UNIVERSITY OF CALGARY

Butyrate and the colonic epithelial barrier: prevention of bacterial transcytosis

By

Kimberley Lewis

A THESIS

SUBMITTED TO THE FACULTY OF GRADUATE STUDIES

IN PARTIAL FULFILMENT OF THE REQUIREMENTS FOR THE

DEGREE OF MASTER OF SCIENCE

DEPARTMENT OF MEDICAL SCIENCES

CALGARY, ALBERTA

AUGUST, 2009

UNIVERSITY OF
CALGARY

Abstract

The epithelial lining of the gastrointestinal tract is the major interface between the external world (i.e. the gut lumen) and the body. As such, the proper maintenance and regulation of epithelial barrier function is a key determinant of digestive health and host well-being. Many enteropathies are associated with increased gut permeability, including Inflammatory Bowel Disease (IBD). Maintaining the barrier function of the epithelium is an energy dependent process. It is therefore thought that metabolic stress can lead to an increase in the permeability of the colonic barrier. One source of metabolic stress is bacterial dysbiosis, or the skewing in the numbers and types of bacteria present in the colon. In the gut of patients with IBD, there is a particular decrease in the *Clostridium* XIVa and IV species which produce butyrate. Butyrate is a short-chain-fatty acid (SCFA) that is the main source of energy for the colonocytes. I hypothesize that increased paracellular permeability as well as internalization and transcellular movement of bacteria in metabolically stressed epithelial cells will be prevented by butyrate treatment.

Our laboratory has found that T84 crypt-like colonic epithelia exposed to 2,4-dinitrophenol (DNP; uncouples oxidative phosphorylation) caused an increase in the internalization and transcellular movement of the non-pathogenic, non-invasive *E. coli* (strains HB101 or F18) and a concomitant decrease in paracellular barrier as gauged by the transepithelial electrical resistance (TER). Co-incubation of butyrate with DNP and *E. coli* strains HB101 and F18 prevented bacterial internalization and translocation, but not the decrease in TER. Likewise, butyrate also prevented mitochondrial swelling and hence, mitochondrial dysfunction that was typically seen with DNP+*E. coli* treated

monolayers. Butyrate also prevented DNP+*E. coli*-induced pseudopodial formation in the T84 cells. This phenomenon was not seen when equi-molar concentrations of acetate (the most abundant SCFA in the colon) was used although the addition of exogenous glucose was also able to prevent bacterial translocation. Butyrate does not only act as an exogenous energy source, but it also prevents NF-κB activation through inhibiting the phosphorylation of the IκB-α inhibitor.

There are many of sources of metabolic stress which can impact the barrier integrity, although not every insult results in prolonged and exaggerated inflammation and disease, such as IBD. However, if an individual has a reduction in barrier as well as a decrease in production (bacterial dysbiosis), uptake (transporters) or metabolism of butyrate, then the individual will lack protection to enhanced bacterial translocation, and disease may occur. Taking butyrate as a prophylactic treatment may be of great assistance in preventing disease relapse in patients with IBD, or even onset of IBD in those that have first degree relatives diagnosed with the disease.

Acknowledgements

To begin, I would like to thank my supervisor Dr. Derek McKay for initially taking me on (albeit reluctantly) as an undergraduate thesis student in 2005. Since then, he has been nothing but kind, supportive, encouraging and helpful throughout both my undergraduate and graduate studies. I will always hold you in the highest of regards, Derek, and I wish both you and Catherine nothing but the best for all that is to come (including the luck that you are going to need in finding a better cat sitter than me!).

I would also like to thank my committee members, Dr. Kevin Rioux and Dr. Wallace MacNaughton, who provided direction and sparked ideas during committee meetings.

I would like to acknowledge the McKay lab members for all of their support throughout my thesis. Dave, Cecile, Van, Arthur, Matt and Smitty, you all have made the past 2 years very enjoyable, and even survivable at times. I would certainly not be where I am today without your continuous friendship. I would like to extend a special thank you to Van, Arthur and Dave P: The three of you have all been so amazing through out my thesis. All of your help did not go unnoticed or unappreciated. THANK YOU! I would also like to thank the ODT for becoming my family out here. Yuan and Dane in particular, you are both honorary members of the McKay lab and I thank you for cheering me up when the cells would crash, the blots didn't work, The Bachelor sent the wrong girl home, or I just needed a hug. You are both very special people and I am thankful to have such amazing friends.

I would also like to thank my parents for always being there to talk (as I was often convinced that that I was the worst M. Sc student ever).

Lastly, thank you to the funding agencies including the Colitis and Crohn's Foundation of Canada, the Canadian Institute of Health Research and the Alberta Heritage Foundation for Medical Research for their generous contributions to my research.

Table of Contents

Abstract i
Acknowledgements iii
Table of Contents v
List of Tables vii
List of Figures viii
List of Abbreviations ix
CHAPTER 1 - Introduction 1
1.1 Intestinal Overview 2
1.1.1 Physiology and Form of the Enteric Epithelium 2
1.1.2 Microbiome 4
1.1.3 Enteric Epithelial Permeability 6
1.1.4 Epithelial Barrier Function and Disease 11
1.2. Inflammatory Bowel Disease (IBD) 13
1.2.1 IBD Introduction 13
1.2.2 Pathogensis of IBD 15
1.3 Metabolic Stress 22
1.3.1 General Description of ATP Production in Colonocytes 22
1.3.2 The Mitochondrion and Metabolic Stress 26
1.3.3 Relevant Sources of Metabolic Stress 26
1.3.4 Sources of Metabolic Stress for Use in the Laboratory 30
1.4 Butyrate 32
1.4.1 Introduction to Dietary Fibers 32
1.4.2 Butyrate and IBD 33
1.4.3 Butyrate as a Treatment for IBD 34
1.5 Aims of Thesis Research 36
CHAPTER 2 - Materials and Methods 38
2.1 Cell lines, Bacteria and Reagents 39
2.2 Measurement of Transepithelial Electrical Resistance and Bacterial Translocation 42
2.3 Bacterial Growth Curves 45
2.4 Internalization Assays 45
2.5 Western Blotting 46
2.6 Enzyme-Linked Immunosorbent Assay (ELISA) for IkB 50
2.7 Transmission Electron Microscopy (TEM) 51
2.8 MTT Assay 52
2.9 Cell Viability 52
2.10 Semi-Quantitative Real Time Polymerase Chain Reaction 54
2.11 Data Presentation and Analysis 57
CHAPTER 3 – Results 58
3.1 DNP Disrupted Mitochondrial Structure Which was Further Exaggerated by the Addition of Commensal Bacteria 59

3.2 Metabolic Stress was Alleviated Through the Addition of Butyrate to Culture Medium 65
3.3 Butyrate Did Not Prevent the Increase in Paracellular Permeability Induced by the Combination of Metabolic Stress and Commensal Bacteria 67
3.4 Butyrate Prevented the Transepithelial Passage of Commensal Bacteria Across .. 73
Metabolically Stressed Colonocytes 73
3.5 Multiple Doses of Butyrate Prevented Enhanced Translocation of *E. coli* at 24 h 79
3.6 The Protective Effect of Butyrate Was Not Common to All Short Chain Fatty Acids, Namely, Acetate 82
3.7 Butyrate Blocked the Increased Bacterial Internalization Caused by Metabolic Stress 84
3.8 The Increase in Intracellular Bacteria Was Not Due to Defective Killing of Internalized Bacteria 87
3.9 Increasing Extracellular Glucose Inhibited the Increased Bacterial Translocation Across Metabolically Stressed T84 Cell Monolayers But Did Not Prevent the Drop in TER 89
3.10 Conditioned Media From Butyrate-Producing Bacteria Did Not Prevent Barrier Dysfunction 91
3.11 Butyrate Prevented DNP+E. coli-Induced NF-κB Activation Via Inhibition of IκB 94
3.12 Mitochondrial Gene Expression Was Not Altered in Patients with CD 99
CHAPTER 4 - Discussion 101
4.1 Experimental Design 103
4.2 Statistical Analysis 107
4.3 Butyrate did not Improve the Paracellular Barrier Integrity in T84 Cell Monolayers 108
4.4 Other SCFAs Cannot Replicate Butryate's Ability to Protect the Transcellular Pathway 110
4.6 Butyrate May Modulate the Barrier by Providing an Energy Source 114
4.7 Future Experiments 115
4.8 Significance 119
References 125

List of Tables

Table Number		Title	Page
Table 1		Characteristics of IBD	14
Table 2		Genes implicated in the pathogenesis of IBD	16
Table 3		Arbitrary unit assignment for bacterial growth on agar plates	44
Table 4		The primary and secondary antibodies used in immunoblotting experiments	49
Table 5		The primers used for semi-quantitative real time PCR	56

List of Figures

Figure		Title	Page
Figure 1		Structure of the tight junctions	9
Figure 2		The pathway of β-oxidation of butyrate	24
Figure 3		Schematic of the experimental set-up	44
Figure 4		Transmission electron microscopy (TEM) revealed that DNP caused mitochondrial dysfunction which was enhanced by the presence of commensal bacteria but prevented by the addition of butyrate	61
Figure 5		Mitochondrial activity of T84s was decreased following exposure to DNP but was regained with the addition of butyrate	66
Figure 6		Increased paracellular permeability across metabolically stressed epithelial cell monolayers exposed to commensal bacteria was not reduced by butyrate co-treatment	68
Figure 7		The decrease in TER was not due to apoptosis	71
Figure 8		Butyrate prevented bacterial transcytosis across metabolically stressed colonocytes	74
Figure 9		Butyrate did not prevent bacterial transcytosis by either killing the bacteria or altering their ability to be taken up by the cell	75
Figure 10		The protective effect of a single dose of butyrate was not sustained over a 24 hour period	77
Figure 11		Acetate did not parallel butyrate's ability to inhibit bacterial transcytosis	81
Figure 12		Butyrate preserved the colonic barrier by preventing bacterial invasion and internalization	85
Figure 13		DNP+*E. coli* HB101 treated monolayers internalized more bacteria that *E. coli* HB101 or *E. coli*+DNP+butyrate treated monolayers and killed the internalized bacteria at a comparable rate	88
Figure 14		Butyrate functioned in part by restoring the energy balance in the cell as exogenous glucose also prevented bacterial translocation	90
Figure 15		The media collected from butyrate-producing bacteria was unable to ameliorate the paracellular and transcellular defects evoked by DNP+*E. coli* HB101	92
Figure 16		Butyrate inhibited T84 epithelial cell mobilization of NF-κB in response to treatment with DNP+*E. coli*	96
Figure 17		Mitochondrial enzyme mRNA was not changed in patients with IBD compared to control patients	100
Figure 18		Butyrate prevents abberant bacterial translocation	122

List of Abbreviations

AP	Activated protein
A/E	Attaching and effacing
ADP	Adenosine diphosphate
AIEC	Adherent Invasive *Escherichia coli*
ASA	Aminosalicyclic acid
ATP	Adenosine triphosphate
BSA	Bovine serum albumin
CAC	Citric acid cycle
CARD	Caspase recruitment domain
CD	Crohn's Disease
CFU	Colony forming units
Co	Coenzyme
Cr-EDTA	Cromium-ethylenediaminetetraacetic acid
dH_20	Distilled water
DMEM	Dulbecco-Vogt modified Eagle medium
DNA	Deoxyribonucleic acid
DNBS	Dinitrobenzene sulphonic acid
DNP	2,4-dinitrophenol
DSS	Dextran sodium sulfate
DZ	Dizygotic
EGF	Epidermal growth factor
ELISA	Enzyme-linked immunosorbent assay
EPEC	Enteropathogenic *Escherichia coli*
ETC	Electron transport chain
F-actin	Filamentous-actin
FAD	Flavin adenine dinucleotide
FBS	Fetal bovine serum
GBF	Germinated barley foodstuff
GI	Gastrointestinal
GTP	Guanosine triphosphate
HEPES	*N*-2-hydroxethyl-piperazine-*N*'-2-ethanesulfonic acid
HRP	Horseradish peroxidase
IBD	Inflammatory Bowel Disease
IEC	Intestinal epithelial cell
IFN-γ	Interferon-γ
Ig	Immunoglobulin
IL	Interleukin
IMM	Inner mitochondrial membrane
JAM	Junctional adhesion molecule
LB	Luria Bertani
LDH	Lactate dehydrogenase
LPS	Lipopolysaccharide
MAPK	Mitogen-activated protein kinase

MCT	Monocarboxylate transporter
MPT	Mitochondrial permeability transitioning
mRNA	Messenger ribonucleic acid
MTT	3-(4,5-dimethyl-thiazol-2-yl)-2,5-diphenyltetrazoliumbromide salt
MZ	Monozygotic
NAD^+	Nicotinamide adenine dinucleotide
NF-κB	Nuclear factor-κB
NOD	Nucleotide-binding oligomerization domain
NSAID	Non-steroidal anti-inflammatory drugs
OD	Optical density
OMM	Outer mitochondrial membrane
PBS	Phosphate buffered saline
PCR	Polymerase chain reaction
P-gp	P-glycoprotein
PI-3K	Phosphatidylinositol-3 kinase
p-IKK	Phosphorylated-IKK
p-IκB-α	Phosphorylated- IκB-α
PMA	Phorbol 12-myristate 13-acetate
PPAR	Peroxisome proliferators-activated receptor
PPS	Plasminogen/plasmin system
PVDF	Polyvinylidene difluoride
RNA	Ribonucleic acid
SCFA	Short-chain fatty acids
SDS	Sodium dodecyl sulfate
SEM	Standard error of the mean
SMCT	Sodium-coupled monocarboxylate transporter
TAD	Transcriptionally active domain
TBST	Tris-biffered saline/0.1% Tween-20
TEM	Transmission electron microscope
TER	Transepithelial electrical resistance
Th-1	T-helper 1
TJ	Tight junction
TLR	Toll-like receptors
TNBS	Trinitrobenzene sulphonic acid
TNF	Tumor necrosis factor
TxA	Toxin A
TxB	Toxin B
Ubc	Ubiquitin-like conjugating enzyme
UC	Ulcerative colitis
ZO	Zonula occluding

CHAPTER 1 - Introduction

1.1 Intestinal Overview

1.1.1 Physiology and Form of the Enteric Epithelium

The gut epithelium is a monolayer of columnar epithelial cells that line the internal aspect of the gastrointestinal (GI) tract. The cells are arranged into crypts and villi, with villi being found only in the small intestine as the colon has crypts with surface epithelium between the crypt openings. This arrangement significantly increases the surface area of the gut tissue, aiding in absorbtion of nutrients and electrolytes, and allowing for water exchange between the gut lumen and the body by enterocytes. In humans, the whole gut epithelium is undergoing continuous renewal that occurs approximately every 3-5 days (1). To mediate this process, stem cells located in the base of the crypts in the intestine undergo division and differentiation to create different cell types. The cells then migrate to the base of the crypts or up the crypt openings, depending on the cell type. For example, secretatory Paneth cells migrate down to the base of the crypts in the small intestine while mucus secreting goblet cells, enteroendocrine cells and absorptive epithelial cells migrate upwards along the villus or to the surface epithelium.

Beneath the epithelium and its basement membrane is a layer of loose connective tissue known as the lamina propria, which contains many blood vessels, nerve endings and immune cells. Below that lies the muscularis mucosae which is a thin layer of smooth muscle. The epithelium, lamina propria and muscularis mucosae are collectively referred to as the mucosa. Beneath this layer lies the submucosa which contains nerve cell bodies in the submucosal plexus that will relay information to and from the mucosa; the primary role of these nerves is believed to be the control of vascular and epithelial

function, such as the regulation of ion transport in the case of the latter. Beyond the submucosa lies the muscularis externa that is responsible for motility in the gut. The muscularis externa is composed of a circular layer of muscle (reduces the diameter of the tube upon contraction) that is surrounded by longitudinal muscle (shortens the tube along its axis). The muscle layer, with the help of the myenteric plexus, which is sandwiched between and enervates the two muscle layers, coordinates gastric and intestinal motility to propel the intestinal contents caudally. The outermost layer of the GI tract is a layer of connective tissue called the serosa (2).

The large surface area of the intestine provides an opportunistic location for pathogens to invade the body. Given that only a single-layer of epithelial cells is responsible for protecting the body proper from antigens and microflora that reside within the lumen, it is not surprising that the intestine is a place of intense immunologic activity. Three broad mechanisms in mammals have developed to protect against infections. The first is the physical barrier (both structural and secreted elements) formed by the enteric epithelial cells and the mucous layer, which is secreted by goblet cells. The second is the innate immune system. Its defense mechanisms include specific pattern recognition receptors located on the epithelium and immune cells in the form of Toll-like receptors (TLRs) and intracellular nucleotide-binding oligomerization domains (NODs) (3). Cells of the innate immune system also produce antimicrobial peptides. These peptides are amphipathic chemicals that interact with and lyse bacterial membranes of both Gram-positive and Gram-negative bacteria. These antimicrobial agents are postulated to have an important role in controlling the normal commensal bacterial population that resides in the GI tract (3).

The third branch of defense for the mucosal surfaces is the lymphocytic or adaptive immune system. The contents of the intestinal lumen are constantly being surveyed as samplings are taken up by highly endocytic microfold cells, which are found in regions of follicle-associated epithelium. The samples are taken to inductive sites called the gut-associated lymphoid tissue and they consist of Peyer's Patches in distal portions of the ileum or lymphoid follicles in the colon and rectum (3). The lymphocytes are immunologicaly naïve and, after being stimulated by their appropriate antigen, will mature, differentiate, traffic back to the lamina propria and re-enter the mucosa to begin their effector functions. Additional levels of protection for the internal environment are offered by the presence of immunoglobulin (Ig)-A, and both intra-epithelial and lamina-propria lymphocytes and natural killer cells.

1.1.2 Microbiome

The GI tract is a complex ecosystem, as it involves the interplay between prokaryotic and eukaryotic cells. The 4 phyla which make up the majority of the bacteria in the human intestines are: *Firmicutes* (49%), *Bacteriodetes* (23%), *Proteobacteria* (21%) and *Actinobacteria* (5%) (4). Interestingly, these subgroups colonize in different locations along the GI tract. For instance, in the human, the small intestine harbours more bacteria from the *Bacillus* subgroup of *Firmicutes* and *Actinobacteria* but have fewer *Bacteriodetes* and *Lachnospiracea* compared to the colon (5).

The commensal bacteria of the alimentary tract confer many benefits to intestinal physiology. The resident bacteria have been found to play a critical role in the maintenance of intestinal epithelial homeostasis by activating TLRs under normal steady

state conditions and may prevent susceptibility to colonic injury (6). They also assist epithelial cell development and differentiation, barrier fortification, angiogenesis and can limit immune activation (7). For instance, when *Bacteriodes thetaiotaomicrons* (a prominent member of the normal microflora of the mouse and human distal intestine) colonize germ-free mice they induce the expression of receptors for trefoil factors that repair damaged epithelia, and decay-accelerating factor, which inhibits cytotoxic damage from microbial activation of complement proteins.

Commensal bacteria play a large role in nutrient uptake and metabolism (7). Colonization of germ-free mice with *B. thetaiotaomicrons* increases the expression of enterocyte genes involved in the absorption of carbohydrates and those responsible for lipid catabolism and absorption. In fact, germ-free mice eat 30% more calories than normal mice each day to maintain their body weight (8). Other metabolic activities of the normal commensal flora include the break down of dietary carcinogens and the synthesis of biotin, folate and vitamin K. The commensal microflora is also critical for the fermentation of dietary fibers (to be discussed later in section 1.4) (8).

Bacteria in the gut are very important for the formation of a normal immune system. At birth, the development of the immune system is incomplete. The normal flora and childhood infections complete the “education” of the immune repertoire. Without a microflora, mucosal-associated lymphoid tissue is rudimentary and there are defects in cell-mediated immunity (9). The colonization of commensal bacteria is important for the fine-tuning of T-cell repertoires and T-helper (Th)-1/Th-2 cytokine profiles (10, 11).

Commensal bacteria also offer protection against infections. Resistance to colonization of pathogens most likely involves several mechanisms including production of anti-microbial factors, such as bacteriocins and lactic acid, that alter the pH and prevent the growth of pathogenic bacteria. The microflora also provides competition for nutrients and epithelial binding sites (8).

1.1.3 Enteric Epithelial Permeability

The epithelial barrier is an active structure that is under the influence of many exogenous stimuli such as bacterial toxins, food antigens and medications. It also receives input from endogenous factors like neuro-endocrine molecules and immune cell messenger molecules. While it is important to prevent the entry of toxins and invasion of pathogens into the sub-mucosa, it is equally important for the barrier to allow the absorption of nutrients, solutes and water into the body so that normal physiological processes may occur. Another possible advantage of a controlled decrease in the epithelial barrier function would be to assist the passage of neutrophils and complement into the gut lumen to combat infections (12).

In the absence of ulcerations or lesions, lumen-derived material crosses the enteric epithelium by either transcellular or paracellular routes. The transcellular pathway involves the movement of materials directly through the cell, with uptake occurring via specific receptor/antibody mediated uptake or non-specific phagocytosis and endocytosis. It has been reported that stabilizers of microtubules (colchicine), microfilaments (jasplankinolide) (13) and clatherin pit endocytosis (pheylarsine oxide) (14) all prevent bacterial internalization and translocation across model gut epithelia, indicating their

importance in transcytosis (15). Paracellular permeability is controlled by tight junctions (TJs) that form a regulated seal at the apex of adjacent cells (16, 17). This pathway is a key regulator of intestinal permeability to macromolecules over 2 kDa such as endotoxins and bacterial products (18, 19). This pathway is both responsive and dynamic as it can change quickly after meals. For example, when the osmolarity of the lumen changes, the permeability characteristics of the TJs also alter. Ingestion of a hypertonic solution or meal-related solutes such as glucose increased paracellular permeability in the small intestine (20, 21).

Tight junctions consist of bands of proteins (composed of transmembrane adhesion proteins and intracellular adaptor proteins) located at the membrane between the apical and basolateral regions of polarized epithelial cells (Figure 1) (16). The transmembrane adhesion proteins include claudins, occludin and junctional adhesion molecules (JAMs) (17, 22). The type and concentration of claudins determines the charge and size selectivity of ions and small molecules allowed to pass via paracellular movement as their extracellular loop is charged. The claudins (which have tissue specific expression) and occludin are associated with intracellular peripheral adaptor proteins called Zonula Occludin (ZO) proteins of which there are 3 isoforms: ZO-1, ZO-2 and ZO-3 (16, 17, 22). Recently, ZO-1 and ZO-2, but not ZO-3, have been implicated in TJ regulation. In addition to these adaptor proteins recruiting cytosolic components such as protein kinases and transcription factors, ZO proteins also anchor the TJ strand to the actin cytoskeleton. There are other scaffolding proteins that are responsible for mediating connections between the transmembrane adhesion proteins and the

cytoskeleton. These proteins include MUPPI, MAGI and cingulin (reviewed in 23; see Figure 1 below).

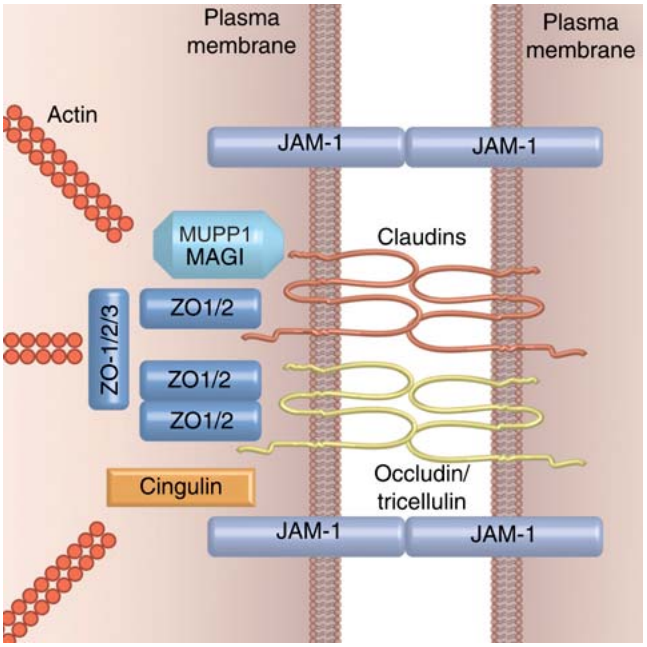

Figure 1. Structure of the tight junctions. There are 3 types of structural transmembrane proteins that are involved with cell-to-cell adhesion at the tight junctional complexes: 1) the 24 member family of the claudins that directly affects paracellular charge and size selectivity, 2) the occludin (or related tricellulin) whose role is currently unknown and 3) the IgG-like family of junctional adhesion molecules (JAMs) that are engaged in homophilic and heterophilic adhesion. These transmembrane adhesion proteins interact with scaffolding proteins such as Zonula Occludin (ZO), MUPP1 and MAGI proteins. The C-terminus of most claudins ends in a PDZ domain which can interact with the first PDZ domain of ZO-1, ZO-2 and ZO-3. The C-terminus of ZOs can then interact with actin, providing a direct link to the cytoskeleton. However, not all scaffolding proteins contain PDZ domains, such as cingulin. Cingulin interacts with ZOs, JAMs, actin and myosin and may be an important regulator of the dynamic nature of TJs (reviewed in and figure adapted from (23)).

Decreased expression of Filamentous (F)-actin, ZO-1 and occludin proteins were concomitant with increased permeability in metabolically-stressed epithelium exposed to commensal bacteria as well as some pathogens (15). The effects of bacteria on the TJ proteins will be discussed in depth in the next section. Studies such as this have revealed the functional importance of TJ proteins and associated proteins in the regulation of epithelial permeability.

There are several different factors that may alter the permeability of the epithelial barrier. The ingestion of a meal can alter the permeability of TJs. Evidence supporting this phenomenon was first described in 1987 when segments of small intestine from rats were mounted in Ussing chambers and the addition of luminal glucose caused an increase in the paracellular permeability (24). This was due to sodium-glucose co-transport-dependent regulation of small intestinal permeability (25, 26) that was linked to the spatial dissociation of ZO-1 and TJ fibers (27).

Additionally, cytokines can influence TJ permeability. For instance, interferon-γ (IFN-γ) is a cytokine that is released by T-cells and natural killer cells. *In vitro* results from the human cancer-derived crypt-like colonic T84 cell line demonstrate that IFN-γ dose-dependently decreases transepithelial electrical resistance (TER; a measure of paracellular permeability) as well as increasing the flux of solutes, such as mannitol, that are believed to cross the epithelium predominantly via a paracellular route (28). IFN-γ also may increase transcellular permeability. The human colorectal adenocarcinoma cell line HT-29, when treated with IFN-γ, exhibited a pronounced flux of apically applied horseradish peroxidase molecules (HRP; a marker of transcellular movement) compared to control cells (29). IFN-γ acts in concert with other cytokines such as tumor necrosis

factor-α (TNF-α) to enhance barrier defects. While TNF-α can cause a direct increase in permeability across renal and some enteric epithelial cell lines (30, 31), it has minimal direct effects on the barrier properties of T84 cell monolayers (32-34). However, when T84s are exposed to TNF-α in the presence of IFN-γ there was a marked redistribution of JAMs in intercellular junctions (35).

There are a wide variety of other cytokines which may alter epithelial permeability. For example, interleukin (IL)-4, which is produced by mucosal lymphocytes, attenuates barrier function (36, 37) and increases the ability of neutrophils to adhere to T84 cell monolayers (38, 39). IL-13 exhibits similar biological effects to IL-4 since it too causes an increase in the paracellular permeability (40, 41) through redistributing claudin-2 (42).

Several different growth factors can modulate epithelial permeability. Hepatocyte growth factor is synthesized by mesenchyme-derived cells and causes decreases in T84 cell TER (43). Not all growth factors cause a decrease in barrier integrity. Transforming growth factor-β has been reported to enhance barrier function in human enterocytes (44) as has epidermal growth factor (EGF) by causing intercellular junctional assembly of subconfluent monolayers (45).

1.1.4 Epithelial Barrier Function and Disease

Anatomical barriers are very important for protecting the body from environmental hazards and toxins. As a simple example, the skin is a primary defense against pathogens that we encounter daily. Loss-of-function mutation in FLG-a gene which encodes for normal epidermal differentiation and maturation- has recently been implicated in the

enhanced percutaneous transfer of allergens, causing atopic disease (46). Thus, given the extent to which the GI tract controls and prevents disease by acting as a barrier, one can imagine the number of pathological disorders that may arise should loss of barrier occur. Several pathogenic bacteria are successful at breaching the enteric barrier. They hijack the normal regulatory mechanisms that control enteric epithelial permeability by delivering virulence factors (i.e. effector proteins) directly into their target cells (47). A common target is the host cytoskeleton (48, 49). For example, attaching and effacing (A/E) bacteria are those that do not invade the cell, but use the actin cytoskeleton to attach intimately to the cell surface, inducing motile actin-rich pedestal formation *in vitro*. A/E pathogens comprise enterohemorrhagic *E. coli*, enteropathogenic *E. coli* (EPEC), *Citrobacter rodentium* and *Hafnia alvei* (50). EPEC infections cause diarrheal disease in pediatric patients by increasing epithelial permeability. EPEC are able to disrupt TJ morphology by inducing the re-organization of the actin cytoskeleton (50). EPEC first inserts Tir, an effector protein, which causes pedestal formation for tight attachment to the epithelium. A second protein, EspF, is injected into the host cell and binds to complexes near the TJ, which causes the redistribution of ZO-1, ZO-2 and actin. This in turn leads to TJ disruption and increases in ion and small molecule fluxes across the epithelium (50).

A variety of bacterial toxins alter the paracellular permeability as well. For example, Toxin A (TxA) and Toxin B (TxB) are produced by *Clostridium difficile* and can induce ileal and colonic epithelial damage. Evidence suggests that the toxins disrupt the barrier by disaggregating actin through glycosylating Rho-family proteins, which open the TJs and decrease the TER in T84 cells. TxA and TxB also induce the release of pro-

inflammatory cytokines from the intestinal epithelial cells (IECs), which can then act in an autocrine-like manner to disrupt TJs (51, 52).

Increased paracellular permeability has been documented in both acute and chronically inflamed intestine (53, 54). Inflammatory Bowel Disease (IBD) is an idiopathic disease consisting primarily of Crohn's disease (CD) and ulcerative colitis (UC) (55). Altered TJ structures and increased epithelial permeability have been observed in IBD (53, 56), although it is unknown if the increase in permeability is a cause or effect of mucosal damage. The implications of barrier defects in this disease will be discussed in depth in the following section.

1.2. Inflammatory Bowel Disease (IBD)

1.2.1 IBD Introduction

CD and UC are typically diagnosed in individuals in their 20s to 40s. However, approximately 20% of patients will develop their symptoms in childhood (57). The characteristics associated with each disease are described in Table 1 below.

	Crohn's Disease	Ulcerative colitis
Afflicted areas (58)	-Anywhere from the oropharynx to the perianal area	-Restricted to the colon with the rectum involved in 95% of cases and will have varying degrees of proximal extensions
Cytokine profile (59)	- Th-1 response: IFN-γ and TNF-α	-Th-2 response: IL-5 and 13
Inflammation characteristics (58, 60)	- Peyer's Patch ulcerations, chronic inflammation of the submucosa, and granuloma formation - Patchy transmural inflammation	-Acute and chronic inflammation of the mucosa by polymorphonuclear leukocytes, crypt abscesses, distortion of the mucosal glands, and goblet cell depletion

Table 1. Characteristics of IBD. Signs and symptoms of the two branches of IBD: Crohn's disease and ulcerative colitis (55).

1.2.2 Pathogensis of IBD

The clinical signs and symptoms of IBD have been characterized, but the cause remains unknown (61). With the incidence rate increasing, it is becoming more pressing to find the triggers for the onset of IBD (62). These triggers are hypothesized to include: genetics, inappropriate reactions to commensal flora, environmental causes and dysfunctions in barrier. However, the prevailing hypothesis is that the interaction of multiple predisposing factors leads to the development of IBD.

a) Genetics

Specific genes have been implicated in causing IBD susceptibility. There is a high concordance rate of disease in identical twins and a 10-25 fold increase in risk in disease propogation if an individual has first degree relatives with CD (61). The discovery of a genetic link occurred in 2001 when NOD2, also known as caspase recruitment domain (CARD)-15, was identified as the first IBD susceptibility gene (62, 63). This gene activates the nuclear factor-κB (NF-κB) pathway in response to bacterial lipopolysaccharide (LPS) (63). NOD2 variant monocytes were found to have an over-active NF-κB pathway (64). Since 2001, there has been an explosion in the number of genes suspected to be involved in the development of IBD. There are now more than 30 genes that are implicated in the pathogenesis of the disease (62, 65), with examples shown in Table 2, below. To date, only the IL23R and ATG16L1 genes are associated with UC, while all the others are linked to CD (62).

Gene	Function
NOD2	Involved in the innate immune response by recognizing bacterial components and activation of NF-κB.
IL23R	Induces IL-17 production, which in turn promotes mucosal inflammation. The IL-23 pathway may also regulate intestinal barrier function. A possible gain of function will lead to dysregulated inflammation.
PTPN2	Encodes a T-cell protein tyrosine phosphatase, a negative regulator of inflammatory responses.
TNFSF15 (TL1A)	Encodes a cytokine of the tumour necrosis factor (TNF) ligand family, which is induced by TNF and can activate NF-κB.
5p13 gene desert	Implicated in the regulation of the prostaglandin E receptor 4 gene (suppression of which enhances colitis in mice).
ATG16L1 and IRGM	Involved in autophagy, which removes intracellular pathogens and supports both the innate and acquired immune response.
NELL1	Encodes a protein containing EGF-like repeats. Aberrant expression in mice is associated with defects in cranial and skeletal development.
NCF4	The regulatory component of the superoxide-producing phagocyte NADPH-oxidase, which is involved in host defense.

Table 2. Genes implicated in the pathogenesis of IBD. The table above provides a description of some IBD-associated gene names and their functions (62).

b) Reaction against the commensal flora

The microflora of the human GI tract consists of roughly 500 different species of bacteria (6). Duchamann *et al.* showed that lamina propria mononuclear cells and peripheral blood mononuclear cells taken from patients with IBD exhibited a robust reaction to both autologous and heterologous gut microflora, while those taken from control patients only reacted to heterologous bacteria (66). This indicated that patients with IBD lack tolerance to antigens present in their own microflora. The IL-10 deficient mouse, if reared in germ-free conditions, does not demonstrate any inflammation or abnormal cytokine levels unlike those that were kept in regular conditions. This indicates that the permeability defect, which precedes normal inflammation (as defined histologically), is only a single step in the development of IBD, as commensal flora must be present to drive immune reactions (67). Likewise, accepted models of colitis including IL-$2^{-/-}$ mice, HLA-B7-transgenic rats and SAMP1/Yit mice, do not develop inflammation in germ-free conditions (68-71). Furthermore, mice with disrupted multidrug resistance gene 1a (*mdr1a*$^{-/-}$) manifest UC-like symptoms (72), but antibiotic treatment reduces colitic symptoms (73).

The translocation of commensal, non-pathogenic bacteria across the enterocytes' barrier occurs in healthy people as indicated by the presence of such bacteria in 5% of cultured mesenteric lymph nodes. However, this positive culture rate jumps to 16-40% in patients with IBD. In addition, patients with CD or UC can have increased antibodies against a broad spectrum of their own commensal bacteria (74). Moreover, the diversion of the fecal stream can improve CD; however, the disease recurs after restoration of bowel continuity or infusion of luminal content into the bypassed ileum (75).

Antibiotics have also proven to be valuable in the treatment of IBD. Antibiotics can decrease bacterial translocation and help to reduce bacterial overgrowth in the colon (76). Broad spectrum antibiotics have been shown to decrease the Crohn's disease activity index in a dose-dependent manner, although they did not prevent relapse rates in all patients with CD (77, 78). However, Rutgeerts *et al.* found that high-doses of antibiotics beginning immediately after resection and continuing for 3 months decreased mucosal ulcerations and prevented clinical recurrence rates for a year (79). In patients with UC, antibiotics have shown to be useful as adjunct therapy to standard treatments (80-82). However, other studies have shown that the use of antibiotics either did not help to improve UC signs and symptoms (83), or their use may have been a plausible trigger for disease onset or relapse (84). Antibiotics can alter the bowel flora which results in the overgrowth of deleterious microbes, thus suppressing the growth of protective bacteria (85). For instance, antibiotics given for *C. difficile* infections have been associated with exacerbation of colitic symptoms (84, 86).

Particular strains of bacteria are also thought to play a role in the pathogenesis of IBD, and these strains are more prevalent in the gut of IBD patients. There are increased concentrations of *Enterobacteriaceae* and *Bacteriodes* species that adhere to the mucosa of patients with IBD (87), and these bacteria are found to invade the mucosa in ulcers (88). Also, patients with CD are statistically more likely to have invasive *E. coli* strains isolated from their gut than normal controls (87, 89-92). These IBD-associated *E. coli* strains, including the CD-associated adherent invasive *E. coli* (AIEC) strain LF82, are able to alter the barrier by causing disorganization of F-actin and ZO-1, resulting in a decrease in the human colonic Caco-2 cell line TER (93, 94). These findings suggest that

there is an antigen or a microbe present in the gut lumen that may induce the pathogenesis of IBD.

c) Environmental Factors

The interplay between genetics and the environment is hypothesized to result in the development of IBD. Several studies have reported a high prevalence of increased intestinal permeability in spouses of CD patients (95-97), indicating an environmental trigger for IBD. Moreover, monozygotic twins (MZ) show concordance rates ranging from 36-58% for CD and 8-16% for UC. Dizygotic twins (DZ) have a lower concordance rate at 4% for both CD and UC (98). Although the higher concordance in MZ twins compared to DZ twins may suggest contributions from genetic risk factors, the high concordance is confounded by shared environmental risk factors. In addition, the approximate 50% lack of concordance for CD and 80% lack of concordance for UC amongst MZ twins suggest that environmental factors can alter the outcome of IBD (98). The incidence of CD also varies in different geographical populations. The highest rates of incidence are found in North America and Europe while the lowest rates of countries studied occur in Japan and New Zealand (99). During the 1970s, there was a high rate of immigration into England from South Asia. At that point in time, the incidence of CD was higher in indigenous Europeans than in the migrant population. However, from 1981-1989, the incidence rate of the migrated Asian population matched that of the indigenous population, suggesting a role for environmental triggers (100).

Smoking has been proposed as an environmental trigger for IBD as well, particularily for CD. It has been found that the percentage of patients with CD that smoke was significantly higher than those in a control population that were matched for

sex and age (45-55% compared to 30-40%, respectively). This is in contrast to UC, where smoking may protect against this form of IBD (101).

While diet and its correlation to IBD has been studied, it has proven to be inconsistent (102). It has been noted that a high consumption of refined carbohydrates and fats (103) may be a factor in the induction of IBD, while consumption of fruits and vegetables may reduce the risk of developing CD (103).

Another environmental factor, albeit controversial, is hygiene and infections (104). Case-control studies have examined patients under 20 years of age and found that recurrent respiratory infections within the first 10 years of life may coincide with an elevated risk for UC (105). Baron *et al.* found an increased risk for UC if the individual shared a bedroom as a child, or if their mother had a disease during pregnancy (106). Likewise, children that stayed in crowded homes, had physician diagnosed infections, or owned a pet were also more likely to eventually be diagnosed with CD (107).

d) Barrier disruption

The importance of a perturbed epithelial barrier in IBD propagation is supported by the large number of first degree relatives of patients with CD who have increased epithelial permeability (108-110). Also, an increase in permeability can be a marker for disease relapse (111-113). In a compelling example, a child with high gut permeability, but no evidence of microscopic or macroscopic disease, was found to develop CD 8 years after the initial impaired barrier function was observed (109). Increases in barrier permeability are of great importance to the development of IBD as it is becoming increasingly apparent that IBD may be due to an aberrant immune reaction to some component of the commensal flora (discussed previously) (114). Normally, the epithelial

barrier is kept tight such that only small amounts of antigen are sampled from the lumen to maintain oral tolerance. However, in situations where the barrier becomes "leaky", excessive amounts of antigen (or perhaps prokaryotes) may cross the epithelium and elicit a defense response causing acute inflammation. If this breach in barrier is prolonged, chronic inflammation may develop. Increases in permeability are often transient and may occur for reasons such as: alcohol consumption, infections and medication administration (eg. Non-steroidal anti-inflammatory drugs; NSAIDs) (115). Certainly, not every individual who consumes a glass of wine will experience prolonged barrier defects with inflammation that may develop into IBD.

There is also evidence from animal models of IBD showing that a barrier defect occurs prior to obvious inflammation. For example, the SAMP1/Yit model (mimics CD) shows increased gut permeability in 3-week-old mice when inflammation is not apparent (116). The *mdr1a*$^{-/-}$ mice manifest defective IECs that lack P-glycoprotein (P-gp), a 170 kDa plasma membrane protein (117, 118). Mice that lack the *mdr1a* gene develop spontaneous colitis (72). The *mdr1a*$^{-/-}$ mice (when placed in conventional housing) are found to experience weight loss, diarrhea, swelling of the colon, colonic neutrophil infiltration, lamina propria thickening, goblet cell depletion, and interestingly, a decrease in the TER across the colon. This increase in permeability is apparent before the onset of symptoms and is matched by an increase in HRP and Fluorescein isothiocyanate-dextran fluxes across the colonic barrier. This observation was found to coincide with decreased levels of phosphorylated occludin, implying a role for improper TJ formation (119). Notably, a subgroup of patients with UC also have an altered *mdr1a* gene and abnormal P-gp distribution (120). The IL-10 knockout mouse also has a disrupted epithelial barrier

associated with the development of IBD-like symptoms (121). Madsen *et al.* found that IL-10 deficient mice exhibited increased ileal and colonic permeability at 2 weeks of age prior to any evidence of histological injury. The defect was associated with increased mucosal secretion of IFN-γ and TNF-α, 2 potent pro-inflammatory cytokines that, as discussed earlier in Section 1.1.3, can have a direct effect on epithelial permeability (67).

The maintenance of the enteric barrier integrity is an energy-dependent process. It has been noted that some patients with CD have swollen mitochondria and misshapen cristae, indicative of decreased levels of adenosine triphosphate (ATP), in enterocytes (110, 122). For instance, there was a decrease in the amount of ATP present in the colons of patients with active CD compared to CD patients that were in remission, or those that had colon cancer (110, 123). Thus, it is possible that metabolic stress may cause a change in epithelial permeability and allow for the movement of antigens across the barrier to elicit an exaggerated immune response. Patients with CD also seem to be more susceptible to the uncoupling of oxidative phosphorylation from the electron transport chain (ETC) (110).

1.3 Metabolic Stress

1.3.1 General Description of ATP Production in Colonocytes

It has been known for many years that butyrate (a c4 short-chained fatty acid; SCFA; see section 1.4.1) is the primary substrate for colonocyte metabolism (124). Since 99% of colonic butyrate exists in the anionic form, very little is absorbed through non-ionic diffusion. Colonocytes absorb the majority of available butyrate through 2 transporters: the monocarboxylate transporter (MCT) (125) and the sodium-coupled

monocarboxylate transporter (SMCT) (126). Butyrate can also be absorbed though anion exchangers. Once butyrate is absorbed by the cells, it undergoes β-oxidation in the mitochondrion (127). There, the SCFA is enzymatically altered into 2 acetyl-Coenzyme (Co) A molecules (127) (Figure 2). This process produces hydrogen gas and 1 nicotinamide adenine dinucleotide (NAD^+) that reduces to NADH. NADH then enters the ETC (described later) (127). Once the 2 acetyl-CoA molecules are produced, they enter the Citric Acid cycle (CAC). This process occurs in the innermost compartment of the mitochondrion: the matrix. The CAC uses the 2 acetyl units from the acetyl-CoA molecules and combines them with oxaloacetate. A series of 8 enzymatic changes then ensues to produce 4 carbon dioxide molecules, 2 guanosine triphosphate (GTP) molecules, 6 NADH molecules and 2 reduced flavin adenine dinucleotide (FAD) molecules. While the GTPs provide the energy equivalency of 1 ATP molecule, the majority of ATP production lies in the reduction of the high-energy electron carriers NAD^+ and FAD to NADH and $FADH_2$ (127).

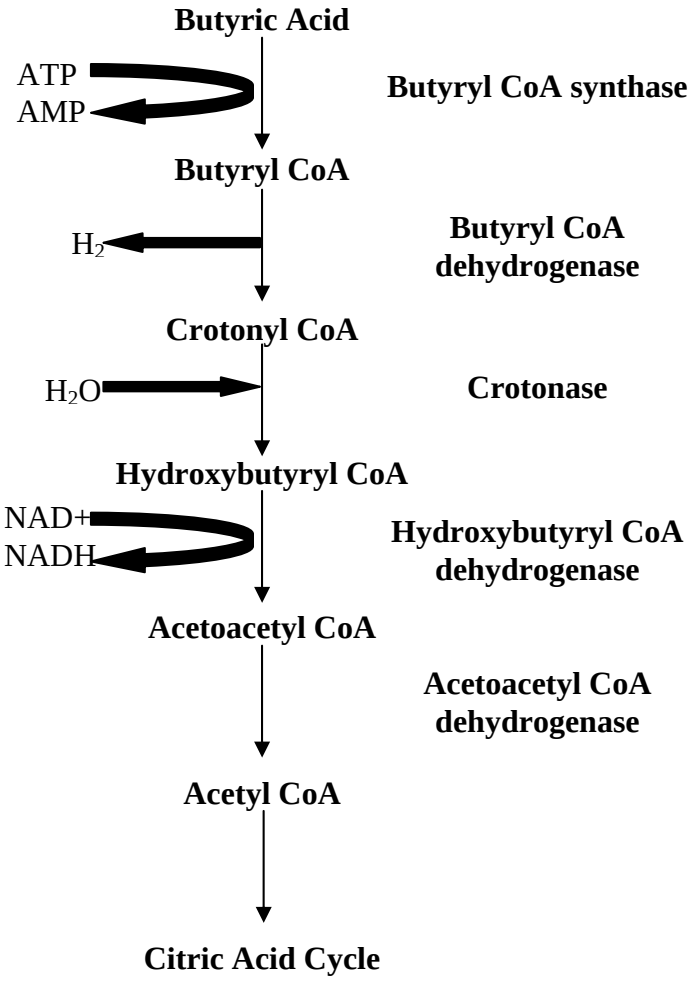

Figure 2. The pathway of β–oxidation of butyrate. Butyrate enters the cell through non-ionic diffusion, ionic exchangers or transports (the monocarboxylate transporter or the sodium coupled monocarboxylate transporter). Once inside the cell, butyrate undergoes β-oxidation in the matrix of mitochondria. The end product of β-oxidation is the production of 2 acetyl-CoA molecules that can enter the citric acid cycle (AMP, adenosine monophosphate). Figure adapted from (128).

The mitochondrion is bound by a smooth outer membrane and contains numerous invaginations, or cristae, of its inner membrane. The inner membrane creates two distinct spaces in the mitochondrion: the intermembrane space and the matrix. Since the outer membrane is very porous, it permits the free diffusion of molecules up to 10 kD, making the intermembrane space equivalent to the cystol in its concentration of metabolites and ions (127). The inner mitochondrial membrane (IMM) is roughly 75% protein by mass. It is only freely permeable to oxygen, carbon dioxide and water (127) while special transporters exist for the passage of metabolites such as ATP and adenosine diphosphate (ADP). It is this selectively permeable membrane that allows for the generation of ion gradients between the matrix (the internal compartment) and the intermembrane space. This ion gradient is key to the production of ATP. The IMM houses a multiprotein complex termed the ETC. When NADH and $FADH_2$ interact with the protein complexes of the ETC on the matrix side, they are oxidized. Protons derived from the oxidative reactions are shuttled out of the matrix into the intermembane space while the electrons pass through the ETC. As the protons are pumped into the intermembrane space, a proton gradient is created and, thus, a positive charge builds up. The protons are allowed to travel back into the matrix via the proton-pumping ATP synthase (127). The electron transport chain and oxidative phosphorylation are tightly coupled as the free energy from the protons passing through the F_1F_0 ATPase generates the production of ATP from ADP+P_i. It takes 3 protons to create 1 molecule of ATP. The protons will be combined with oxygen that has accepted electrons from the ETC to make water, which can then freely diffuse out of the matrix, into the intermembrane space and eventually into the cytosol (127).

1.3.2 The Mitochondrion and Metabolic Stress

Swelling of mitochondria due to the uncoupling of oxidative phosphorylation has been reported in other tissues. For example, ischemia causes an increase in the IMM permeability and mitochondrial swelling in brain cells (129). This event is called mitochondrial permeability transitioning (MPT) (130) and involves the opening of a pore in the IMM that allows for the free diffusion of ions or molecules greater than 1.5 kDa (129, 130). This disrupts the proton motor force (the proton gradient that was established) and leads to the uncoupling of oxidative phosphorylation. MPT causes the ATP synthase to operate in reverse, consuming ATP in a futile attempt to restore the proton gradient. Thus, the occurrence of a mitochondrial permeability transition pore accelerates cellular energy depletion. More than simple energy depletion, it also causes mitochondrial swelling. The alteration of the ionic gradient promotes H_2O uptake, causing internal swelling and loss of cristae structure. As the surface area of the IMM increases compared to the outer mitochondrial membrane (OMM), the IMM pushes on the OMM and causes the mitochondrion to swell (131).

1.3.3 Relevant Sources of Metabolic Stress

a) Bacterial dysbiosis

There are distinct shifts in the microbial flora in IBD patients compared to control patients (4). This alteration in relative gut diversity has been termed "bacterial dysbiosis" and may be a potential source of metabolic stress. For instance, Macichanh *et al.* saw a marked reduction in the number of Gram-positive Firmiculate bacteria in 6 patients with CD. There was a particular decrease in *Clostridium leptum* and *Clostridium coccoides*

compared to control subjects (132). These organisms are major producers of butyrate, which is both an energy source for the colonocytes and possesses anti-inflammatory properties (133, 134). Thus, it may be suggested that a loss of butyrate-producing bacteria will ultimately reduce the amount of ATP production in the epithelium.

b) Infection

As described above, several pathogens can inhibit proper mitochondrial function and induce morphological changes. For example, *Campylobacter jejujni* infections (135) and *E. coli* strain C25 (136) can induce mitochondrial swelling in human epithelia as is also seen in murine epithelial cells infected with the mouse pathogen *Citrobacter rodentium* (137). Also, *C. difficile* TxA migrates to the mitochondria, induces morphological changes, halts ATP production and causes actin filament disaggregation (138). Moreover, rotavirus infections can deplete energy in Caco-2 epithelial cells and cause a redistribution of TJ proteins (139).

c) Psychological stress

Human psychological stress

The gut is controlled by a highly autonomous endocrine system, with its control being exerted by higher cortical impulses. IBD is a transient disease that alternates between active and quiescent periods with disease relapse questionably corresponding to stressful life events. Several studies claim that there is no correlation between major life events and the re-activation of IBD (140). However, recent investigations appear to reveal that daily hassle and perceived stress contribute to reactivation of IBD, or exacerbation of clinical symptoms (141-144).

Stress may increase the permeability of the enteric barrier (145). For instance, repeated immersions of a subject's hand in cold water resulted in a change in barrier as noted by an increase in jejunal water secretion (146). A stress-induced increase in enteric permeability was also seen in a study completed a decade earlier where Barclay and Turnberg saw a decrease in the intestinal fluid absorption by healthy volunteers when they were subjected to cold pain stress (145).

Animal Psychological Stress

The effects of psychological stress on the intestinal barrier have been closely examined in animal models. Saunders *et al*. (1994) found that when rats were physically restrained there was an increase in gut permeability as gauged by increases in the flux of ^{3}H-mannitol, ^{51}Chromium-ethylenediaminetetraacetic acid (^{51}Cr-EDTA) and HRP across Ussing-chambered intestine (147). Levels of corticotrophin releasing hormone were highest in animals that had the largest increase in permeability. Adrenalectomized animals or animals given an inhibitor of glucocorticoids prior to being stressed did not experience an increase in permeability, nor did animals that received vehicle treatment (148).

Murine models of chronic stress also indicate that stress can induce changes in gut epithelial permeability. Soderholm *et al.* demonstrated that when rats were placed under mild but prolonged psychological stress, such as repeated water avoidance stress, they experienced an increase in gut permeability, an increase in bacterial attachment and perturbed mitochondrial structure. These 3 conditions have also been observed in humans with IBD. Thus, psychological acute or chronic stress in the rodent appears to result in an aberrant intestinal barrier (147, 149, 150).

d) Medications

Evidence of prescription anti-inflammatory drugs in permeability induction has also been documented. NSAID drugs are the single most prescribed antirheumatic drug (151). However, NSAIDs induce GI complications in the form of inflammation of the large intestine and increases in intestinal permeability (152). Although the exact mechanism is controversial, NSAIDs may alter the enteric barrier by metabolically stressing the enterocytes, thus destroying the energy-dependent TJs. It is believed that NSAIDs either uncouple oxidative phosphorylation or inhibit the ETC, both of which decrease ATP production (151). Moreover, morphological changes occured in bowel mitochondria after NSAID administration: mitochondria were swollen and the cristae were deranged (151, 153, 154). NSAIDs are not the only drugs that may inhibit energy production and consequently increase epithelial permeability. For instance, Tacolimus (FK507) is an immunosuppressive drug that inhibits T-cell activation; however, it also reduces mitochondrial activity and thus may impair the colonic barrier (155, 156).

e) Ischemia/Surgery

Hypoxia is another condition that affects mitochondria structure/function. In extreme sepsis, the ability of tissues to extract oxygen from the blood is severely impaired and oxygen metabolism in the mitochondrion is altered (157). Mitochondria were found to have diminished ETC activity during sepsis, indicating decreased ATP production (158).

Other means of ischemia may occur as well during surgical stress. It has been shown that there is an increase in intestinal permeability even if surgery is done at a remote location (159). Studies have shown that oxidative stress in enterocytes might

promote decreased epithelial barrier integrity and enteric mitochondrial swelling during surgical procedures such as bowel manipulation or laparotomy (160).

1.3.4 Sources of Metabolic Stress for Use in the Laboratory

There are several metabolic stressors which can be used *in vitro* to reduce the amount of ATP produced by the cells. For instance, reducing the concentration of glucose in the media would lower ATP production. However, this would also stop glycolysis from occurring, and not be a true measure of mitochondrial dysfunction.

Hydrogen peroxide (H_2O_2) is a physiologically relevant source of metabolic stress as it is produced *in vivo* in order to fight infections. Many proteins with transition metals in their composition are susceptible to oxidative damage by H_2O_2. H_2O_2 will interact with transition metals to induce the release of free metal ions that could initiate a series of free radical reactions (161). In particular, H_2O_2 reacts with the iron in cytochrome *c*, which is localized on the IMM and is part of the ETC. The reaction between H_2O_2 and cytochrome *c* leads to the release of iron ions and the production of the powerful oxidizing hydroxide radical, which will oxidize many macromolecules including deoxyribonucleic acid (DNA), protein, lipids and carbohydrates (161-165). H_2O_2 has many non-mitochondrial effects such as the activation of the NF-κB and activator protein-1 (AP-1) pathways (166, 167).

NSAIDs can induce metabolic stress; however, they are anti-inflammatory agents that effect many targets such as cyclooxygenase (168), peroxisome proliferator-activated receptor (PPAR)-γ (169) and the NF-κB pathway (170), to name a few. The promiscuity of NSAIDs makes them an inappropriate choice for a metabolic stressor.

The chemical 2,4-dinitrophenol (DNP) is a model compound that induces metabolic stress. The IMM potential is created by the selective pumping of protons to the intermembrane space of the mitochondrion. DNP is a protonophore that facilitates the movement of protons through the IMM. Thus, DNP destroys the proton gradient by picking up protons in the acidic intermembrane space, passing through the IMM and then releasing the protons in the matrix. The anionic DNP is then able to pass back through the IMM and repeat the cycle (171), uncoupling oxidative phosphorylation from the ETC and arresting ATP production.

Cancer-derived, crypt-like colonic T84 epithelial cell monolayers did not experience a DNP (0.1 mM)-induced decrease in TER after 24 h of incubation. Commensally derived microbes such as *E. coli* strain HB101 (non-pathogenic, non-invasive; 10^6 cfu) also did not increase the paracellular permeability or translocate across the T84 cell monolayers to any significant level. However, co-incubation of the DNP+*E. coli* HB101 induced a drastic decrease to roughly 40% of the pre-treatment TER value and had increased amounts of bacterial translocation across the monolayers. These results were replicated when another metabolic stressor, indomethicin (an NSAID), was substituted for DNP (122). Additional experiments revealed that the bacteria had to be viable and that the DNP was not "changing" the bacteria to become a more invasive or pathogenic strain. Moreover, delivery of DNP into a rat ileum caused distorted and swollen mitochondria. Thus, the metabolically stressed enterocytes responded to the commensal-derived bacterial strain in a manner reminiscent of the changes in epithelial function that are seen in IBD. Alteration of the paracellular pathway in T84 cells by DNP+*E. coli* HB101 was the result of dissociated F-actin from the peri-junctional ring

and focal condensation of F-actin and α-actinin. There was also a re-distribution or loss of ZO-1 and occludin (122).

1.4 Butyrate

1.4.1 Introduction to Dietary Fibers

Dietary fibers are non-starch polysaccharides that come from the indigestible portion of plants (e.g. psyllium husk, fruits, vegetables, oats and barley) and are classified as either soluble or insoluble fibers. Insoluble fibers, such as lignin, cellulose, and some hemicelluloses, are unable to undergo fermentation. They increase fecal bulk, which dilutes carcinogens and toxins in the colon while increasing the rate at which these toxins pass through the intestines. They also bind bile salts to decrease levels of cholesterol in the blood, which has implications for improved cardiovascular health (172, 173). Soluble fibers are not digested in the small intestine; instead, they pass into the colon where they undergo fermentation by colonic bacteria, namely *Clostridium* clusters I, III, IV, VII, IX, XIVa, XV and XVI (174). Molecules that can be fermented by bacteria include non-starch dietary fibers such as oligosaccharides, pectin, psyllium and bran as well as proteins and glycoprotein precursors in the colon (173, 175-177). The products of fermentation are SCFAs which are 2-6 carbon organic acids. The 3 main SCFAs produced in the human colon are acetate (c2), proprionate (c3) and butyrate (c4) (178), and occur in a molar ratio of 60:20:20, respectively (179). Isobutyrate (c4), valerate (c5), isovalerate (c5), and hexonate (c6) are also produced in smaller amounts in the colon (representing 5-10% of the total SCFAs) (180). The total amount of SCFAs is greatest in the proximal colon, where concentrations range from 70-140 mM and fall to 20-70 mM

in the distal colon (178). The SCFAs are rapidly taken up by the colonocyte where they are either used immediately, or passed into the blood to be circulated. Three types of cells metabolize SCFAs: colonocytes, hepatocytes and myocytes. Butyrate is almost completely metabolized in the colon while only 50% of the available acetate and proprionate are used at this location. Also, dependence on glucose metabolism becomes more important towards the distal end of the colon (180). Hepatocytes metabolize butyrate and propionate in gluconeogenesis and metabolize 50-70% of the available acetate. Muscle cells use the remaining acetate to produce energy (181).

1.4.2 Butyrate and IBD

Seventy-five percent of the oxygen consumption in the colon is attributed to butyrate metabolism (124). In fact, rat colonocytes preferentially oxidized butyrate over acetoacetate, glutamine or glucose (182). Impaired availability or utilization of butyrate can be hypothesized to play a role in the causation of IBD. For instance, it was found that butyrate oxidation was much lower in active and quiescent UC patients than in control subjects (124, 183, 184). Rats given an inhibitor of β-oxidation developed symptoms that were reminiscent of IBD including weight loss, bloody diarrhea and ulceration (185). Moreover, it appears that, in some patients with UC, the severity of disease correlates with an increase in the concentration of luminal butyrate, indicating impaired absorption (186). This may not be surprising as the transporter of butyrate can be impaired in patients with IBD. Both IBD patients and rats with dextran sodium sulfate (DSS)-induced colitis have reduced levels of MCT-1 messenger ribonucleic acid (mRNA) and protein (187). This down-regulation may be due to the pro-inflammatory

cytokines that are ubiquitous in patients with IBD, since HT-29 epithelia exposed to a combination of TNF-α and IFN-γ down-regulated transcription of the MCT-1 gene (187, 188).

1.4.3 Butyrate as a Treatment for IBD

The administration of butyrate as a treatment for IBD has been attempted in cohorts of patients with CD or UC (189, 190). Butyrate administered to patients with CD induced a positive response in some individuals with a reduction in their disease activity scores and the induction of clinical remission (191, 192). Patients who relapsed on standard treatment (2.5 g of mesalazine) were given 2 g of butyrate twice a day in an enteric-coated tablet in addition to their pre-existing medicine regime throughout an 8 week study. The butyrate treatment group experienced clinical improvements and remission. They also showed improvements in endoscopic and histological scores in the terminal ileum and cecum and a significant reduction in mucosal levels of IL-1β and NF-κB activation (193).

Topical butyrate has been used to treat patients with UC. Ten patients with refractory distal UC treated with sodium butyrate (100 mmol/L) enemas experienced decreased bowel movements, improved endoscopic and histological scores and the presence of blood in the stool ceased in 9/10 patients (194). Fifty-one patients who were refractory to topical 5-aminosalicyclic acid (5-ASA)/cortisone were placed into random groups who received 2 g of 5-ASA and a butyrate enema, or 5-ASA and a saline enema. It was found that the butyrate not only improved the overall disease activity scores, but

also accelerated the rate of improvement. Endoscopic results also improved, while the histological scores did not (189, 195-197).

SCFA enemas have also been used as a treatment. Ten patients with distal UC were treated with twice daily enemas of a SCFA mixture of: 60 mM sodium acetate, 30 mM sodium proprionate and 40 mM sodium butyrate for 6 weeks. Fifty percent of the patients experienced an improvement, although this study lacked placebo controls (198). In addition, 40 patients with mild to moderate distal colitis were given a SCFA enema of 100 mL twice a day. Overall, the SCFA group improved as indicated by a decrease in intestinal bleeding (196). Another group found that the irrigation of the colon with a SCFA enema improved endoscopic scores and enhanced cessation of rectal bleeding compared to the placebo controls during the 5 weeks that the enemas were administered (199).

The use of butyrate is not always effective as some UC patients that were treated with butyrate enemas either experienced similar or diminished levels of improvement when compared to placebo control groups (200, 201). A subsequent study performed on 13 patients with diversion colitis demonstrated that a SCFA enema made up of 60 mM acetate, 30 mM proprionate and 40 mM butyrate failed to improve both endoscopic and histological scores (202), demonstrating that butyrate treatment is not ideal for all patients.

Prebiotics are another method of delivering SCFAs to patients with IBD. Prebiotics are soluble dietary fibers which undergo fermentation by colonic bacteria. *Plantago ovata* husk is primarily a soluble fiber. The administration of the husk to quiescent UC patients maintained remission and reduced GI discomfort to similar levels

as mesalamine treated patients (203). This phenomenon could be attributed to increased butyrate production as the concentration of butyrate significantly increased in the distal colon (204). Germinated barley foodstuff (GBF) administered to patients with mild to moderate active UC used in conjunction with standard treatment (5-ASA and/or steroids) reduced mucosal damage, prevented disease relapse, improved endoscopic scores and decreased the clinical activity index when compared to the patients that received the standard treatment alone (205-208). GBF also helped to modulate the intestinal microflora to produce more *Bifidobacteria* while reducing harmful strains of *Bacteriodes* (206). However, more research needs to be done as the administration of oligofructose to patients who were undergoing elective abdominal surgery did not improvement the gut barrier function as measured by bacterial translocation (209).

1.5 Aims of Thesis Research

Based on the evidence supporting a role for butyrate in gut homeostasis coupled with the effects of metabolic stress on diminished gut integrity, **we hypothesized that increased paracellular permeability and transcellular movement of bacteria in metabolically stressed epithelium could be prevented by exogenous butyrate treatment**.

To test this hypothesis, the aims of my Masters studies were:

1- To determine if DNP mimics the metabolic state seen in some patients with IBD

2- To determine if butyrate can prevent the increased internalization of bacteria into enterocytes exposed to DNP and the increased transcytosis of bacteria across metabolically-stressed epithelia

3- To assess the mechanism by which butyrate can reduce bacterial internalization transcytosis across epithelial monolayers, concentrating on the NF-κB pathway

To address these issues I have used an *in vitro* approach employing a human colon-derived crypt-like T84 cell line. The above parameters were measured in these cells following exposure to the classic uncoupler of oxidative phosphorylation (DNP), sodium-butyrate and non-pathogenic, non-invasive laboratory strains of *E. coli* (strain HB101 or F18).

CHAPTER 2 - Materials and Methods

2.1 Cell lines, Bacteria and Reagents

Monolayers of cancer-derived human colonic epithelial crypt-like T84 (passages 42-88; ATCC, Manassa, VA) cells were maintained on plastic culture flasks at 37˚C and 5% CO_2 in an equal volume mixture of Dulbecco-Vogt modified Eagle medium (DMEM) and Ham's F-12 (Invitrogen corporation, Burlington, ON) supplemented with 10% fetal bovine serum (FBS; CanSera, Toronto, ON, Canada), 2% (vol/vol) penicillin-streptomycin, 0.6% L-glutamine and 1.9% sodium bicarbonate (Invitrogen Technologies, Burlington, ON, Canada) (T84 medium). The medium was changed every 1-2 days and the cells were passaged once a week (typically on days 6-8). One million T84 cells were seeded on transwell filter-supports with pore sizes of 0.4 μm or 3.0 μm (Costar Inc., Cambridge, MA). Medium was changed every 1-2 days in the transwells until the monolayers reached a transepithelial electrical resistance (TER) $\geq$ 750 Ω/cm^2 at which point they were deemed ready to be used in experiments (typically 6-8 days). The epithelial monolayers used in this research had starting TERs of 750-3090 Ω/cm^2. Alternatively, $2.5x10^5$ T84 cells/ml were seeded on 12 well plastic plates or 35 cm plastic dishes and allowed to grow to ~70% confluence (determined by phase contrast microscopy).

The human epithelial HT-29 (ATCC, Manassa, VA) cell line was maintained on plastic culture flasks at 37˚C and 5% CO_2 in DMEM supplemented with 5% FBS, 1% (vol/vol) penicillin-streptomycin, 0.1% L-glutamine, and 0.5% sodium bicarbonate (HT-29 medium). The medium was changed every 1-2 days and the cells were passaged once a week (typically on days 6-8). One million HT-29 cells were seeded on transwell filter-supports with pore sizes of 0.4 μm or 3.0 μm. Medium was changed every 1-2 days in

the transwells until the monolayers reached a transepithelial electrical resistance (TER) ≥ 250 Ω/cm^2 at which point they were deemed ready to be used in experiments (typically 8-12 days).

The human THP-1 monocytic cell line (ATCC, Manassa, VA) was grown in suspension at 37˚C and 5% CO_2 in RPMI-1640 medium (Invitrogen Inc., Burlington, ON) supplemented with 2% (vol/vol) penicillin-streptomycin, 10% FBS and 36 µM 1.5% *N*-2-hydroxethyl-piperazine-*N*'-2-ethanesulfonic acid (HEPES; Invitrogen Life Technologies, Burlington, ON, Canada) (THP-1 medium). The cells were seeded onto 6 well tissue culture plates (Sarsted Inc., Montreal, QC) at $5x10^5$ cells/well. They were then differentiated into a macrophage-like phenotype through the addition of Phorbol 12-myristate 13-acetate (PMA; 10nM, Sigma-Aldrich, Oakville, ON). Seventy-two h later, the medium was replaced with antibiotic-free THP-1 media and the cells were allowed to rest for 24 h followed by treatment.

Escherichia coli strains HB101 and F18 (obtained from Dr. Philip Sherman, University of Toronto, Toronto, ON) were inoculated for experiments in 10 ml of Luria Bertani (LB) broth (BD Biosciences, Missisauga, ON) in a 50 ml tube and placed in an orbital shaker incubator (Forma Scientific, Marietta, OH) rotating at 250 rpm and heated to 37°C for 15 h. Following that, the bacteria were pelleted through centrifugation at 2500 rpm for 15 minutes and re-suspended in fresh antibiotic-free T84 medium. The optical density (OD) was determined using a Victor3V spectrophotometer (595 nm; PerkinElmer, Waltham, MA) where 1.0 OD unit equals 10^{10} colony forming units (cfu)/ml. The absorbency reading does include dead *E. coli*; however this measurement

has been standardized by our laboratory through dilution analysis every 4 months. The bacteria were then diluted to approximately 10^6 cfu/ml.

Salmonella typhimurium were generously donated by Dr. Mike Surrette (University of Calgary, Calgary, AB). *S. typhimurium* were grown overnight for 15 h in the orbital shaker at 250 rpm (37°C) in LB broth. After this time, a 1:33 dilution in LB broth was done and the *S. typhimurium* were shaken for an additional 3 h so that the bacteria would be in the late log phase of growth, which is when they would be expressing the majority of their invasive genes. One ml of the *S. typhimurium* culture was then centrifuged for 2 minutes at 7000 rpm. The supernatant was removed and the bacteria were re-suspended in 1 ml of antibiotic-free T84 medium.

A 10 mM 2,4-dinitrophenol (DNP, from Sigma Chemical Co., St. Louis, MO) solution was prepared by doing a 1:10 dilution of a 100 mM DNP solution (made by adding 0.1841g DNP into 10 ml of absolute ethanol) into 70% ethanol. Adding 10 µl of the 10 mM solution into 1 ml of media produced a working concentration of 0.1 mM. DNP at a concentration of 0.1 mM was previously reported by our laboratory to be non-toxic to *E. coli* HB101, but still induced metabolic stress in T84 cells (122). Sodium-butyrate (Sigma Aldrich) was kept in 500 µl aliquots of 500 mM in the -20°C freezer. Butyrate concentrations that were used in the experiments ranged from 0.1-100 mM, although the majority of experiments were performed using 3 mM butyrate. Lipopolysaccharide (LPS; 1 µg/ml, Sigma Aldrich) and tumor necrosis factor-α (TNF-α; 10 ng/ml; R&D Systems, Minneapolis, MN) were both used as positive controls. 3-O-methyl-D-glucopyranose, glucose and mannitol were all prepared in antibiotic free medium to give a 25 mM working concentrations and were all sterile-filtered before use

(all from Sigma). Conditioned media collected from the butyrate-producing bacterium *Fusobacteriaum gonidiaformans* strain 21115R, was sterile-filtered and frozen in aliquots in the -80°C freezer until needed (a gift from Dr. Emma Allen-Vercoe, Guelph University, Guelph, ON).

2.2 Measurement of Transepithelial Electrical Resistance and Bacterial Translocation

One million T84 cells added to tissue culture-treated semi-permeable transwell support filters were grown until they reached a consistent TER of 750 Ω/cm^2 or greater (typically resulting in values $\geq$1000 Ω/cm^2) as measured with a voltmeter and associated chop-stick electrodes (Millicell-ERS; Millipore, Bedford, MA). Once confluent on the transwells, a new culture plate was obtained. One ml of antibiotic-free medium was added to the outer well. The filters were then transferred from the original plate to the new plate and 0.5 ml of antibiotic-free medium was added to the inner well (i.e. the apical side of the cells). Then, 0.1 mM DNP, and 5 µL (i.e. 10^6 cfu/ml) of *E. coli* HB101 or F18 were simultaneously added to the apical side of the cells in addition to butyrate (3 mM). The treated T84 cell monolayers were incubated at 37°C in 5% CO_2 for up to 72 h. The controls were as follows: 1) time-matched naïve monolayers 2) butyrate only 3) *E. coli* HB101 or *E. coli* F18 only 4) *E. coli* HB101 or *E. coli* F18 and DNP 5) butyrate and *E. coli* HB101 or *E. coli* F18. The last treatment was the test condition and consisted of butyrate, *E. coli* HB101 or *E. coli* F18 and DNP (Figure 3). TER was examined before the experiments began, then at 2, 4, 6, 8, 12, 16 and finally 24 h post-treatment. TER was used as a measurement of the integrity of the tight junctions of the cells, which directly

correlated with paracellular permeability. Data were expressed as a percentage of the pre-treatment TER values. The same protocol was followed using HT-29 cells, only confluent monolayers were assumed to be present when the TER reached 250 Ω/cm^2. Also, only varying amounts of butyrate was added (1 mM-6 mM) was added to the cell monolayers and TER was assessed at 2, 4, 6, 8, 12, 16 and 24 h post-treatment and data were expressed as a percentage of the pre-treatment TER.

Translocation was assessed simultaneously with TER (i.e. 2, 4, 6, 8, 12, 16 and 24 h post-treatment). To do so, 10 µL aliquots were taken from the basolateral compartment of the transwell (the outer well) and then plated onto an LB agar plate. The aliquot was spread over the surface of the plate using a Lazy-L-Spreader™ (Cole-Parmer, Montreal, QC). The plates were incubated at 37°C and 5% CO_2 for 24 h post-collection. The LB agar plates were then examined and bacterial colonies were counted, if present. A scale was established based on the number of bacterial colonies counted to semi-quantitatively judge the amount of bacteria present (210) (Table 3).

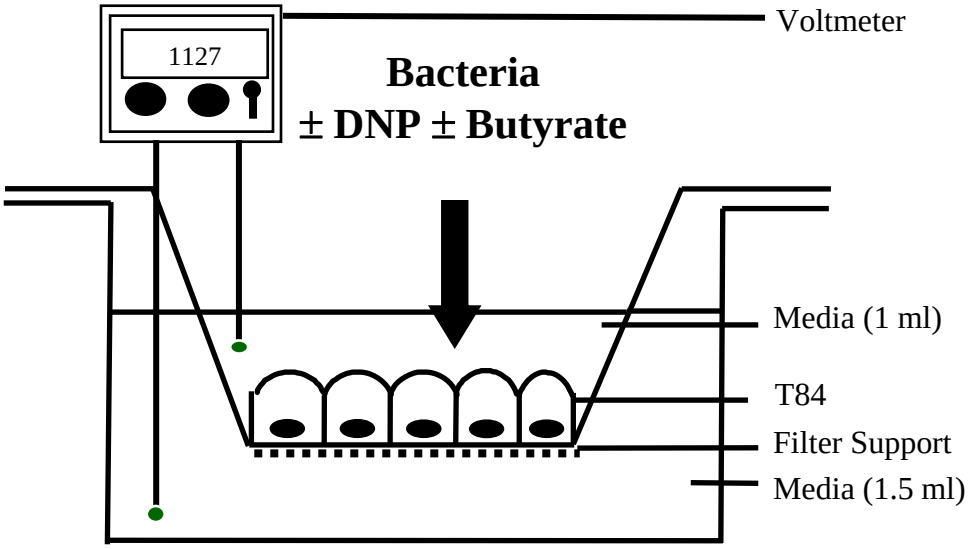

Figure 3. Schematic of the experimental set-up. One million T84 colonic cancer-like crypt derived epithelial cells were seeded on a 0.4 or 3.0 μm pore transwell support filter and were allowed to grow to confluence (reaching a TER > 750 Ω/cm^2 on day 6, 7, 8). In the apical portion of the transwell support filter (representing the lumen of the gut), 0.1 mM of DNP, 3 mM of butyrate and 10^6 *E. coli* HB101/F18/*Salmonella typhimurium* were added to antibiotic free media. All treatments were added simultaneously.

Bacteria Visualized on the Agar Plate (Number of colonies)	**Corresponding Scale**
0	0
1-10	1
10-100	2
>100	3
Uncountable, however individual colonies were visible	4
Bacterial lawn	5

Table 3. Arbitrary unit assignment for bacterial growth on agar plates.

2.3 Bacterial Growth Curves

To determine if butyrate was killing bacteria, *E. coli* HB101 or *E. coli* F18 (10^6 cfu) were incubated with LB broth or LB broth+butyrate (3 mM), and the bacteria were placed in the orbital shaker incubator at 250 rpm at 37°C. Samples were taken and the OD was measured at 2, 4, 6, 14 and 24 h.

2.4 Internalization Assays

Semi-confluent monolayers of T84 cells were grown in 12 well plates and inoculated with *E. coli* HB101, *E. coli* F18 or *S. typhimurium* (10^6 cfu/ml)±DNP (0.1 mM)±butyrate (3mM) and were incubated for 4 h at 37ºC. Semi-confluent monolayers were used instead of confluent monolayers to prevent overgrowth and death of the cells during the incubation period of the assay. A sample of the media at 4 h post-treatment was collected and a log-fold serial dilution was performed. Three 10 µl aliquots from each dilution for each condition were pipetted onto LB agar plates that were then incubated overnight at 37°C and 5% CO_2. Meanwhile, the T84 cell monolayers were washed twice with room temperature sterile phosphate buffered saline (PBS) and were treated with gentamicin (200 µg/ml, diluted in T84 media; Sigma Chemical Co.) for 1.5 h, 4 h, 8 h or 24 h. To be certain that the extracellular bacteria had been killed, 3 samples (10 µl) from randomly selected wells after the gentamicin treatment were plated onto an LB agar dish labeled as "Test plate" and were placed in an incubator overnight. After that, the epithelia were rinsed with sterile PBS and lysed with 1.0 ml of 0.75% Triton X-100/PBS (20 minutes at 4ºC). Samples from the lysed T84s underwent log-fold dilutions and then were pipetted onto LB agar plates and were incubated overnight (37°C and 5%

CO_2). After the overnight incubation period, all plates were removed from the incubator. The experiment was discarded if the "Test plate" had any visible bacterial colonies growing on it. The dilution that had between 20-100 bacterial colonies present on the agar dish per aliquot was used for the enumeration of the bacteria. Using that selected dilution, the average number of bacterial colonies of the 3 aliquots was calculated. The total number of extracellular and intracellular bacteria for each condition was then calculated by multiplying the average number of bacterial colonies by the dilution factor by the total volume of media or Triton-X used in the wells divided by the 10 µl aliquot sample. The number of internalized, viable bacteria was determined and presented as a percentage of the number of external bacteria.

2.5 <u>Western Blotting</u>

Cells were grown and treated with butyrate only, *E. coli* HB101 (10^6 cfu/ml) only, butyrate (3 mM)+*E. coli* HB101, DNP (0.1 mM)+*E. coli* HB101, butyrate+DNP+*E. coli* HB101 on transwell filters. PMA-differentiated THP-1 cells grown on 12 well plastic plates were treated with LPS (1 µg/ml) and used as a positive control. Cells were rinsed twice in 4°C PBS and then lysed with 80 µl ice-cold lysis buffer (20 mM Tris [pH 7.5], 150 mM NaCl, 1 mM EDTA, 1 mM EGTA, 1% Triton X-100, 2.5 mM sodium pyrophosphate, 1 mM $NaVO_3$; all from Sigma Aldrich) and a complete protease inhibitor complex (Roche, Indianapolis, IN), scraped from the filters and collected. Extracts were then frozen at -80˚C for 24 h. The samples were removed from the freezer and thawed on ice. They were then sonicated twice for 10-seconds (Microson™ Ultrasonic Cell Disruptor, SPI supplies, West Chester, PA). Lysates were clarified through

centrifugation (13,000 rpm for 5 minutes at 3˚C) and protein concentrations were determined using the Bio-Rad/Bradford assay (Bio-Rad, Hercules, CA). Briefly, samples underwent a 1:4 dilution in distilled water (dH_2O) and 10 µl were added in duplicate to a 96 well plate. Bovine serum albumin (BSA) standards underwent a two-fold serial dilution seven times to prepare a standard curve that ranged from 1.0-0.0156 mg/ml. Ten µl of each dilution was added in duplicate to the 96 well plate. Two hundred µl of the acidic Coomassie® Brilliant Blue G-250 dye was added to all samples and standards in the 96 well plate (including a dH_2O blank) and incubated at room temperature for 5 minutes. During this time, the dye bound to basic and aromatic amino acids (211), which induced a color change of the dye to varying degrees depending upon the concentration of the proteins that were present in the samples (212). The absorbance was read at 595 nm and protein concentrations were determined (213). Four µL of sodium dodecyl sulfate (SDS) loading buffer (2% SDS, 50 mM Tris-HCl,100 mM dithiothreitol, 1% bromophenol blue, 5% glycerol; all from Sigma-Aldrich) was added to 40 µg of protein from each sample. The samples and SDS loading buffer mixtures were then placed in a boiling water bath for 5 minutes to denature the proteins. They were then loaded into a SDS-10% polyacrylamide gel and run for 2.5 h at 100 V for all blots except for the Cullin-1 and NEDD8 experiments, which were run for 5 h at 100 V in SDS-8% polyacrylamine gels. The separated proteins were electroblotted to polyvinylidene difluoride membranes (PVDF; VWR, Mississauga, Ontario, Canada) overnight at 30 V at 4˚C. The PVDF membranes were blocked the following day with 5% nonfat Carnation™ powdered milk in Tris-biffered saline/0.1% Tween-20 (TBST; reduces non-specific antibody binding) or 5% BSA-TBST (if examining a phospho-protein) for 2 h at room

temperature. The blots were then washed three times with TBST (vigorously shaken for 7 minutes each time). The administration and incubation of primary antibodies followed (see Table 4 for specific details). Membranes were washed three times with TBST (vigorously shaken for 7 minutes each time) and then incubated with the appropriate secondary antibody (see Table 4 for specific details). The blots were then washed 5 times for 5 minutes in TBST and once in PBS for 5 minutes. The immunoreactive proteins were visualized by using enhanced chemiluminescence (Amersham Pharmacia, Piscataway, NJ) and exposed to Kodak XB-a film (Eastman Kodak company, Rochester, NY). It should be noted that after the phospho-proteins had been visualized (e.g. p-IκB-α), the PVDF membrane was stripped of the primary and secondary antibodies. This was done by adding 10 ml of Stripping buffer (0.76 g Tris, 2 g SDS, 700 µl 2-mercaptoethanol, 100 ml dH_2O, pH 7.4) to the PVDF membrane. The membrane and Stripping buffer were placed in a 50 ml conical tube, heated to 65 ^oC and rotated for 10 minutes at that temperature (VWR Hybridization Oven, West Chester, PA). The blots were then washed twice with TBST for 5 minutes and once with dH_2O for 5 minutes. The PVDF membranes were blocked again for 2 h at room temperature, and then probed for total protein levels (e.g. IκB-α) as described above. Density of the bands was calculated using Image J. Density was expressed as phospho-protein/total protein (arb. units).

Protein	Primary Antibody [dilution]	Primary Antibody Incubation Time and Temperature	Source of Primary Antibody	Secondary Antibody	Secondary Antibody [dilution]	Secondary Antibody Incubation Time and Temperature	Source of Secondary Antibody
p-IκB-α monoclonal	1:1000	1 h at room temperature	Santa Cruz Bio-technology, Santa Cruz, CA	Goat anti-mouse IgG-HRP	1:10000	1 h at room temperature	Santa Cruz Biotechnology, Sanra Cruz, CA
IκB-α polyclonal	1:1000	1 h at room temperature	Santa Cruz Bio-technology, Santa Cruz, CA	Goat anti-rabbit IgG-HRP	1:5000	1 h at room temperature	Santa Cruz Biotechnology, Sanra Cruz, CA
IKK-β polyclonal	1:1000	1 h at room temperature	Cell Signaling Technology, Beverly, MA	Goat anti-rabbit IgG-HRP	1:7000	1 h at room temperature	Santa Cruz Biotechnology, Sanra Cruz, CA
p-IKK-β monoclonal	1:1000	1 h at room temperature	Cell Signaling Technology, Beverly, MA	Goat anti-rabbit IgG-HRP	1:7000	1 h at room temperature	Santa Cruz Biotechnology, Sanra Cruz, CA
Cullin- 1 polyclonal	1:1000	Overnight at 4^{o}C	Zymed Laboratories, San Francisco, CA	Goat anti-rabbit IgG-HRP	1:7000	Overnight at 4^{o}C	Santa Cruz Biotechnology, Sanra Cruz, CA
NEDD8 polyclonal	1:1000	Overnight at 4^{o}C	Zymed Laboratories, San Francisco, CA	Goat anti-rabbit IgG-HRP	1:7000	Overnight at 4^{o}C	Santa Cruz Biotechnology, Sanra Cruz, CA
Cleaved Caspase-3	1:1000	1 h at room temperature	Cell Signaling Technology, Beverly, MA	Goat anti-rabbit IgG-HRP	1:5000	1 h at room temperature	Santa Cruz Biotechnology, Sanra Cruz, CA
Caspase-3	1:1000	1 h at room temperature	Cell Signaling Technology, Beverly, MA	Goat anti-rabbit IgG-HRP	1:5000	1 h at room temperature	Santa Cruz Biotechnology, Sanra Cruz, CA

Table 4. The primary and secondary antibodies used in immunoblotting experiments.

2.6 Enzyme-Linked Immunosorbent Assay (ELISA) for IkB

A p-IκB ELISA kit was purchased from Invitrogen Molecular Probes and the manufacturer's protocol was followed. Briefly, T84 cells were grown on transwell filters and incubated for 4 h with antibiotic free media only, 0.1 mM DNP+*E. coli* HB101 (10^6 cfu/ml), or butyrate (3 mM)+*E. coli* HB101+DNP. T84 cells were also exposed to 10 ng/ml TNF-α (R&D Systems Inc) for 24 h to serve as a positive control. The samples were then rinsed twice in cold PBS and lysed with 80 µl ice-cold lysis buffer (20 mM Tris [pH 7.5], 150 mM NaCl, 1 mM EDTA, 1 mM EGTA, 1% Triton X-100, 2.5 mM sodium pyrophosphate, 1 mM $NaVO_3$) containing complete protease inhibitor complex, scraped from the filters and collected. They were then frozen at -80˚C for 24 h. The samples were removed from the freezer, thawed on ice and then sonicated twice for 10 seconds. Lysates were clarified through centrifugation (13,000 rpm for 5 minutes at 3˚C). Fifty µl of samples (added neat) and p-IκB-α standards (ranging from 0-100 Units/ml) were individually co-incubated with 50 µl rabbit anti-p-IκB-α overnight (14-18 h) at room temperature on the provided p-IκB-α antibody coated 96 well plate . The following day, the plates were then washed 4 times with the provided wash buffer, incubated for 30 minutes with 100 µl anti-rabbit IgG-HRP, washed four more times, then 100 µl tetramethylbenzidine (a stabilized chromogen) was added and incubated in the dark at room temperature for 30 minutes after which time 100 µl Stop Solution was added to all wells. The OD was determined spectrophotometrically at 450 nm using a microplate reader (Perkin-Elmer, Waltham, MA).

2.7 Transmission Electron Microscopy (TEM)

T84 cells were seeded into 35 cm Petri dishes and grown to ~70% confluence. The cells were incubated at 37°C and 5% CO_2 for 6 h with *E. coli* HB101 (10^6 cfu)±DNP (0.1 mM)±butyrate (3 mM), TNF-α (10 ng/ml)±LPS (*E. coli*-derived 1 μg/ml; Sigma Chemical Co.). The cells were then rinsed with 0.1 M cacodylate buffer, pH 7.4 and fixed with 1.6% paraformaldehyde and 2.5% glutaraldehyde in 0.1 M cacodylate buffer, pH 7.4 overnight at 4˚C. After washing 3 times with 0.1 M cacodylate buffer, pH 7.4, the cells were post-fixed with cacodylate buffered 1% osmium tetroxide for 1 h at room temperature. Cells were then dehydrated through graded acetone and embedded in Epon mixture. After polymerizing, the hardened Epon layer containing the embedded cells was separated from the plastic culture dish. Under a light microscope a representative area was selected, trimmed and glued to a resin stub for sectioning. Ultra thin sections (0.1 μm) were cut with a diamond knife on an ultramicrotome (Ultracut, Reichert-Jung, Vienna, Austria) and collected on single hole grids with Formvar supporting film. The sections were stained with 2% aqueous uranyl acetate and Reynolds's lead citrate and observed under a Hitachi H-7650 TEM (Pleasanton, CA) at 80 kV. The images were acquired with an AMT16000 digital camera mounted on the microscope. Images (6-15/monolayer) were captured and pictures were analyzed by an observer blinded to the experimental conditions. The length of pseudopodial extension/20 μm of plasmalemma was counted and calculated. The processing was performed by Wei Dong and I thank him for his assistance.

2.8 MTT Assay

The 3-(4,5-dimethyl-thiazol-2-yl)-2,5-diphenyltetrazoliumbromide salt (MTT) assay examines mitochondrial activity. MTT is a water soluble salt that produces a yellow colour when it is dissolved in phenol red-free medium. Mitochondrial dehydrogenase converts the MTT molecule into water-insoluble purple formazan. The formazan is soluble in isopropanol and when the alcohol is added to the cultures, colour changes may be measured spectrophotometrically to determine the concentration of the formazan, providing an indication of the level of mitochondrial activity (214). 1 $x10^5$ T84 cells/well were seeded in a 96 well and were grown to confluence. The cells were exposed for 2, 4 and 24 h to butyrate (3 mM), DNP (0.1 mM), butyrate+DNP or 5 μM staurasporine. After the treatment period, the cells were washed with phenol-free RPMI medium, supplemented with 10% FBS and 36 μM HEPES. Following 4 h of incubation with 100 μl MTT (0.5 mg/ml) at 37˚C, the medium was replaced with 50 μl acidic isopropanol (0.04 N HCL in absolute isopropanol). Absorbance was then measured at 595 nm and results expressed in arbitrary units. I would like to thank Femke Lutgendorff for performing the MTT assay.

2.9 Cell Viability

To test for apoptosis, DNA laddering was assessed. The cells were seeded in 12 well plastic plates and were treated with butyrate (3 mM), DNP (0.1 mM), *E. coli* HB101 (10^6 cfu), *E. coli*+butyrate, *E. coli*+DNP and *E. coli*+DNP+butyrate for 24 h. Twenty-four h staurosporine (5 μM)-treated T84s served as a positive control. The cells were collected and then centrifuged at 800 rpm for 5 minutes. They were then re-suspended in

sterile PBS and centrifuged again. The supernatant was aspirated and the cells were frozen in the -20°C freezer overnight. A TE buffer was then prepared using 10 mM TRIS and 1 mM EDTA, and 0.5 ml was added to each sample. The tubes were vortexed twice for 5 seconds each time to lyse the cells and cause the release of DNA. The cells were then placed in a boiling water bath for 5 minutes. After, the samples were centrifuged (13000 rpm for 10 minutes) and the supernatant was collected. The amount of DNA was quantified spectrophotometrically using Nanodrop (Thermo Scientific, Wilmington, DE). A 2.5% agarose gel was made and 0.5 µg/ml of ethydium bromide was added to the gel before cooling occurred. One µl of 10x loading dye was added to the samples. The samples were then run on the gel at 80 V for 3 h. A picture was then taken (SynGene G Box, Synoptics Ltd.).

Lactate dehydrogenase (LDH) is a stable cytosolic enzyme that is released upon cell lysis. Released LDH in a culture medium can be measured in a colorometric assay. The amount of LDH is nessesary to convert tetrazolium salts into a red formazan product, which can then be measured. The amount of LDH released into the cytosol was determined using the manufacturer's instructions (CytoTox96® Non-Radioactive Cytotoxicity Assay, Promega Corp., Madison, WI, USA). Briefly, T84 cells were seeded in a 96 well plate and when confluent, *E. coli* HB101 (10^6 cfu)±DNP (0.1 mM) treatments were administered to the cells for 24 h. The cells were then lysed and the plate was centrifuged at 250*g* for 4 minutes. Fifty µl aliquots extracted from all wells were transferred to a new 96 well plate and were incubated with 50 µl of the provided Substrate Mix. The plate was then incubated for 30 minutes, 50 µl/well of Stop Solution was added and the absorbance was recorded at 490 nm. Staurosporine treated cells (5

μM, 24 h) were used as a positive control. I would like to extend my gratitude to Van Phan for performing the LDH assay.

2.10 Semi-Quantitative Real Time Polymerase Chain Reaction

Gene expression of ATP synthase, NADH Coenzyme Q and Succinate dehydrogenase was determined in pinch biopsies taken from the inflamed or non-inflamed areas of the ascending colon of patients with CD and colon cancer patients by semi-quantitative real time polymerase chain reaction (PCR). The tissue samples were provided by the IBD tissue bank at the University of Calgary. Following homogenization of the tissue, total ribonucleic acid (RNA) was extracted from the tissue homogonates using the TRIzol method as directed by the manufacturer (Invitrogen Inc). RNA was quantified spectrophotometrically using the Nanodrop and 1 μg of the RNA was used to make cDNA by using an iSCRIPT reverse transcription kit (Bio-Rad Laboratories, Hercules, CA). The reaction protocol consisted of a 5 minute incubation at 25˚C, 90 minutes at 42˚C, and lastly 5 minutes at 80˚C. The Primer 3 program (http://frodo.wi.mit.edu/cgi-bin/primer3/primer3_www.cgi) was used to design the primers for human β-actin (housekeeping gene), human NADH Coenzyme Q, human ATP synthase and human Succinate dehydrogenase (Table 5). Spidey (www.ncbi.nlm.nih.gov/IEB/Research/Otell/Spidey/) was used to examine the intron/exon boundaries while ePCR (www.ncbi.nlm.nih.gov/sutils/e-pcr/) on the NCBI website was used to verify primer accuracy. Real time PCR was done on the Eppendorf Mastercycler realplex^2 reader (Eppendorf, Mississauga, ON) using 10 μl of 2x Bio-Rad iQ Sybr Green Supermix, 1 μl cDNA, primers (300 μM) and add dH_2O was added to give

a total volume of 20 µl. The reaction protocol consisted of a 2 minute activation at 95˚C, 95˚C for 15 seconds denaturing step, 55˚C for 15 seconds annealing step and a 68˚C for 20 seconds extension step. A melting curve analysis was then performed to ensure the primer specificity (95˚C for 15 seconds, 60˚C for 15 seconds and 20 minutes of slowly ramping the temperature). 40 cycles were completed and the computer derived threshold was used. The reciprocal of the difference between the gene of interest and β-actin was determined and averaged from 4 different patients for each gene and condition to determine the relative expression of the gene of interest. Thank you to Dave Prescott and Matthew Klompus for assisting in the primer design and real time PCR execution.

Gene	Forward	Reverse
Human β-actin	GGACTTCGAGCAAGAGATGG	AGCACTGTGTTGGCGTACAG
Human NADH Coenzyme Q	CCACCATCAACTACCCGTTC	AAGCCGCAGTAGATGCACTT;
Human ATP Synthase	GCAGATTTTGGCAGGTGAAT	AGGGGCAAGGAGAGAGACA
Human Succinate dehydrogenase	GCTGCAACAGTGTGTGACCT	GCTGCAACAGTGTGTGACCT

Table 5. The primers used for semi-quantitative real time PCR.

2.11 Data Presentation and Analysis

Data for TER, bacterial internalization, densitometry and spectrophometric analysis are presented as the mean ± standard error of the mean (SEM), where n values represent the number of individual epithelial monolayers from a certain number of indicated experiments. Statistical analysis of variance was done using a one-way ANOVA followed by a post-hoc Tukeys test for pair-wise comparisons. Data from bacterial translocation studies were assessed using Pearson- chi^2 analysis as data was binomial, non-parametric and non-linear. The Pearson-chi^2 test examined the p-value, and the null hypothesis (being that the level of translocation a monolayer experienced was independent of the treatment) was either accepted or rejected. If rejected, the phi^2 value was then examined to determine if there was a statistic correlation between the treatment and level of translocation. If there was a correlation between the treatment level and level of translocation, the p-value for each level of translocation was then assessed using a chi-goodness of fit test. A statistically significant difference was accepted at $p<0.05$. To determine linear correlation, the Pearson coefficient was calculated. Thank you to Emmanuel Thompson for all of his assistance in the statistical analysis and interpretation of the translocation data.

CHAPTER 3 – Results

3.1 DNP Disrupted Mitochondrial Structure Which was Further Exaggerated by the Addition of Commensal Bacteria

The chemical 2,4-dinitrophenol (DNP; 0.1 mM) was used *in vitro* to model the mitochondrial dysfunction observed in patients with IBD since DNP is known to inhibit oxidative phosphorylation and halt ATP synthesis. Crypt-like colonic T84 cell monolayers were exposed to DNP for 6 h, fixed and processed for transmission electron microscopy (TEM). Micrographs revealed that DNP-treated cells displayed increased mitochondrial swelling (Fig 4A) as compared to control cells (Fig 4B). This was not surprising as we have previously reported that DNP decreased ATP levels in T84 cells at 24 h post-treatment, which confirmed the ability of DNP to perturb mitochondrial function (15). The metabolically stressed T84 cells had a significant increase in the number of pseudopodial extensions of 0.5-1.0 μm and >1 μm in length (Fig 4C). These changes were not present in T84s treated with non-pathogenic, non-invasive *E. coli* (strain HB101, 10^6 cfu) (Fig 4D). However, co-incubation of *E. coli* HB101 with DNP caused a statistically significant exaggeration (i.e. ~20-fold increase over control levels) in the number of pseudopodial extensions of both sizes compared to DNP-only treated cells (Fig 4C and 4E). The membrane morphological changes were not NF-κB driven as TNF-α+LPS (10 ng/ml and1 μg/ml, respectively; combination activates the NF-κB pathway; Fig 4F) did not induce an increase in the number of pseudopodial extensions of either size in the cells. Interestingly, the addition of butyrate (3 mM) to T84s exposed to *E. coli* HB101+DNP was able to significantly prevent not only the increase in pseudopodial extensions of both sizes (Fig 4C), but also the appearance of swollen

mitochondria. The mitochondria were smaller, rounded and had a cytoplasmic enclosure, which is indicative of mitochondrial regenesis or prevention of injury(Fig 4G).

A: DNP

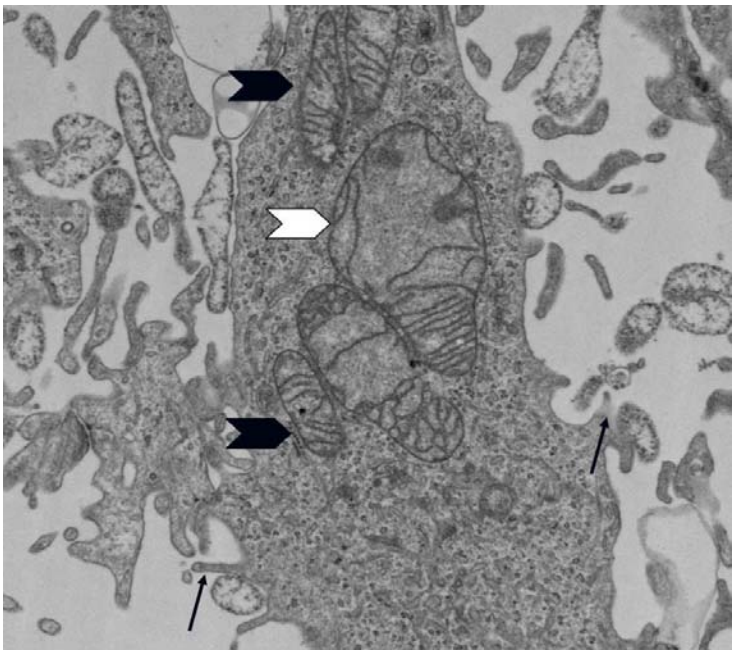

B: Control

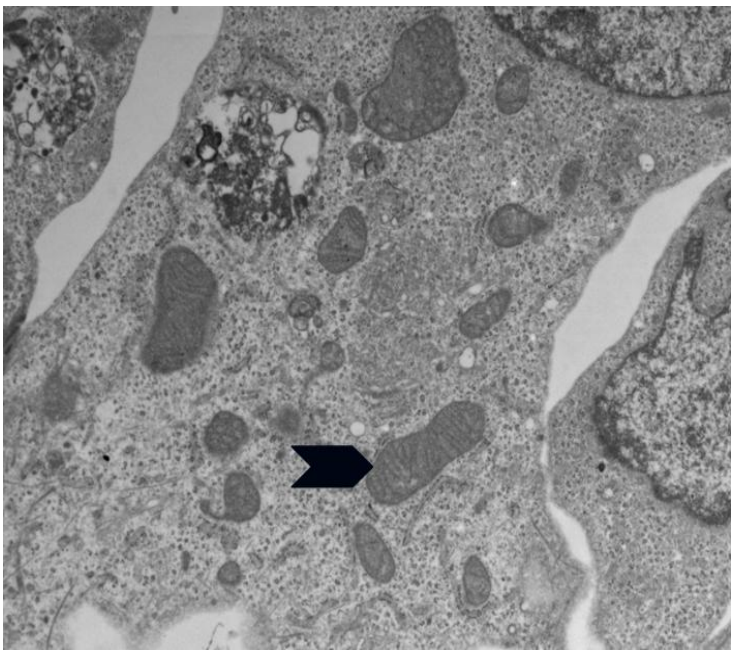

C

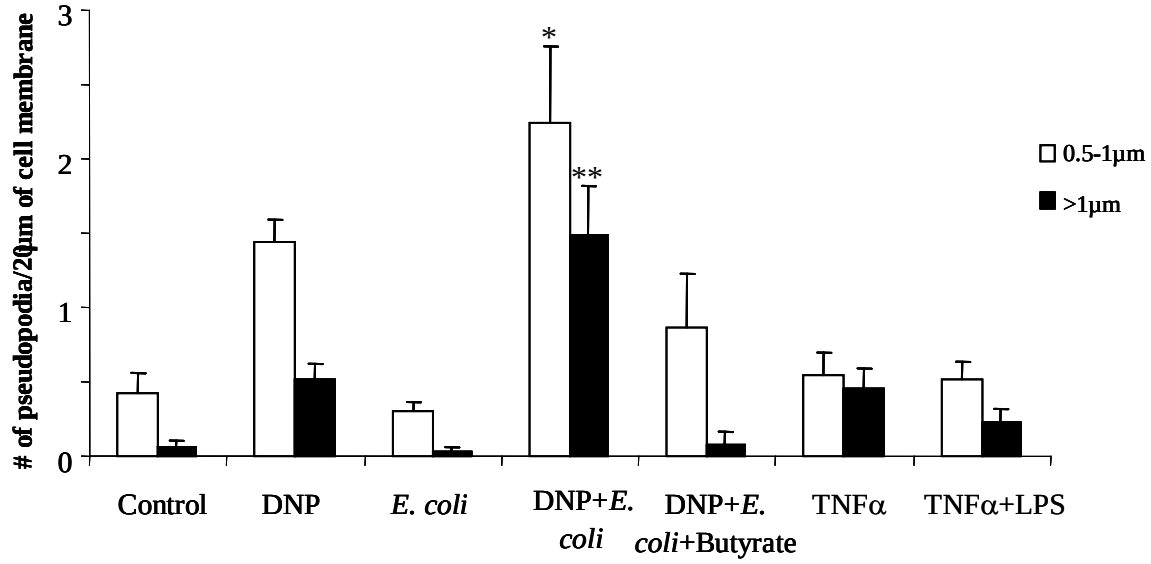

D: *E. coli* HB101

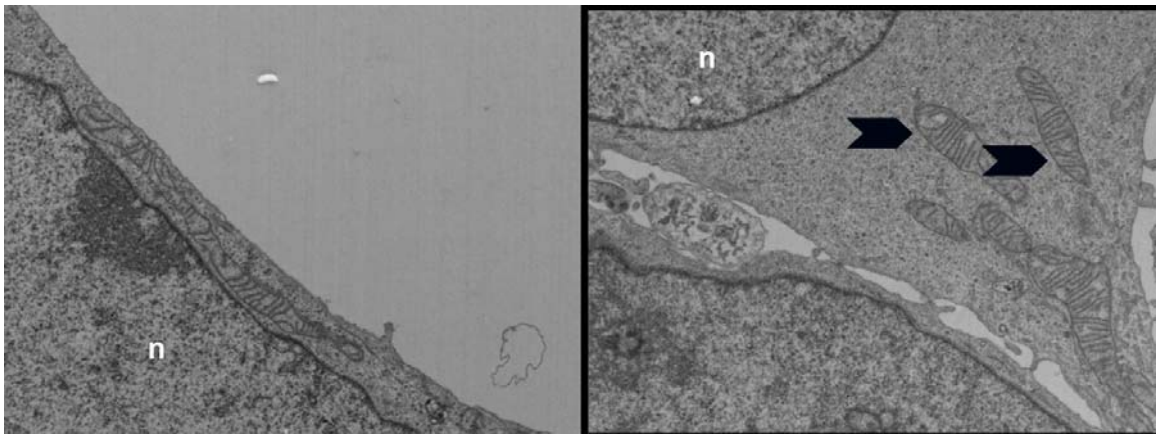

E: DNP+*E.coli* HB101

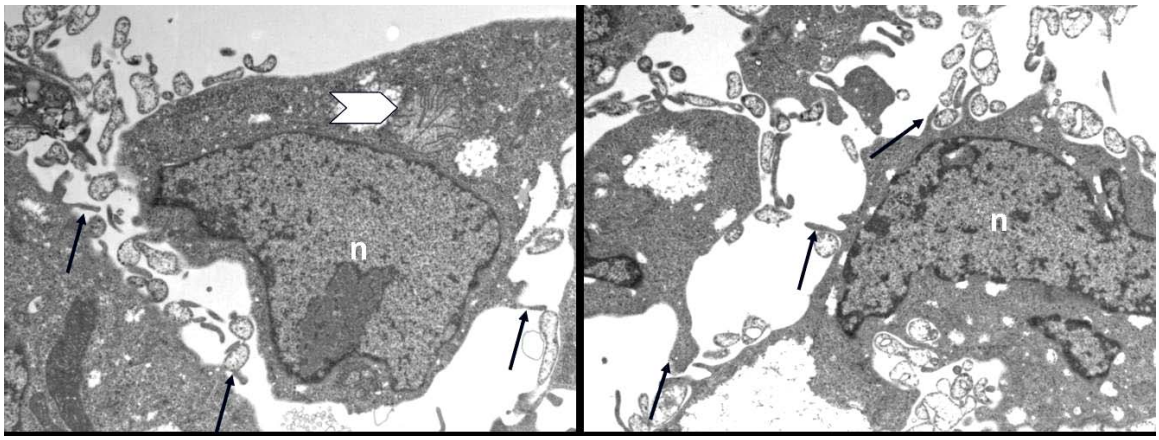

F: TNF-α+LPS

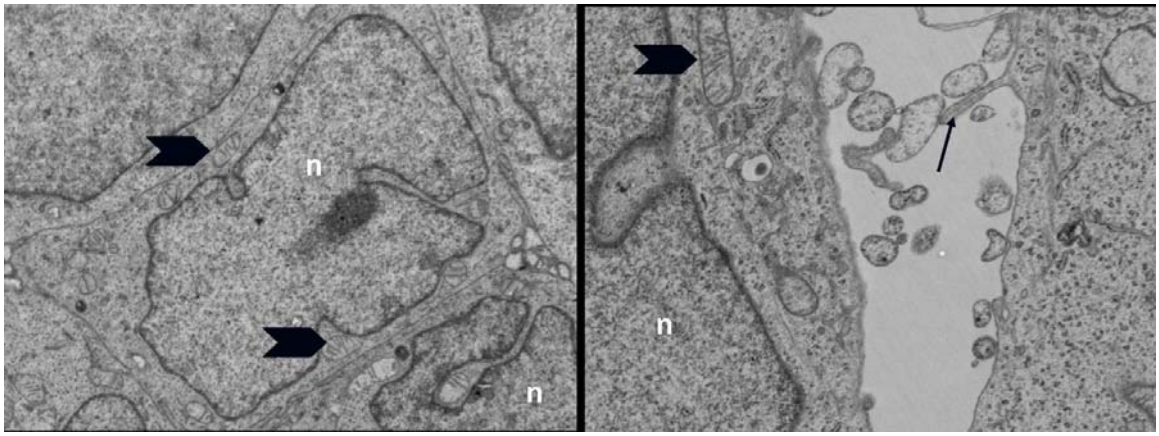

G: DNP+*E. coli* HB101+Butyrate

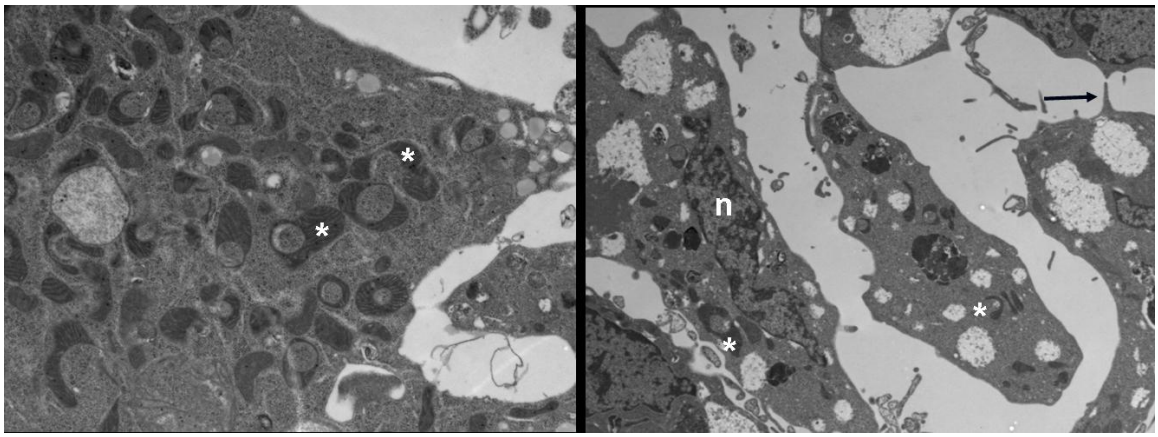

Figure 4. Transmission electron microscopy (TEM) revealed that DNP caused mitochondrial dysfunction which was enhanced by the presence of commensal bacteria but prevented by the addition of butyrate. T84 crypt-like colonic monolayers grown to 70% confluence on plastic culture plates were treated for 6 h, fixed and then prepared for microscopy. TEM images of DNP (0.1 mM)-treated T84 cells (panel A) showed swollen mitochondria and disrupted cristae compared to control cells (panel B). The DNP also caused an increase in the number of pseudopodial extentions, which augmented significantly in both number and length upon the addition of *E. coli* HB101 (10^6 cfu) to the culture media (panel C). DNP+*E. coli* treated T84s also had enlarged mitochondria (panel E) compared to *E. coli* HB101 alone, which did not induce membrane ruffling or mitochondrial swelling (panel D). Butyrate (3 mM) prevented pseudopodial extension formation/mitochondrial swelling and induced mitochondrial regeneration (panel G). The mitochondrial swelling and pseudopodial formation was not due to NF-κB activation as TNFα+LPS (10 ng/ml and 1 μg/ml, respectively; panel F) failed to induce the same morphological changes that DNP did. Images are representative of 3 monolayers per condition (10-20 sections/T84 cell monolayer; *,

p>0.05 compared to control **, p>0.01 compared to control; data are represented as mean±SEM; black arrowheads depict normal mitochondria, white arrowheads highlight swollen mitochondria with irregular cristae, black arrows point to pseudopodial extensions, N= nucleus and * =putative regenerating mitochondria).

3.2 Metabolic Stress was Alleviated Through the Addition of Butyrate to Culture Medium

The 3-(4,5-Dimethylthiazol-2-yl)-2,5-diphenyltetrazolium bromide (MTT) assay was used to assess mitochondrial function. The addition of 0.1 mM DNP to T84 cells significantly reduced mitochondrial activity at 24 h, but not at 2 or 4 h as assessed by OD readings at 595 nm wavelengths. In fact, DNP reduced the cleavage of the MTT (and hence inhibited proper mitochondrial function) to comparable levels of the PKC inhibitor and inducer of apoptosis, staurospaurine (5 μM), which was used as a positive control. Butyrate (3 mM) when added by itself to the culture media did not increase the rate of cleavage of MTT at 24 h. However, co-incubation of butyrate with DNP prevented part of the DNP-induced mitochondrial dysfunction as gauged by MTT cleavage (Figure 5).

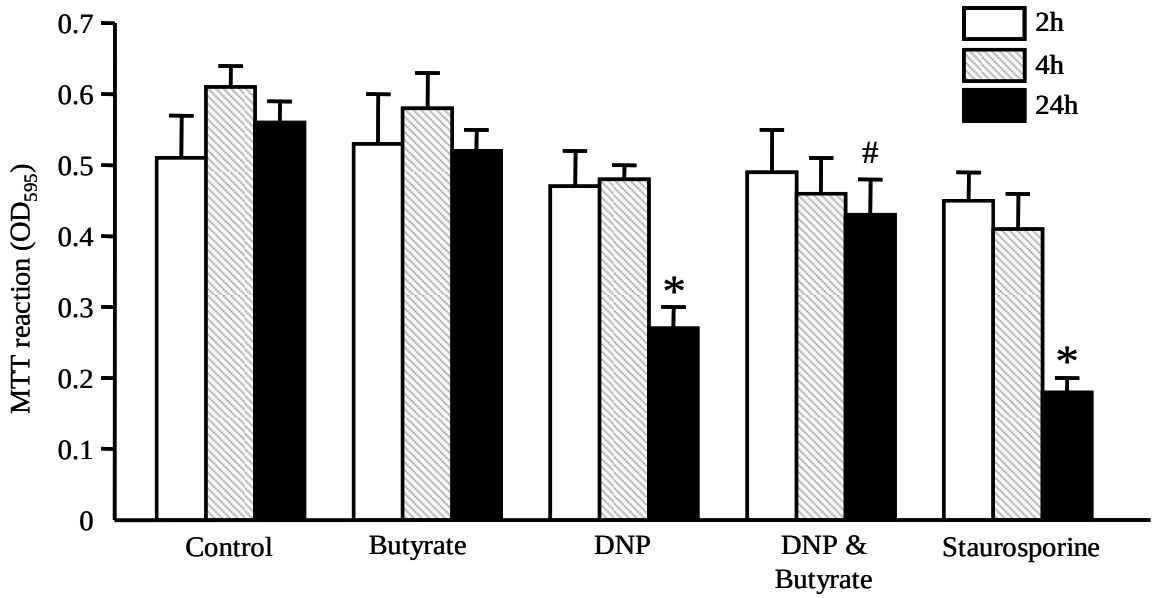

Figure 5. Mitochondrial activity of T84s was decreased following exposure to DNP but was regained with the addition of butyrate. T84 cells were treated with DNP (0.1 mM) for 2, 4 or 24 h. DNP acted in a time-dependent manner to decrease the conversion of the yellow MTT reagent by mitochondria to the insoluble purple formazan. The values were determined spectrophometrically at 595 nm. Butyrate (3 mM), while unable to increase the amount of mitochondrial action at any time point, was able to prevent some mitochondrial dysfunction when co-incubated with DNP. Staurosporine (5 µM; PKC inhibitor) induced apoptosis, and thus stops mitochondrial function. Incubation of T84 cells with staurosporine caused a decrease in MTT cleavage comparable to that of DNP treated cells (n=8 monolayers per treatment from 2 experiments;*,$p<0.05$ compared to control, #, $p<0.05$ compared to 24 h DNP; data are mean±SEM).

3.3 Butyrate Did Not Prevent the Increase in Paracellular Permeability Induced by the Combination of Metabolic Stress and Commensal Bacteria

Addition of butyrate only (0.1-100 mM) to confluent monolayers of T84 cells for 48 h did not lead to an increase in TER. However, ≥20 mM butyrate caused a significant decrease in TER to ~50% of the pre-treatment value by 48 h post-treatment (Fig 6A). The same phenomenon was observed in HT-29 epithelial cells as butyrate concentrations ≤6 mM did not increase or decrease the TER over a 72 h period (Fig 6B). Butyrate (3 mM) was added daily to filter-grown T84 cells 3 days after seeding, but butyrate did not increase the rate at which monolayers formed as gauged by TER (Fig 6C).

As previously shown, when *E. coli* HB101 (10^6 cfu) and DNP (0.1 mM) were added to T84 cell monolayers alone, they did not cause a consistent, statistically significant decrease in TER (122). However, simultaneous addition of DNP (0.1 mM) and *E. coli* HB101 or F18 (10^6 cfu) caused decreases in TER that were unaffected by butyrate addition to the co-culture well (Fig 6D). The decrease in TER was not due to apoptosis as revealed by a lack of DNA laddering and cleavage of caspase-3 (Fig 7A and 7B). Similarly, a lack of cell death was corroborated by LDH measurements that revealed no differences between controls (normalized to 100%) and DNP+*E. coli* treated (95±8% of control values) filter-grown T84 cell monolayers (Fig 7B). Also, previously published results have revealed no cell death by either necrosis or apoptosis (210).

A

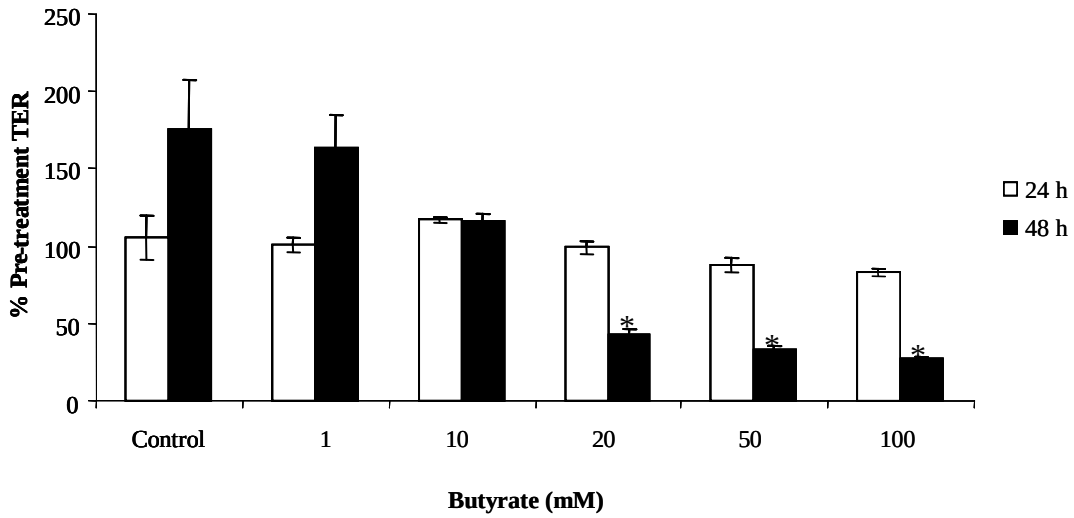
250
200
150
100
50
0
% Pre-treatment TER
24 h
48 h
*
*
*
Control
1
10
20
50
100
Butyrate (mM)

B

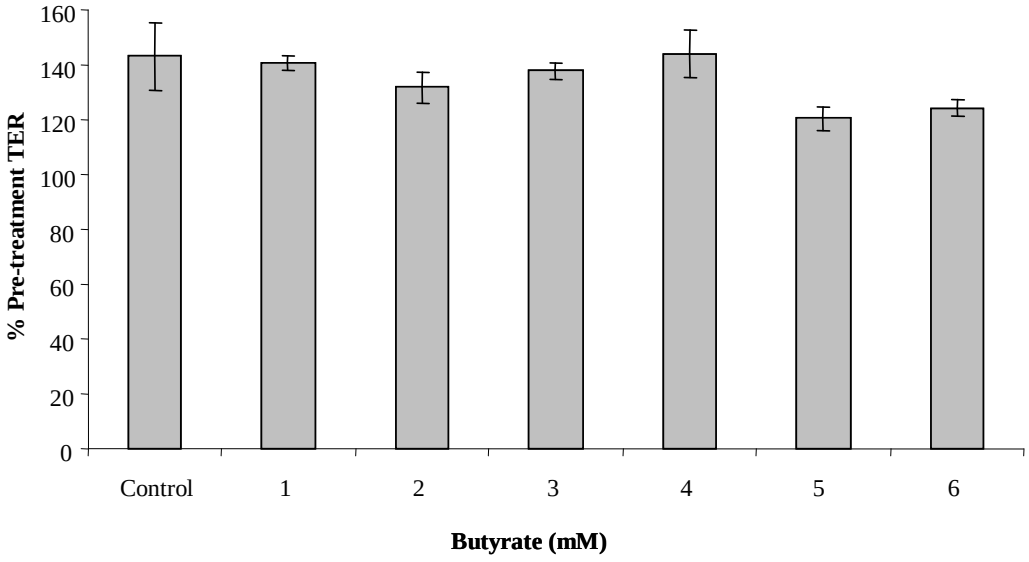
160
140
120
100
80
60
40
20
0
% Pre-treatment TER
Control
1
2
3
4
5
6
Butyrate (mM)

C

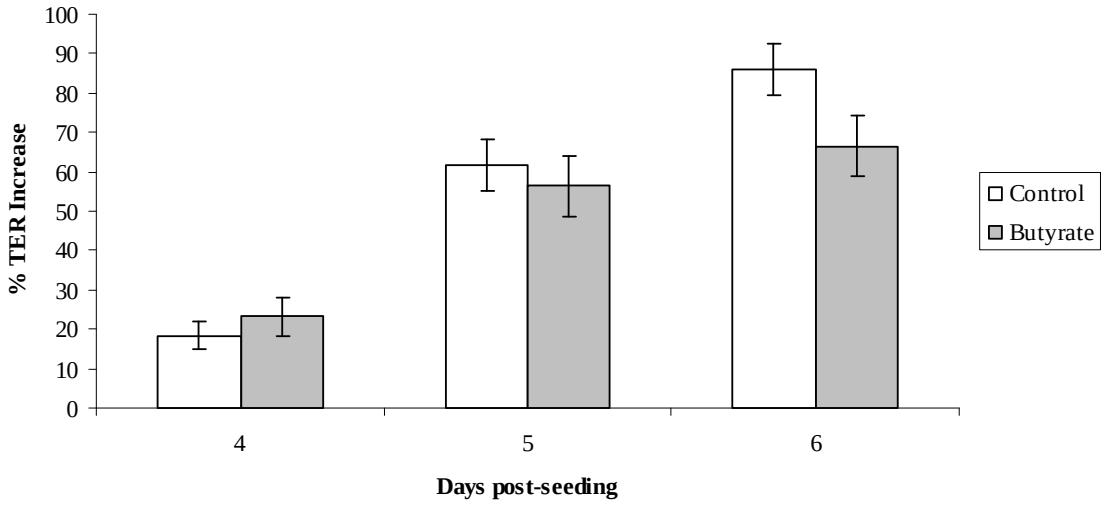

D

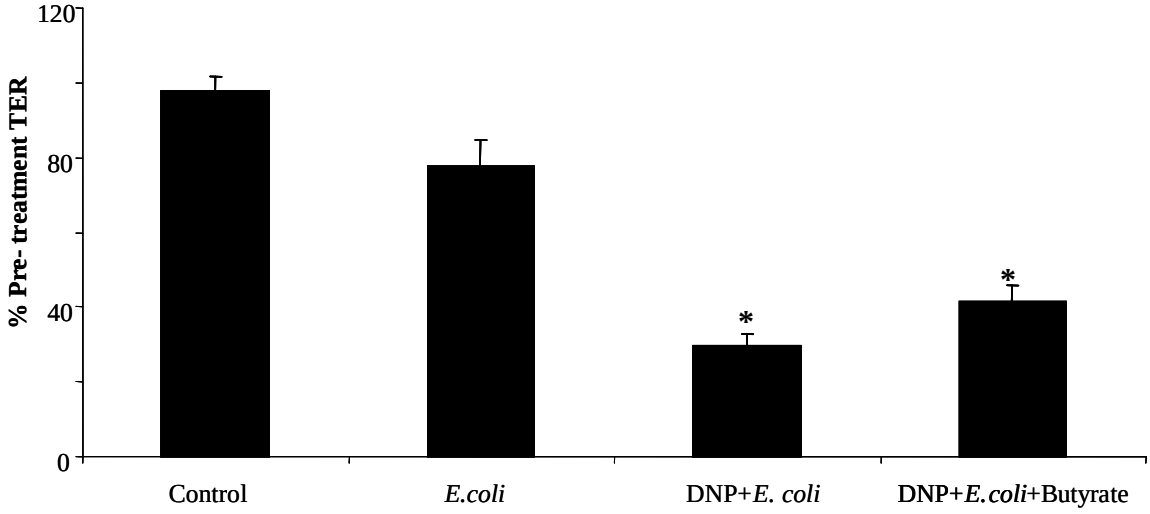

Figure 6. Increased paracellular permeability across metabolically stressed epithelial cell monolayers exposed to commensal bacteria was not reduced by butyrate co-treatment. A: bar graph showing that 24 or 48 h exposure of confluent T84 cell monolayers to butyrate (0.1-100 mM) did not increase the transepithelial electrical resistance (TER). However, butyrate when given at doses ≥20 mM diminished the TER at 72 h post-treatment (data are mean±SEM; n=4-14 T84 cell monolayers per condition from 7 experiments; *, $p<0.05$ compared to control). B: shows that butyrate concentrations at or below 6 mM did not alter the paracellular barrier in confluent HT-29 cell monolayers (data are mean±SEM; n=6 monolayers per condition from 3 experiments). C: butyrate was administered daily, commencing 3 days after seeding T84 cells. Butyrate did not enhance monolayer formation as measured by changes in TER (n=18 monolayers per condition from 3 individual experiments; data are mean±SEM;

butyrate, 3 mM). D: butyrate (3 mM) added to T84 cell monolayers did not prevent the decrease in TER caused by 24 h exposure to DNP (0.1 mM) and *E. coli* (HB101, 10^6 cfu) (data are mean±SEM; n=14 T84 cell monolayers from 7 experiments for each condition; *, $p<0.05$ compared to control).

A: DNA Laddering

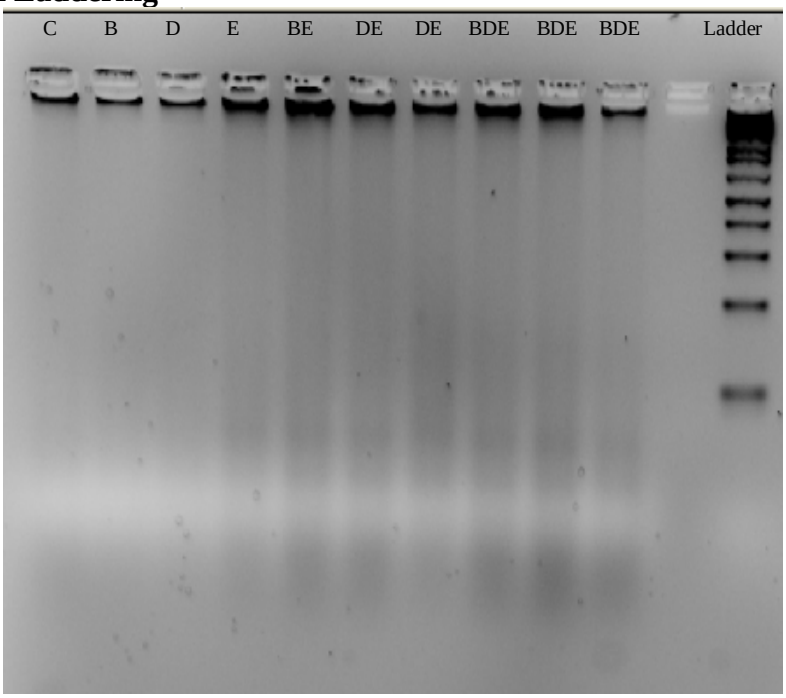

B: Caspase Immunoblot

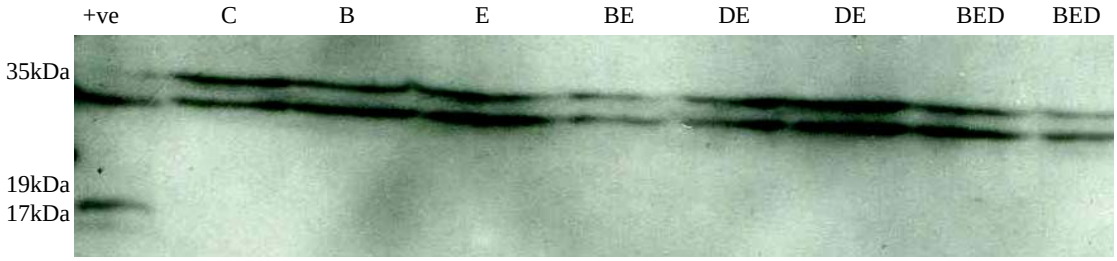

C

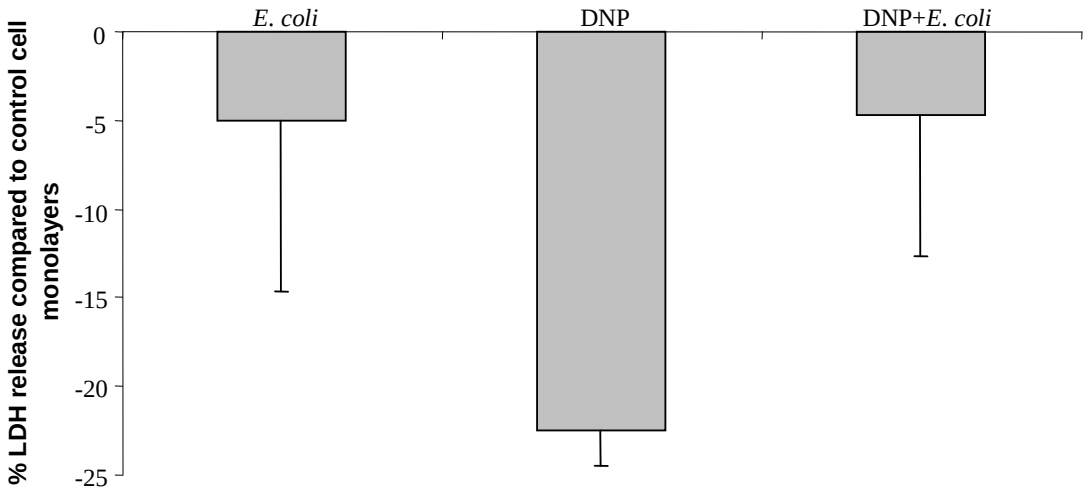

Figure 7. The decrease in TER was not due to apoptosis or necrosis. Seventy percent confluent T84 cell monolayers grown on 12 well plastic culture plates were incubated for 24 h with butyrate (3 mM), *E. coli* HB101 (10^6 cfu), DNP (0.1 mM), *E. coli* HB101+ butyrate, *E. coli* HB101+DNP, *E. coli* HB101+DNP+butyrate. The cells were then rinsed with PBS twice, lysed with DNA lysis buffer and vortexed. The amount of DNA was then measured, loaded and run through a 2% agarose gel. There were no signs of DNA laddering, a classic indicator of apoptosis (panel A, n=4 monolayers per condition from 2 experiments; C=control, E=*E. coli*, B=Butyrate, D=DNP). Likewise, western blotting from whole cell lysates also failed to reveal cleaved caspase-3 (panel B). Lactate dehydrogenase is a classic indicator of cell necrosis. T84 cells were seeded into a 96 well plate and were exposed to *E. coli* (10^6 cfu)±DNP (0.1 mM) for 24 h upon reaching confluence. The amounts of LDH were assessed for each condition using a colourimetric assay. Statistically, there was no difference in the amount of LDH between control cells, DNP treated cells, *E. coli* HB101 treated cells or DNP+*E. coli* HB101 treated cells (panel B, n=3 mololayers per condition, data are mean±SEM).

3.4 Butyrate Prevented the Transepithelial Passage of Commensal Bacteria Across Metabolically Stressed Colonocytes

In contrast to paracellular permeability, butyrate was able to prevent the enhanced translocation of *E. coli* across DNP co-treated T84 cell monolayers. For instance, every T84 cell monolayer exposed to *E. coli* (HB101 or F18; 10^6 cfu)+DNP (0.1 mM) for a duration of 4 h showed bacterial translocation (Fig 8A & 8B); however, the co-incubation of butyrate (3 mM) with DNP+ *E. coli* (HB101 or F18) reduced the level of bacterial translocation. For example, 65% of the monolayers treated with butyrate+DNP+*E. coli* (HB101) did not show any bacterial translocation (Fig 8A). We found that bacterial transmigration was independent of changes in TER (Fig 8C). Bacterial translocation occurred at 4 h post-treatment, despite the lack of obvious changes in paracellular

permeability in both DNP+*E. coli* and DNP+*E. coli*+butyrate treated monolayers (TER remaining at 89±7% and 88±4% of the pre-treatment values, respectively). Moreover, statistical analysis revealed no correlation between changes in TER and bacterial transcytosis (Pearson coefficient is -0.4 for DNP+*E. coli* and 0.2 for DNP+*E. coli*+butyrate).

Butyrate could have prevented transcytosis by killing the bacteria or, conversely, altering the bacteria in some manner that made them more resistant to up-take by colonocytes. We accounted for both of these possibilities as 1) 24 h growth curves for both *E. coli* F18 (Fig 9A) and HB101 (Fig 9B) were identical in the presence of 3 mM butyrate (n=3) and 2) *E. coli* grown in butyrate-containing LB broth overnight and then washed showed similar translocation levels as the bacteria grown in LB broth alone (Fig 9C), indicating that the butyrate was inhibiting transcytosis through an epithelial cell-mediated mechanism.

A

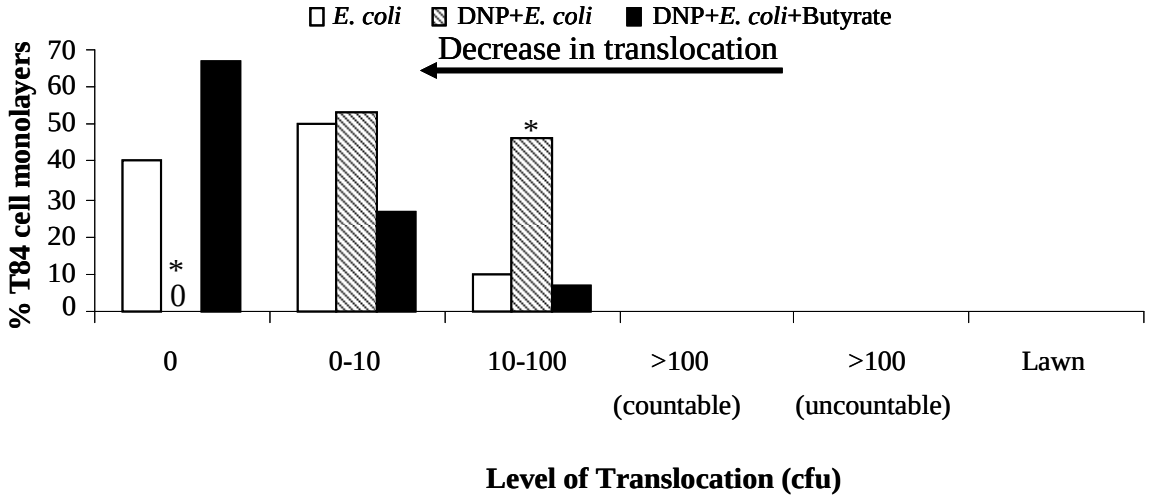
E. coli
DNP+E. coli
DNP+E. coli+Butyrate
Decrease in translocation
% T84 cell monolayers
70
60
50
40
30
20
10
0
*
0
*
0
0-10
10-100
>100
(countable)
>100
(uncountable)
Lawn
Level of Translocation (cfu)

B

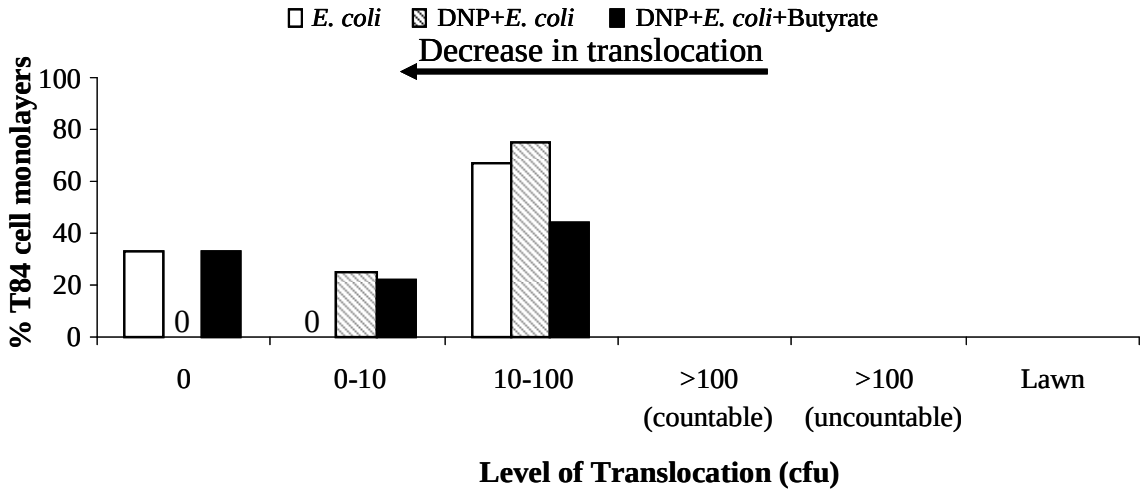
E. coli
DNP+E. coli
DNP+E. coli+Butyrate
Decrease in translocation
% T84 cell monolayers
100
80
60
40
20
0
0
0
0-10
10-100
>100
(countable)
>100
(uncountable)
Lawn
Level of Translocation (cfu)

C

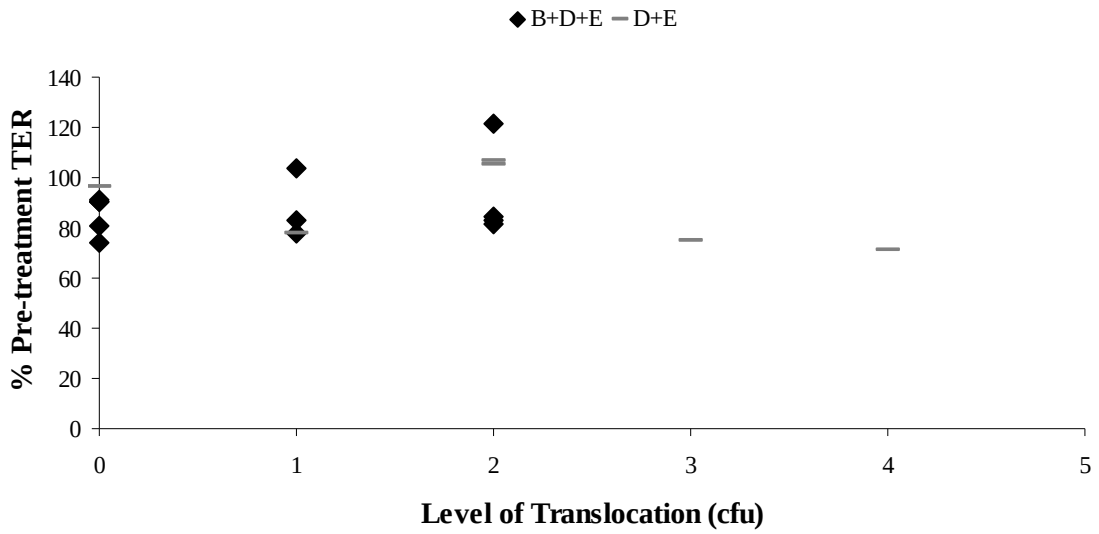

Figure 8. Butyrate prevented bacterial transcytosis across metabolically stressed colonocytes. In contrast to the paracellular pathway, butyrate reduced bacterial translocation (*E. coli* HB101 (panel A) and *E. coli* F18 (panel B)) across DNP-co-treated confluent T84 cell monolayers at 4 h post-treatment (panel A, *, $p<0.01$ compared to *E. coli* HB101 only and DNP+*E. coli* HB101+butyrate treated monolayers; n=16-21 monolayers per condition from 7 experiments; panel B, n=8-12 monolayers per condition from 4 experiments; see Materials and Methods for the interpretation of bacterial translocation; scores with "0" indicating no translocation at this level). Panel C: The increase in transcellular permeability was not significantly correlated with a decrease in the paracellular permeability at 4 h post-treatment (Pearson coefficient is -0.4 for DNP+*E. coli* and 0.2 for DNP+*E. coli*+butyrate) (n=6-12 monolayers for each condition from 4 individual experiments; see Materials and Methods for the interpretation of bacterial translocation scores; DNP 0.1 mM; *E. coli* HB101 10^6 cfu; butyrate 3 mM).

A

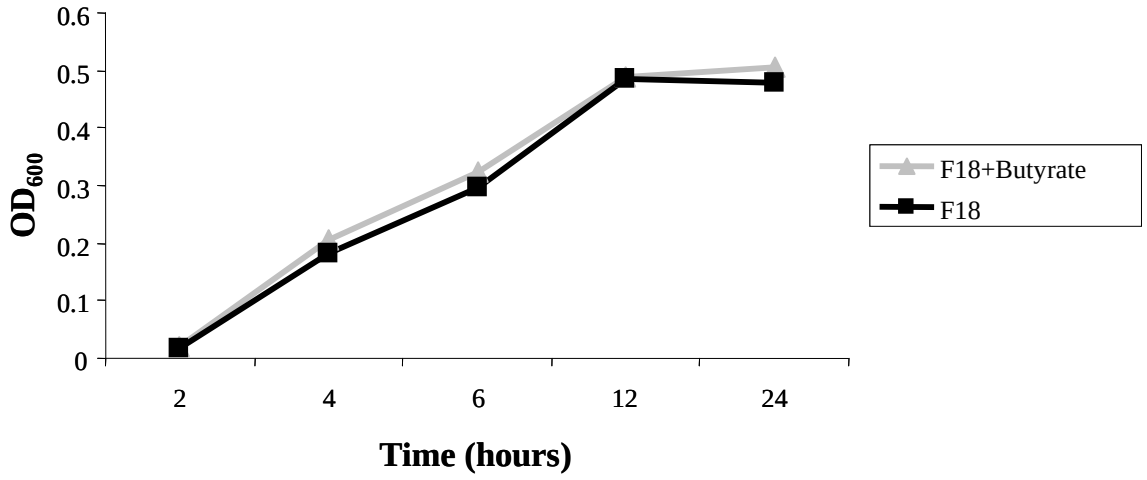
0.6
0.5
0.4
0.3
0.2
0.1
0
OD600
2
4
6
12
24
Time (hours)
F18+Butyrate
F18

B

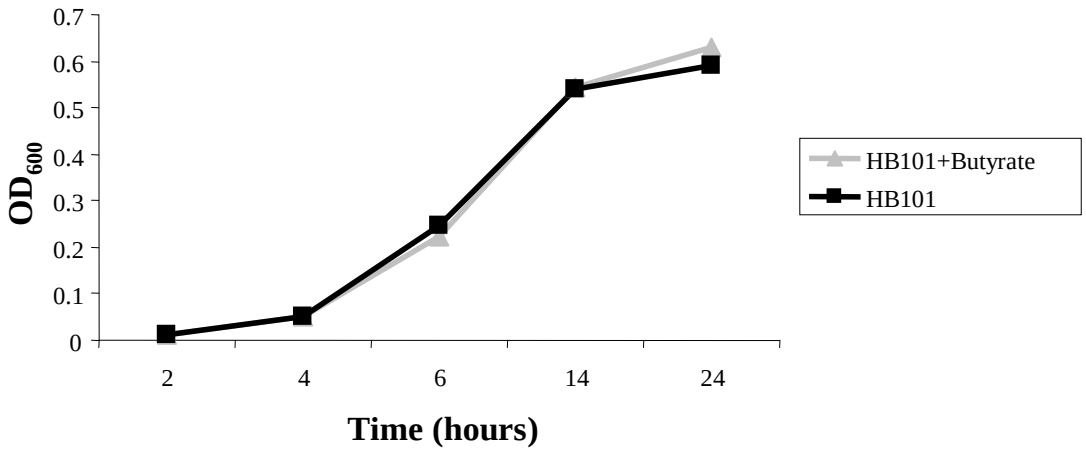
0.7
0.6
0.5
0.4
0.3
0.2
0.1
0
OD600
2
4
6
14
24
Time (hours)
HB101+Butyrate
HB101

C

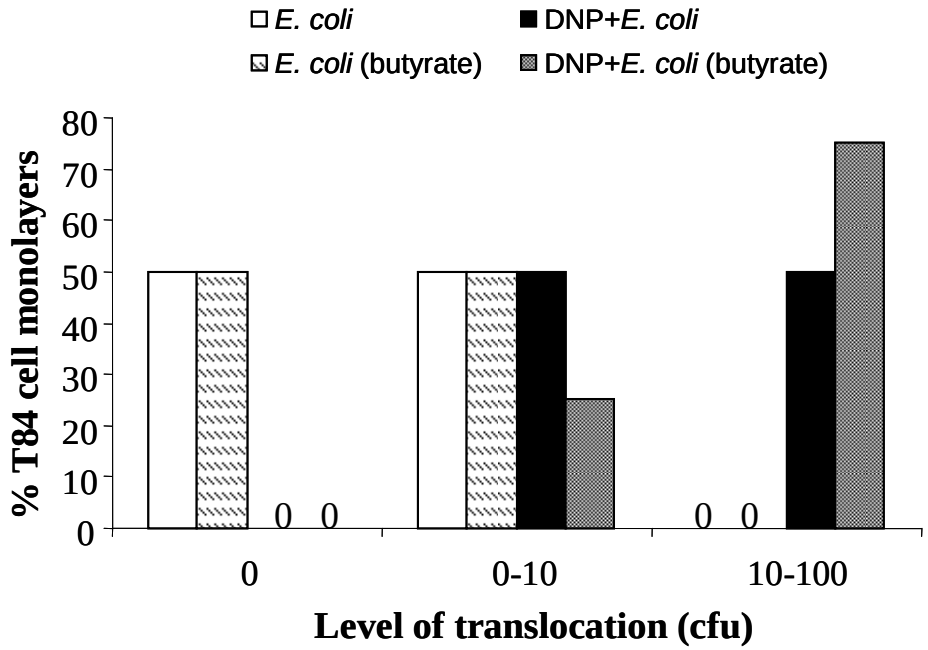

Figure 9. Butyrate did not prevent bacterial transcytosis by either killing the bacteria or altering their ability to be taken up by the cell. *E. coli* F18 (panel A) and HB101 (panel B) were grown either in LB broth alone, or in LB broth containing butyrate (3 mM). At various time points, a 1 mL sample was taken from the inoculums and the optical density (OD) was measured as a gauge of bacterial growth and division. There was not any difference in OD between butyrate-treated bacteria or those grown in LB broth alone (n=2 experiments). Also, bacteria that were grown in butyrate for 24 hours were compared to bacteria that were grown in LB broth alone for their ability to undergo translocation by the cells. The butyrate-grown bacteria (*E. coli* HB101) were washed prior to their addition to the T84 cell monolayers to ensure that little butyrate was being added to the monolayer to confound the results. The pre-incubation of *E. coli* HB101 with butyrate did not prevent bacterial translocation (panel C; n=4 monolayers per condition from 2 experiments; see Materials and Methods for the interpretation of bacterial translocation; scores with 0 indicating no translocation at this level).

3.5 Multiple Doses of Butyrate Prevented Enhanced Translocation of *E. coli* at 24 h Post-Treatment

By 24 h post-treatment the effect of butyrate had waned and the differences in translocation between DNP+*E. coli* and butyrate+DNP+*E. coli* treated T84 cell monolayers were no longer apparent (Fig 10A and 10B, HB101 and F18, respectively). It was hypothesized that since butyrate is the primary energy source for the colonic epithelial cells (215), perhaps the observed loss of protection was due to a consequence of complete butyrate metabolism by the colonocyte. Butyrate was therefore administered every 4 h over a 24 h period. When bacterial translocation levels were assessed at the end of the 24 h treatment period, almost 40% of the butyrate+DNP+*E. coli* HB101 treated T84 cell monolayers displayed no bacterial translocation whereas epithelia treated with DNP+*E. coli* all showed translocation levels of 100 cfu or more (Fig 10C).

A

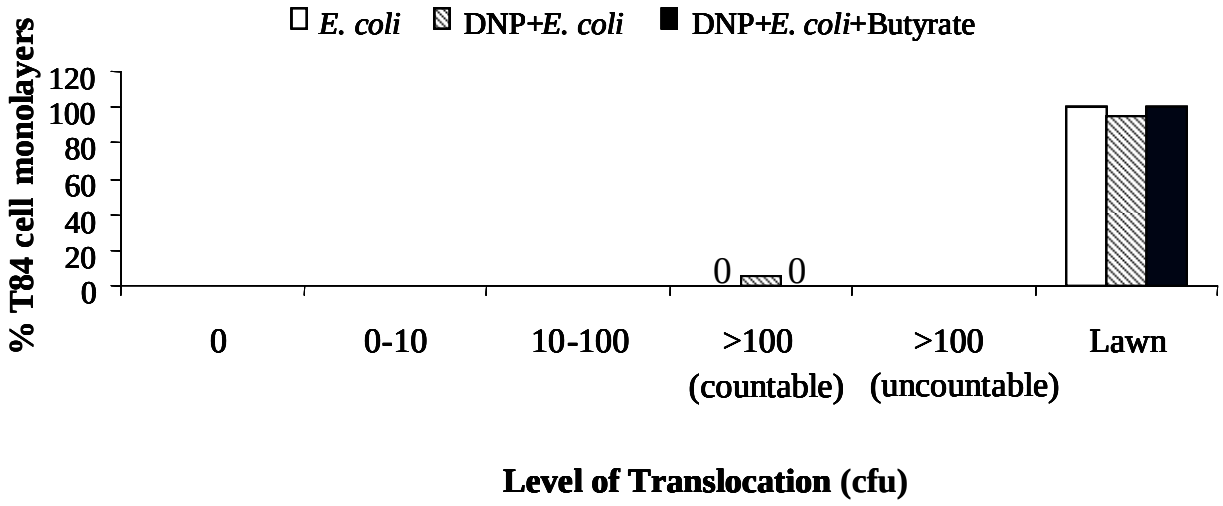
E. coli
DNP+E. coli
DNP+E. coli+Butyrate
% T84 cell monolayers
120
100
80
60
40
20
0
0
0
0
0-10
10-100
>100 (countable)
>100 (uncountable)
Lawn
Level of Translocation (cfu)

B

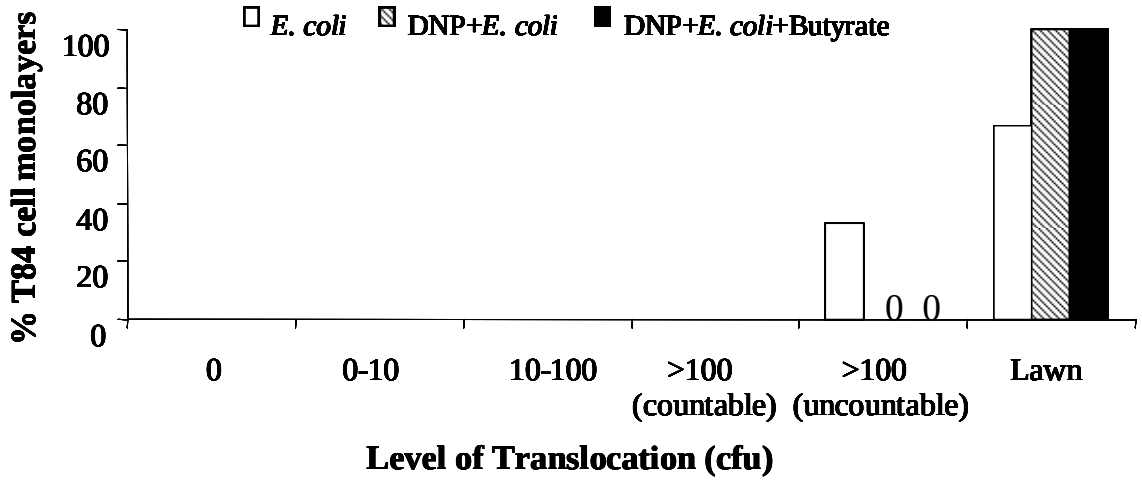
E. coli
DNP+E. coli
DNP+E. coli+Butyrate
% T84 cell monolayers
100
80
60
40
20
0
0
0
0
0-10
10-100
>100 (countable)
>100 (uncountable)
Lawn
Level of Translocation (cfu)

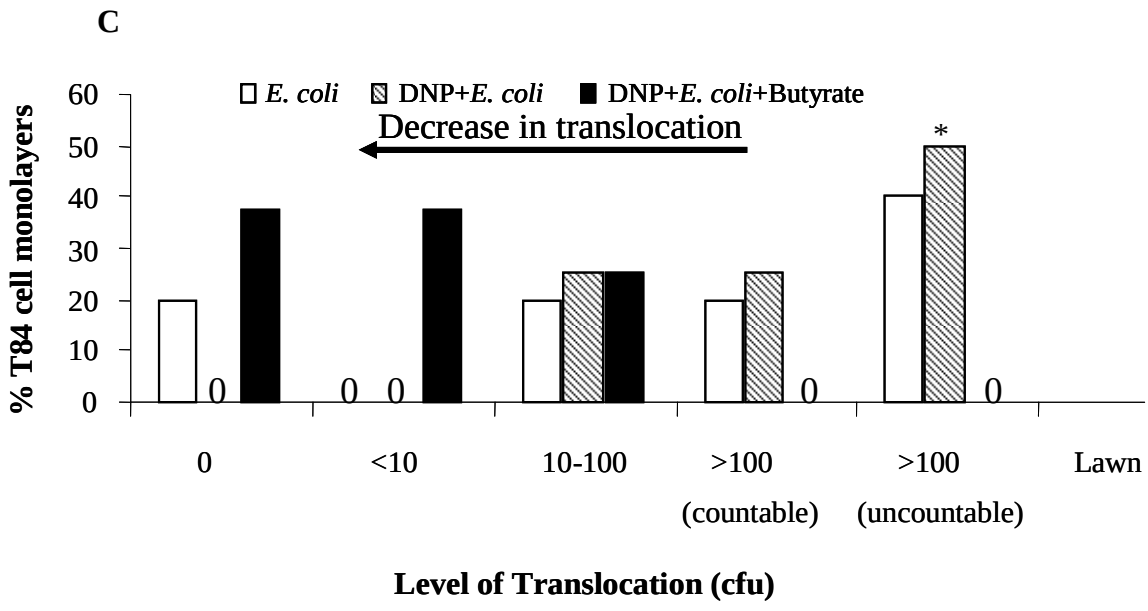

Figure 10. The protective effect of a single administration of butyrate was not sustained over a 24 hour period. At 24 h post-treatment, the amount of bacterial translocation was comparable between *E. coli*+DNP and *E.* coli+DNP+butyrate for both the HB101 (panel A) and F18 strains (panel B). C: bar graph showing that delivery of butyrate (to a final concentration of 3 mM) into the culture well every 4 h reduced bacterial translocation across T84 monolayers exposed to DNP (0.1 mM) and *E. coli* (HB101, 10^6 cfu) (*, $p<0.01$ compared to DNP+*E. coli*+butyrate at the specified level; n=6-9 monolayers from 3 experiments; bacterial transcytosis was assessed 24 h post DNP+*E. coli* treatment; see Materials and Methods for the interpretation of bacterial translocation; scores with 0 indicating no translocation at this level).

3.6 The Protective Effect of Butyrate Was Not Common to All Short Chain Fatty Acids, Namely, Acetate

The ability of butyrate to inhibit bacterial transytosis could be due to a property held by all SCFAs. To test this, the most abundant SCFA found in the colon, acetate (c2), was used as a comparator molecule. We observed no ability of acetate to ablate the enhancement of *E. coli* HB101 translocation across metabolically stressed T84 cell monolayers (n=6 epithelial preparations from 3 experiments; Figure 11).

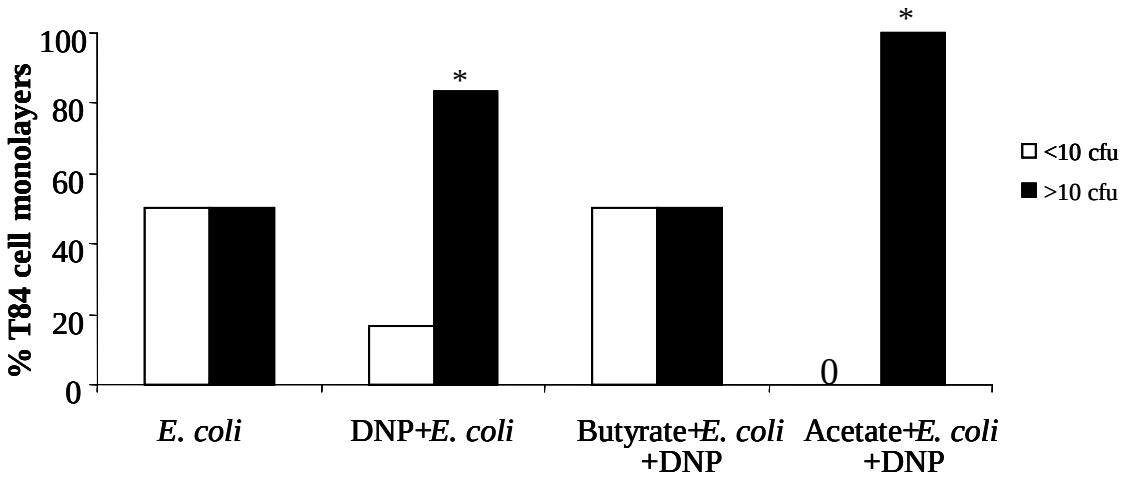

Figure 11. Acetate did not parallel butyrate's ability to inhibit bacterial transcytosis. Acetate is the most abundant SCFA produced in the colon. When added to T84 cell monolayers in addition to DNP+*E. coli* HB101, acetate was unable to prevent the transcellular breach in permeability, as marked by bacterial transcytosis at 12 h post-treatment (*, $p<0.05$ when compared to *E. coli* HB101 only or butyrate+*E. coli*+DNP at that particular level of translocation; n=6 monolayers per condition from 3 experiments; DNP, 0.1mM, *E. coli* HB101, 10^6 cfu; acetate, 3 mM, butyrate, 3 mM; see Materials and Methods for the interpretation of bacterial translocation; scores with 0 indicating no translocation at this level).

3.7 Butyrate Blocked the Increased Bacterial Internalization Caused by Metabolic Stress

Bacteria can cross the epithelium by passing between the tight junctions or via a transcellular route. Bacterial internalization into the enterocytes was assessed by the gentamicin exclusion assay. The gentamicin assay involved incubating sub-confluent T84 cell monolayers with *E. coli* HB101±DNP±butyrate, killing the extracellular bacteria with the antibiotic gentamicin, and then lysing the T84 cells with detergent. The lysed cells were then plated on agar dishes and bacteria were grown overnight. The numbers of internalized bacteria were then counted. As shown in Figure 12A, T84 cell internalization of *E. coli* HB101 was significantly increased 4 h post co-treatment with DNP and this was reduced by simultaneous butyrate treatment. Butyrate also prevented the internalization of *E. coli* strain F18 at 4 h post-treatment (Fig 12B). Given the relatively low percentage of internalization, experiments were conducted with invasive *Salmonella typhimurium* and exactly the same pattern was observed: increased intracellular *S. typhimurium* amounts were found in DNP only-treated T84 cells, but internalization was reduced in the presence of butyrate+DNP (Fig 12C).

A

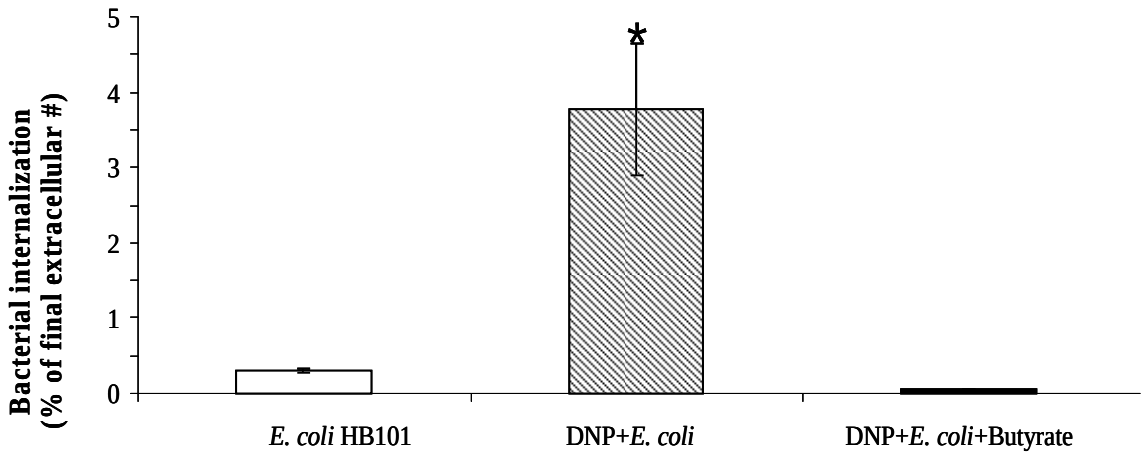
Bacterial internalization
(% of final extracellular #)
5
4
3
2
1
0
*
E. coli HB101
DNP+E. coli
DNP+E. coli+Butyrate

B

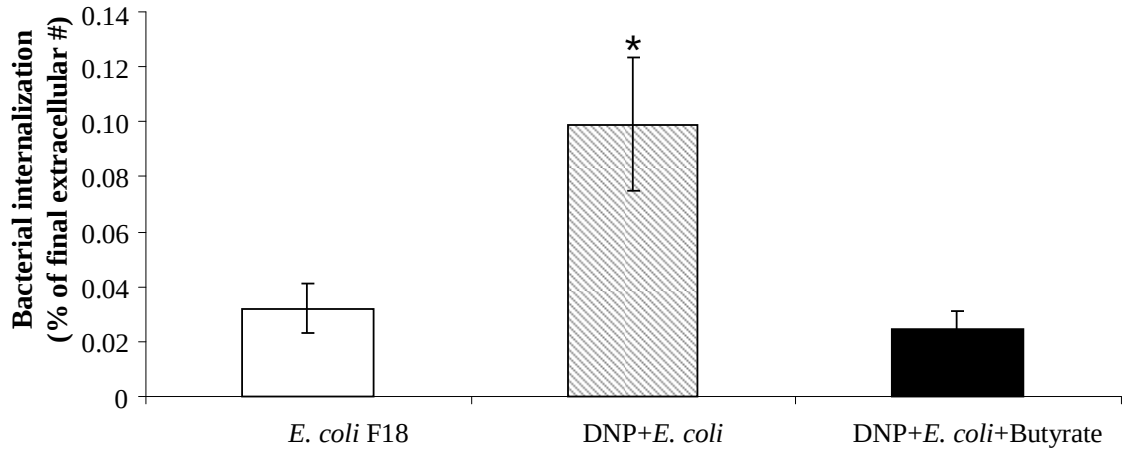
Bacterial internalization
(% of final extracellular #)
0.14
0.12
0.10
0.08
0.06
0.04
0.02
0
*
E. coli F18
DNP+E. coli
DNP+E. coli+Butyrate

C

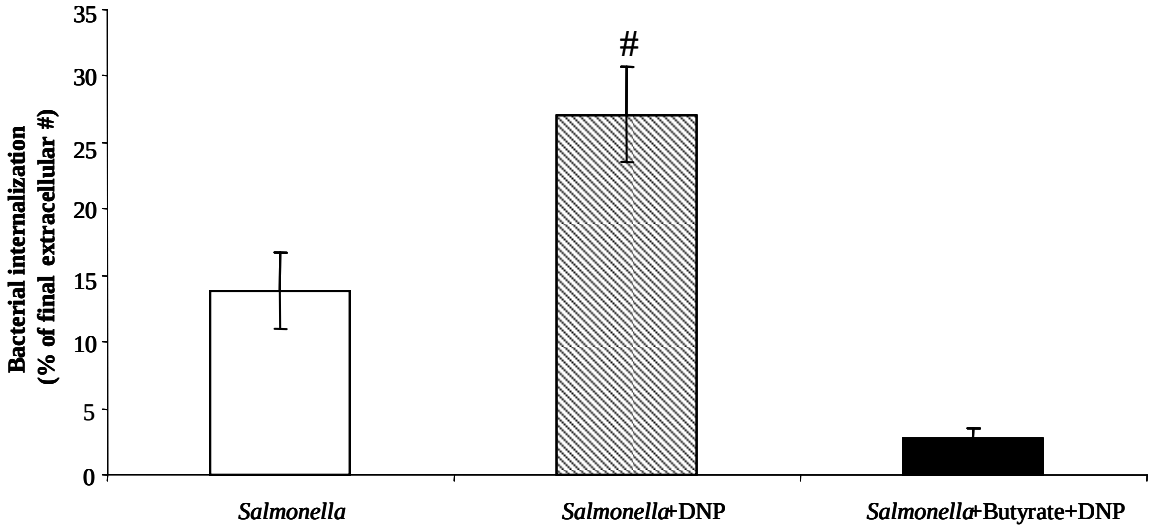

Figure 12. Butyrate preserved the colonic barrier by preventing bacterial invasion and internalization. Since bacteria can pass by either a paracellular or transcellular route, bacterial internalization into sub-confluent T84 cell monolayers was assessed using a gentamicin exclusion assay where the monolayers were incubated with bacteria alone (*E. coli* HB101 or *E. coli* F18 or *Salmonella typhimurium*), bacteria+DNP, or bacteria+DNP+butyrate. The extracellular bacteria were counted, then killed using the aminoglycoside gentamicin (200 μg/ml), and finally the T84 cells were lysed and the number of internalized bacteria were counted. Butyrate prevented the internalization of the non-pathogenic, non-invasive *E. coli* HB101 (panel A, n=16 monolayers from 4 experiments for each condition) as well as other commensal-derived bacterial strains such as *E. coli* F18 (panel B; n=20 monolayers from 5 experiments for each condition). Butyrate also prevented the invasion of *Salmonella typhimurium* into T84 cells (panel C; n=6-12 monolayers from 5 experiments for each condition) (#, $p < 0.01$ when compared with *Salmonella* alone and *Salmonella*+DNP+butyrate; *, $p<0.05$ when compared to *E. coli* only and *E. coli*+DNP+butyrate; DNP, 0.1 mM, *E. coli* HB101, *E. coli* F18 and *S. typimurium* all inoculated at 10^6 cfu; Butyrate, 3 mM).

3.8 The Increase in Intracellular Bacteria Was Not Due to Defective Killing of Internalized Bacteria

The increase in intracellular bacteria in the DNP+*E. coli* treated monolayers could have been due to either an increased rate of internalization or a decreased ability of the metabolically-stressed epithelia to kill the internalized bacteria. To test this, T84 cells were treated for 4 h with DNP+*E. coli*±butyrate, then treated with gentamicin for 4, 8 or 24 h, at which point the cells were lysed and viable bacteria enumerated. Using this approach we found that by 24 h, the numbers of intracellular bacteria were similar in all conditions suggesting that the increased internalization was not due to a reduced ability to kill the bacteria. The rate of killing may have even been enhanced in the DNP-treated monolayers given that the increased numbers seen after 4 h of gentamycin had been reduced to control levels by 24 h after antibiotic treatment (Fig 13).

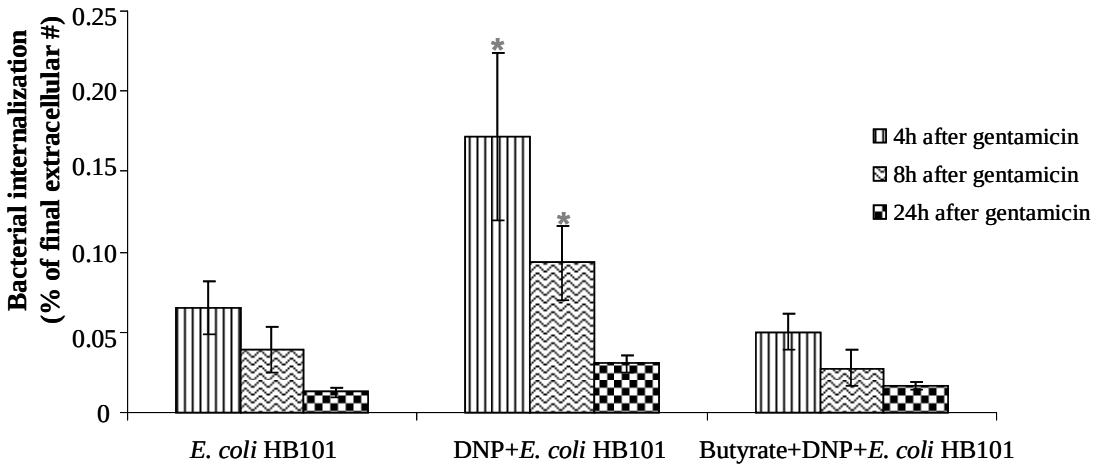

Figure 13. DNP+*E. coli* HB101 treated monolayers internalized more bacteria than *E. coli* HB101 or *E. coli*+DNP+butyrate treated monolayers and killed the internalized bacteria at a comparable rate. Bar graph showing that the metabolic stress induced by exposure to DNP (0.1 mM) did not inhibit the ability of T84 epithelial cells to kill internalized bacterial, as levels of intracellular *E. coli* HB101 (10^6 cfu) were similar at 24 h after extracellular bacteria were killed by treatment with gentamicin to prevent any further internalization of viable *E. coli* (n=4-6 monolayers from 4 experiments; data are mean±SEM; *, $p<0.01$ compared with control at the time-matched point; butyrate at 3 mM).

3.9 Increasing Extracellular Glucose Inhibited the Increased Bacterial Translocation Across Metabolically Stressed T84 Cell Monolayers But Did Not Prevent the Drop in TER

As stated above, butyrate's primary role is that of an energy source, and a decrease in the colonic concentration of butyrate due to bacterial dysbiosis could create an environment where there are insufficient nutrients for the colonocytes. Given that, the addition of exogenous energy sources, such as 25 mM glucose, should restore, at least in part, the metabolic homeostasis. The addition of exogenous glucose significantly enhanced the TJ defect by reducing the TER (Fig 14A) to the extent seen with high concentrations (≥20 mM) of butyrate (Fig 6A). However, the exogenous glucose did prevent bacteria transcytosis as a consequence of treatment of DNP+*E. coli* after 4 h of incubation (Fig 14B). The addition of equi-molar mannitol did not prevent bacterial translocation, indicating that this was not due to an osmotic effect. The glucose-induced prevention of bacterial transcytosis was also not due to the activation or opening of glucose transporters because 3-ortho-methyl-D-glucopyranose, which is taken up with similar kinetics to glucose but cannot be metabolized, did not reproduce the effect of glucose (Fig 14B).

A

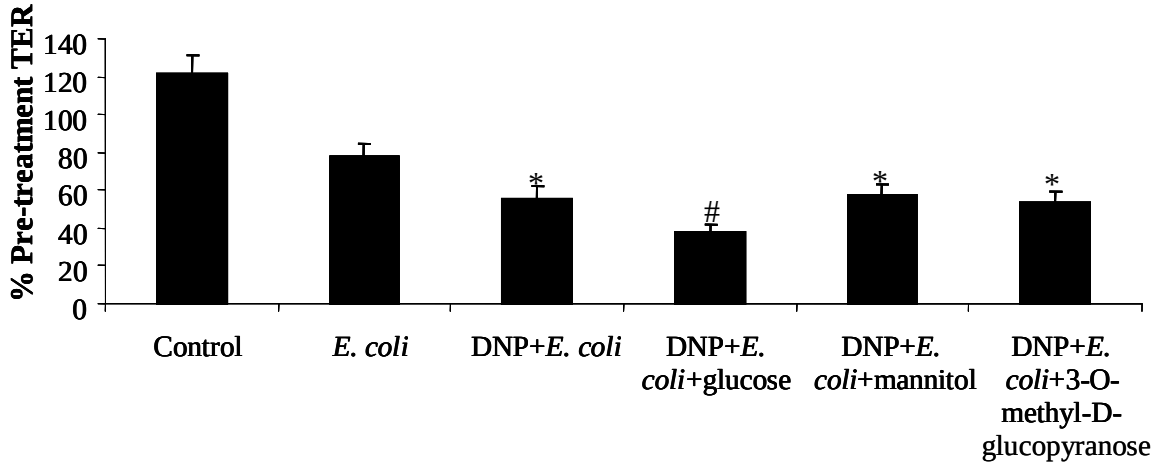

B

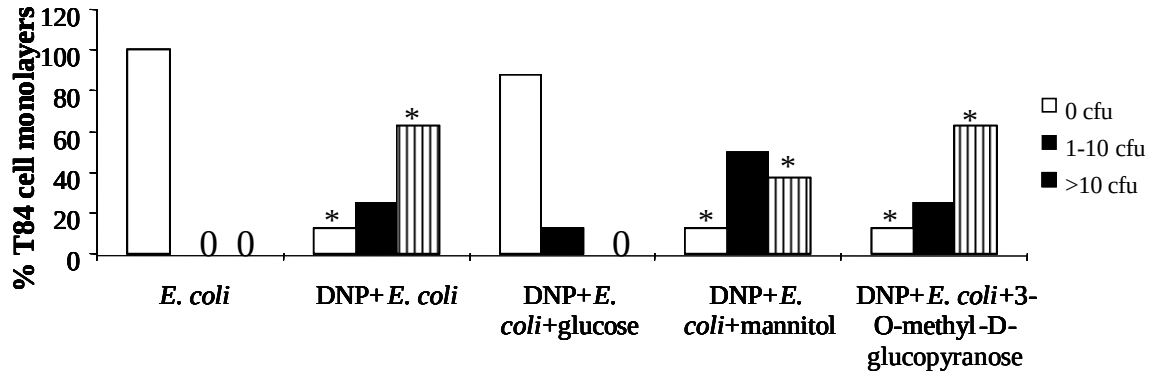

Figure 14. Butyrate functioned in part by restoring the energy balance in the cell as exogenous glucose also prevented bacterial translocation. Bar graph (panel A) showing that increasing amounts of extracellular glucose to 25 mM did not prevent the drop in TER caused by a 24 h treatment of DNP (0.1 mM)+*E. coli* (HB101, 10^6 cfu), but actually enhanced the barrier defect. In contrast, exogenous glucose inhibited bacterial translocation across metabolically stressed confluent T84 cell monolayers (panel B), and this was not observed when equi-molar mannitol or the non-metabolizable 3-O-methyl-D-glucopyranose was substituted for glucose (data are mean±SEM; n=7-8 monolayers from 3 experiments for each condition; panel A: *, $p<0.05$ compared to control; #, $p<0.05$ compared to DNP+*E. coli*; panel B: bacterial transcytosis was assessed 24 h post DNP+*E. coli* treatment;*, $p<0.05$ compared to DNP+*E. coli*+glucose; see Materials and Methods for the interpretation of bacterial translocation; scores with 0 indicating no translocation at this level).

3.10 Conditioned Media From Butyrate-Producing Bacteria Did Not Prevent Barrier Dysfunction

Fusobacteriaum gonidiaformans strain 21115R are known butyrate producers. The addition of cultured medium from these bacteria to T84 cells exposed to DNP+*E. coli* HB101 did not prevent either the decrease in paracellular (Fig 15A) or transcellular (Fig 15B) permeability.

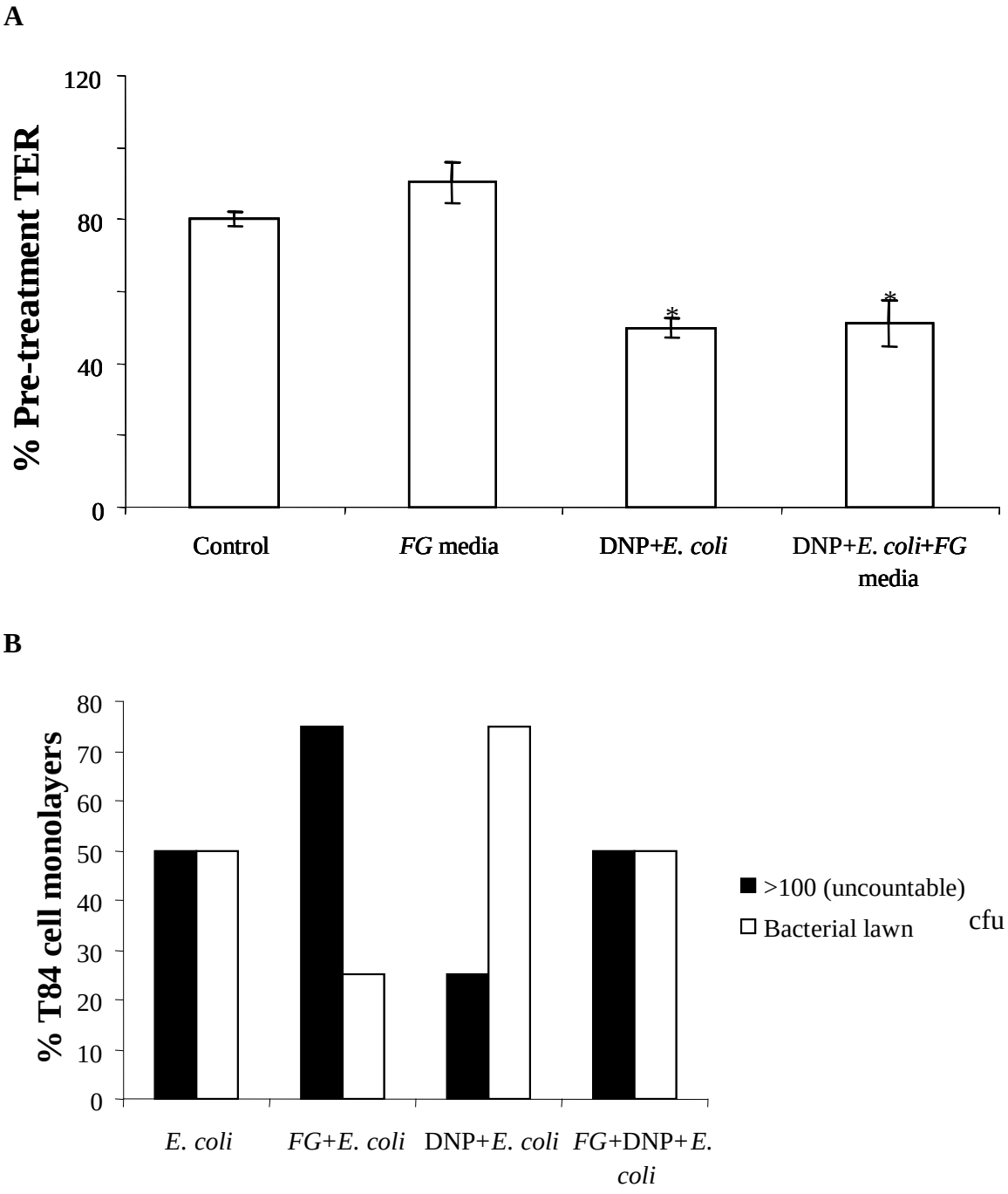

Figure 15. The media collected from butyrate-producing bacteria was unable to ameliorate the paracellular and transcellular defects evoked by DNP+*E. coli* HB101. Conditioned media collected from the butyrate producing *F. gonidiaformans* strain 21115R was filtered for bacteria and diluted in anti-biotic free T84 media (1:4 dilution) before being added to the T84 cell monolayers in addition to *E. coli* HB101±DNP. Cultured medium was unable to prevent the decrease in TER at 24 h post-treatment

(panel A) and the increased bacterial translocation (panel B) (n=4 monolayers/condition from 2 experiments; data are mean+SEM; *, $p<0.05$ as compared to control; see Materials and Methods for the interpretation of bacterial translocation; *FG*= *F. gonidiaformans* strain 21115R conditioned; DNP 0.1 mM; *E. coli* HB101 10^6 cfu).

3.11 Butyrate Prevented DNP+*E. coli*-Induced NF-κB Activation Via Inhibition of IκB

We postulated that the effect of butyrate could be via inhibition of the NF-κB pathway as pharmacological inhibitors of the NF-κB activation reduced bacterial transcytosis across DNP-treated T84 cell monolayers (210). IκB acts as an inhibitor of NF-κB activation, however phosphoryation and subsequent ubiquitination of this molecule liberates the NF-κB dimers to migrate to the nucleus and regulate transcription. The phosphorylation of IκB is performed by the IKK enzyme, which itself must be phosphorylated on residue serine$^{176/180}$ in the case of IKK-α and serine$^{177/181}$ in the case of IKK-β to become functionally active (216). While there was no difference in the upstream phosphorylation of the IKK enzymes between DNP+*E. coli* and butyrate+DNP+*E. coli* samples (n=3 experiments, Figure 16D), butyrate reduced the increase in phosphorylated (p)-IκB-α levels that are characteristically caused by DNP+*E. coli* treatment at 1 h post-treatment (Fig 16A and 16B). The decreased levels of p-IκB-α were confirmed by the use of an ELISA for p-IκB-α (Fig 16C). Levels of p-IκB-α of the DNP+*E. coli* HB101 treated T84s were comparable to the epithelia that were exposed to TNF-α at 24 h post-treatment (5.61±0.53 vs 7.23±0.52, relatively).

Another upstream level of control for the NF-κB pathway is the ubiquitin-like conjugating enzyme (Ubc)-12. The Ubc-12 is responsible for neddylating the Cullin-1 subunit of E3-SCF (the enzyme that is responsible for ubiquitinating p-IκB). A recent study by Kumar *et al.* showed that butyrate can inhibit baseline levels of NEDD8 conjugation to the Cullin-1 subunit of E3-SCF (217). However, using the same

antibodies and technique, we did not observe butyrate-induced alterations in NEDD8-Cullin-1 conjugation in T84s (Fig 16E).

A

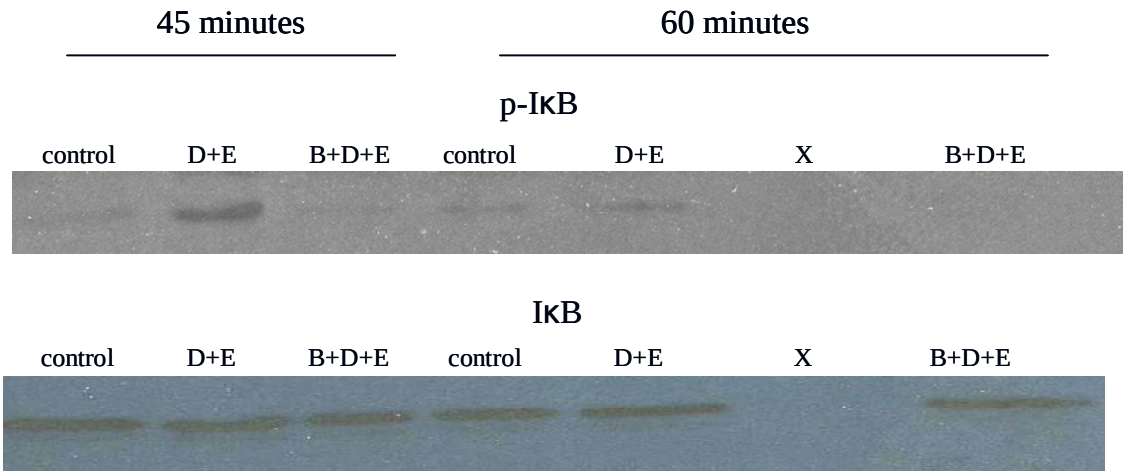
45 minutes
60 minutes
p-IκB
control
D+E
B+D+E
control
D+E
X
B+D+E
IκB
control
D+E
B+D+E
control
D+E
X
B+D+E

B

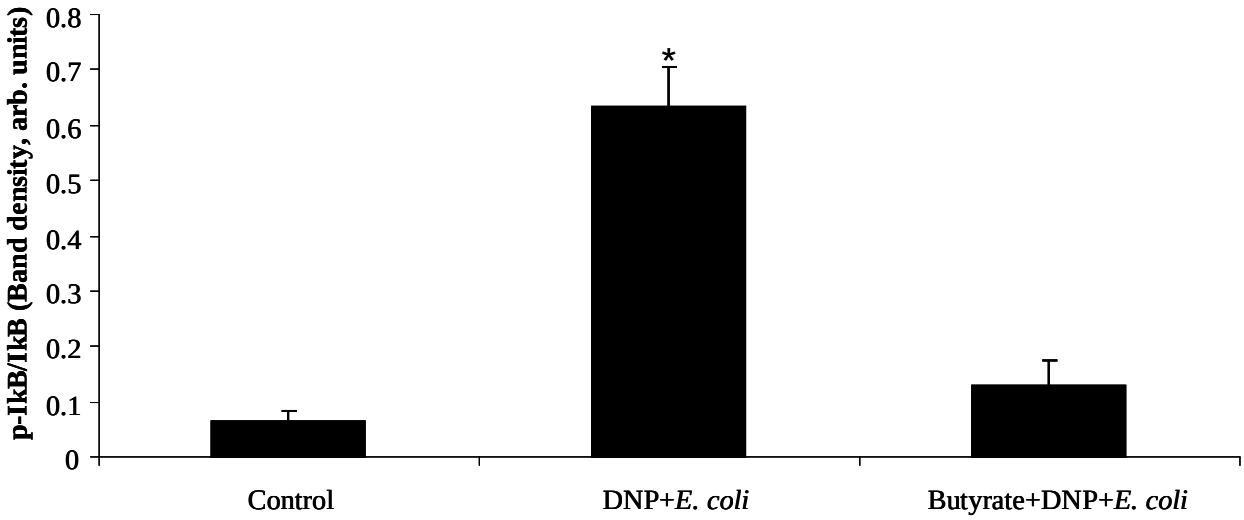
p-IkB/IkB (Band density, arb. units)
0.8
0.7
0.6
0.5
0.4
0.3
0.2
0.1
0
*
Control
DNP+E. coli
Butyrate+DNP+E. coli

C

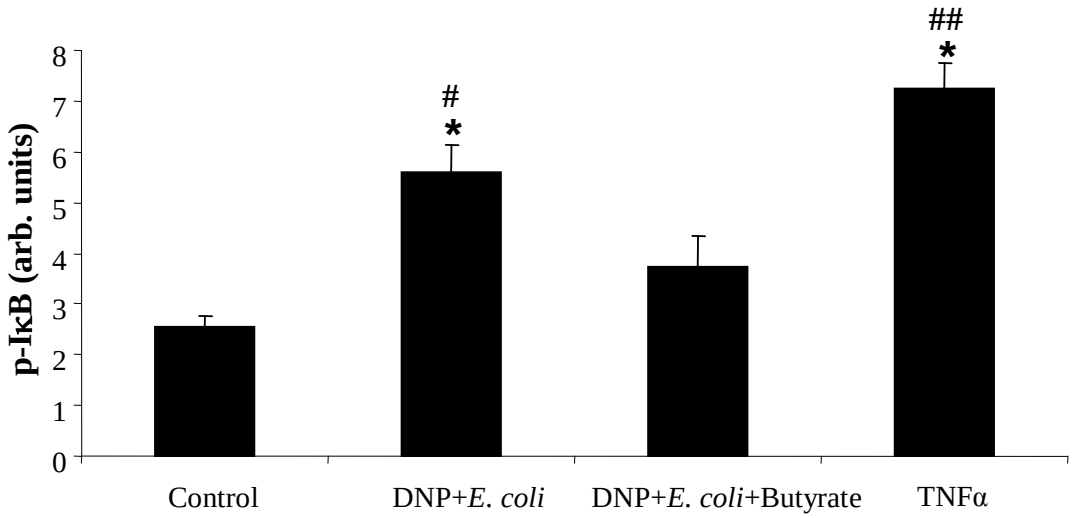

D

p-IKK-β

IKK-β

E

Figure 16. Butyrate inhibited T84 epithelial cell mobilization of NF-κB in response to treatment with DNP+*E. coli*. A: representative immunoblots from whole cell T84 lysates collected at 45 and 60 minutes after treatment (con, control; D, DNP at 0.1 mM; E, *E. coli* at 10^6 cfu; B, butyrate at 3 mM; X, blank lane; p-IκB, phosphorylated IκB-α). B: densitometry of immunoblots revealed a statistically significant increase in the phosphorylation of IκB-α in response to DNP+*E. coli* that was inhibited by co-treatment with butyrate (data are mean±SEM; n=3-9 T84 cell preparations from 4 experiments; *, $p<0.05$ compare to other groups). C: ELISA for the phosphorylated form of IκB-α supports the analysis of immunoblotting shown in panel B (n=3-6 T84 cell preparations from 5 experiments; *, $p<0.01$ compared to control; #, $p<0.05$ compared to butyrate; ##, $p<0.01$ compared to butyratel cells were collected 1 h post-treatment). D: immunoblot of p-IKK-β and IKK-β that demonstrated that butyrate did not alter the level of the IκB-α regulator (n=3 experiments; MW, molecular weight; c, control; D, DNP at 0.1 mM; E, *E. coli* HB101 at 10^6 cfu; B, butyrate at 3 mM; +ve, positive control; X, blank lane; p-IKK-β, phosphorylated IKK–β). E: Immunoblot showing that butyrate did not inhibit the process of conjugation of NEDD8 to the Cullin-1 subunit of E3-SCF (n=3 experiments; MW, molecular weight; c, control; D, DNP at 0.1 mM; E, *E. coli* HB101 at 10^6 cfu; B, butyrate at 5 mM; +ve, positive control; X, blank lane; Cul-1, Cullin-1).

3.12 Mitochondrial Gene Expression Was Not Altered in Patients with CD

We and others have reported that patients with IBD can have swollen and misshapen mitochondria (110, 122). These morphological changes are indicative of disrupted mitochondrial function. While there may have been a change in the mitochondrial morphology, we were unable to detect significant differences in message for mitochondrial enzymes (ATP synthase, succinate dehydrogenase and NADH Coenzyme Q) from RNA isolates obtained from colonic tissue collected from patients of CD (both active and inactive sites) compared to colon cancer patients (Fig 17).

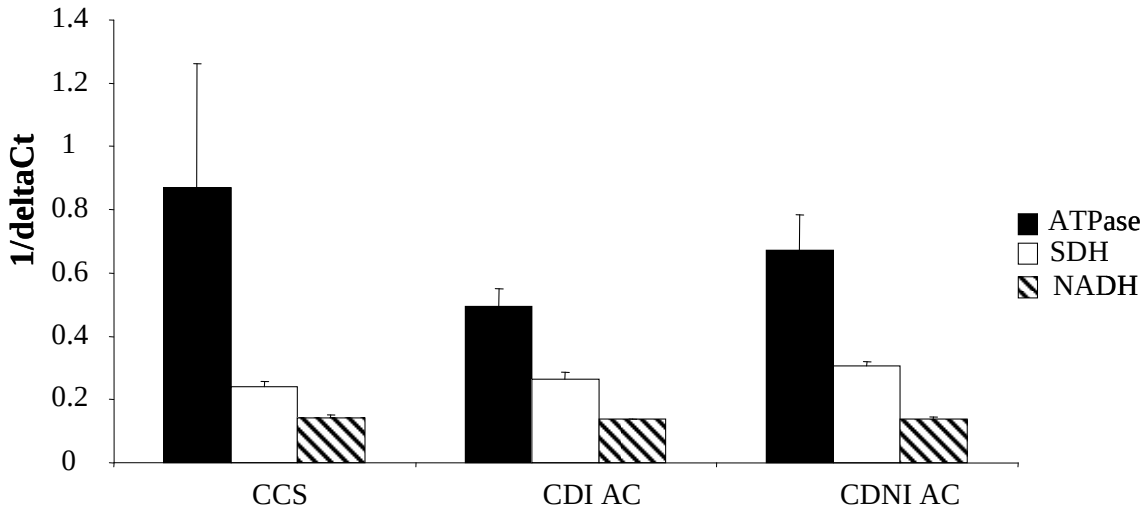

Figure 17. Mitochondrial enzyme mRNA was not changed in patients with IBD compared to control patients. Colonic pinch biopsy extracted from CD inflamed ascending colon (CDIAC), CD non-inflamed ascending colon (CDNIAC) and colon cancer patients samples (CCS) were subjected to TRIzol for a total RNA extraction. The samples were then converted to cDNA and amplified by real-time PCR for the desired genes (ATP synthase (ATPase), succinate dehydrogenase (SDH) and NADH Coenzyme Q). The results revealed no significant decrease in the level of mitochondrial enzymes of CD patients compared to colon cancer patients. The graph represents the delta CT compared to β-actin (n=4 samples per treatment; data are mean+SEM).

CHAPTER 4 - Discussion

The ~500 different commensal bacteria of the human microbiome are non-pathogenic in their intended environment –the lumen of the GI tract– and play an important role in maintaining gut homeostasis (6). A breach in the single cell layer of epithelium that separates these bacteria from the internal environment may result in the enhanced passage of bacteria into the submucosa, which can result in potentially pathogenic consequences. Evidence now indicates that commensal bacteria may trigger idiopathic intestinal inflammatory diseases, such as IBD (218). For example, many different mouse models of colitis, whether spontaneous or chemically induced, are less severe if the animals are raised in germ-free conditions (219). In some cases of human IBD, inflammation is present in parts of the gut containing the highest bacterial concentrations, and antibiotic treatment can offer some CD patients relief (219).

Enhanced mucosal permeability would cause excessive transmigration of bacteria, and this may play a pivotal role in either causing or maintaining a chronic inflammatory state. An interesting case was reported where a 13 year-old girl was identified as having increased gut permeability to ^{51}Cr-EDTA during a cross-sectional study of patients and their first-degree relatives. She was asymptomatic and lacked microscopic and macroscopic inflammation at the time, which led the authors to believe that the increase in permeability was a primary defect as she went on to develop ileocolonic CD (109). This account provides support of the hypothesis that increased gut permeability to macromolecules and bacteria is an early step in the pathogenesis of IBD. Despite whether increases in permeability are a cause or effect of disease, intestinal permeability in some patients with CD is increased proportionally to disease activity and may be used to predict the clinical course of disease (219). The enhanced permeability may be in the

form of either increased paracellular permeability (i.e., movement of materials between the cells across the TJs) or transcellular permeability (i.e., movement through the cells).

There is evidence to suggest that an increase in permeability may be linked to an impaired metabolic state of the enteric epithelium. Various stressors may disrupt proper mitochondrial function, thus inhibiting ATP production and causing an increase in permeability. Infections (220), ischemia (160) psychological stress (221) and medications (152) have all been identified as promoters of barrier disruptions. Recently, bacterial dysbiosis has been identified in some patients with CD (4, 132), and is implicated as a potential source of metabolic stress. Subsets of patients with IBD have a decrease in the number of *Clostridium* bacteria, which are the main producers of the colonic energy source, butyrate (215). Accordingly, reduced mucosal ATP levels have been reported in patients with IBD (222). Our laboratory has shown that *in vivo* and *in vitro* models of metabolic stress resulted in increased paracellular permeability and enhanced bacterial translocation of non-pathogenic, non-invasive bacteria across colonic epithelium via the trancellular pathway (15, 122, 210). In light of these findings, we hypothesized that the addition of exogenous butyrate to metabolically stressed colonic epithelium reduces the transcellular flux of non-pathogenic, non-invasive bacteria.

4.1 Experimental Design

T84 cells are a tissue culture model of the colonic epithelium that was derived from a lung metastasis of a colonic carcinoma (223). These cells secrete chloride and, when grown on glass, plastic or collagen-coated nylon mesh in the presence of serum, will form an electrically tight monolayer (224). Freeze-fracture examination also

demonstrates the presence of tight junctions (TJs) between the cells, signifying the ability of the cells to maintain polarity like that of a typical differentiated epithelial cell (223). These cells were appropriate to use for our studies as they formed monolayers that reached high TERs. The integrity of the TJs was key to being able to study minute changes in the TER and translocation that may not have been apparent in other colonic cell lines such as Caco-2 and HT-29. The presence of a confluent monolayer and polarized properties allowed for the examination of transcellular migration independent of paracellular flux. We found that bacterial transmigration was independent of changes in TER (Fig 18). Bacterial translocation occurred at 4 h post-treatment, despite the lack of obvious changes in paracellular permeability in both DNP+*E. coli* and DNP+*E. coli*+butyrate treated monolayers as seen in Figure 8C.

As metabolic stress was a key component of our model of disease, it was important that we used a metabolic stressor that specifically acted on the mitochondrion to reduce cellular ATP levels. We chose to induce metabolic stress in T84s by the use of 2,4-dintrophenol (DNP) as it uncouples oxidative phosphorylation from the electron transport chain by disrupting the mitochondrial proton gradient (see section 1.3.4 for a further explanation of DNP). When used at 0.1 mM, DNP significantly reduced the amount of ATP inside a T84 cell at as soon as 4 h post-treatment (15). Other investigators have also found that DNP (1 mM) inhibited ATP production by 50% in the human Jurkat T-cell lymphoma cell line after a 6 h incubation (225). Moreover, other chemically induced models of metabolic stress activate different signaling pathways and intracellular changes that DNP does not (see section 1.3.4). For example, H_2O_2 activates the NF-κB pathway (166). This made DNP an ideal choice of metabolic stressor.

It is possible that the changes seen in the T84 cell monolayers such as decreased TER and increased bacterial transcytosis were the result of cell death (15, 122, 210). However, we found that DNP (0.1 mM) was unable to induce caspase-3-mediated apoptosis in the T84 cell lines after a 24 h incubation period (210). We showed that there was no increase in LDH (a marker of tissue breakdown, Figure 7B) and no observed DNA laddering in Figure 7A. We have also previously shown that the pan-caspase inhibitor, benzyloxycarbonyl-Val-Ala-Asp fluoromethylketone (10-100 μM), affected neither the DNP+*E. coli* HB101-induced drop in TER nor the increase in bacterial translocation (15). In addition, administration of 1 mM DNP to Jurkat cells for 6 h did not induce apoptosis through a caspase-mediated pathway nor did it induce the release of cytochrome *c* from the mitochondrion (225). This was expected, as apoptosis is an energy-regulated mechanism. ATP depletion has been negatively associated with Fas-induced apoptosis in HeLa and Jurkat cells (226). Conversely, quick ATP depletion may induce necrosis (227). However, a trypan-blue staining assay revealed that DNP did not induce necrosis in T84 cells after 24 h (210).

Moreover, although DNP did not provoke the activation of the NF-κB pathway directly, there was an increase in NF-κB activation via phosphorylation of the IκB-α molecule when T84 cells were simultaneously exposed to both DNP and *E. coli* HB101 (Fig 16A and B). Interestingly, NF-κB activation is known to suppress apoptosis. An anti-tumor and anti-inflammatory molecule used in cancer treatment (Denbinobin) has been shown to inhibit the NF-κB pathway, induce mitochondrial dysfunction and increase apoptosis in Jurkat cells (228). Thus, DNP (0.1 mM) appears to be a suitable choice of metabolic stress as it did not cause cell death by apoptosis or necrosis in T84

cells but was still able to decrease ATP levels and induce mitochondrial swelling (Fig 4C and E), similar to that which has been seen in patients with IBD.

The composition of the microbiome in patients with IBD may contribute to disease propagation. As stated earlier, 99% of the gut microbiome is composed of *Firmicutes*, *Bacteriodes*, *Proteobacteria* and *Actinobacteria*. Sixty-four percent of those bacteria are *Firmicutes*, comprised mainly of the *Clostridium* XIVa and IV species (4). In patients with IBD, there is reduced diversity in the phylum *Firmicutes*, with particular decreases in *Clostridium leptum* group, specifically, the *Faecalibacterium prausnitzii* member (4, 132, 218, 229). In fact, low concentrations of *F. prausnitzii* at the time of ileal resection in patients with CD is a predictor of relapse (230). There is also marked expansions in the number of colonic *Proteobacteria* in some patients with IBD (4). *Proteobacteria* are Gram-negative bacteria and encompass a wide range of bacteria, including *Escherichia coli*, which have been implicated in IBD pathogenesis. Modifications in luminal concentrations of *E. coli* have been observed in patients with CD (4) and greater numbers of *E. coli* have been isolated in the ileum and mesenteric lymph nodes of patients with CD compared to controls (231-233). Antibody titers to *E. coli* are also much higher in the serum of patients with CD compared to controls (234). For instance, antibodies to *E. coli* are present in 37-55% of patients with CD, but in less than 5% of control subjects (235). *E. coli* have also been found in the colonic mucus layer of patients with UC (236).

Given the potentially important role that *E. coli* may play in the pathogenesis of IBD and barrier dysfunction, *E. coli* strain HB101 and F18 were the predominant bacterial strains used in our studies. These non-invasive and non-pathogenic strains of *E.*

coli were selected as many virulent forms of *E. coli* can cause alterations in paracellular permeability. For example, the adherent invasive strain of *E. coli* (AIEC) LF82s have been found in patients with CD. AIEC strains colonize the intestinal mucosa by adhering to epithelial cells. AIEC are also able to invade the epithelial cell through a macropinocytic-like process, ultimately resulting in their intracellular survival and replication. They can subsequently move into the mucosa and infect more cells including macrophages, where they are also able to survive and replicate extensively (90, 94, 237). This type of bacterium would not be ideal to use in this model system as any changes in barrier could not be directly attributed to metabolic stress. In addition, we were more interested in looking at how the epithelial cell interacts with commensal bacteria after being exposed to metabolic stress, induced in our studies by the chemical DNP.

4.2 Statistical Analysis

Sample sizes play a large role in statistics. Due to the nature of the experiments, it is possible that not all assays had sufficiently large enough sample sizes, thus accounting for the lack of significance. For instance, the F18 translocation scores at 4 h were found to be insignificant (Figure 8B) despite the apparent trend for reduced bacterial translocation upon the addition of butyrate to DNP+*E. coli* treated cells. This could be due to the fact that there were only 8-12 monolayers per treatment from 4 individual experiments. More repetitions of the experiment could be done to determine if the findings are significant.

4.3 Butyrate did not Improve the Paracellular Barrier Integrity in T84 Cell Monolayers

As previously mentioned, the intestinal barrier is highly regulated and many different exogenous and endogenous factors may influence its permeability. Several experiments have found that butyrate may act in a paradoxical fashion as it can both improve and worsen the barrier integrity in different situations. We found that butyrate (0.1-100 mM) when added alone to confluent T84s, as seen in Figure 6A, does not induce a change in the transepithelial electrical resistance (TER) before 48 h. Other studies have shown that T84 epithelial cell monolayers and segments of rat caecum mounted in Ussing chambers did not experience changes in permeability when exposed to 20 mM butyrate (238). Conversely, low concentrations (<5 mM) of butyrate increased the TER across Caco-2 monolayers (239-241). This was most likely due to butyrate's ability to induce Caco-2 differentiation while slowing cell division (239, 241). Butyrate was able to increase Caco-2 production of alkaline phosphatase, a hydrolase enzyme found in the brush border of the small intestine that is a known marker of cellular differentiation (242). There was also an increase in the doming of the cells, another indicator of a differentiated cell as they become polarized for vectoral secretion (239, 242). As cells differentiate, the TJ strand count increases, resulting in an increased TER (243). Undifferentiated cells originate in the crypts but differentiate as they migrate up the crypt wall. At the top of the villus (or at the crypt surface in the colon), the cells are exposed to more antigens than cells in the crypts below, accounting for the increased requirement for more TJs. Since butyrate does not induce differentiation in T84s in the same manner as in the Caco-2 cell line, it is likely that no further TJ strand assembly occurred and, thus,

the TER did not change. Butyrate also failed to alter brush-border hydrolase activity in human colonic C2/bbe (C2) monolayers, indicating that butyrate does not alter differentiation in all intestinal epithelial cell lines (244).

Some concentrations of butyrate impair the colonic barrier. We found that concentrations ≥20 mM induced drastic decreases in the TER (Fig 6A). Likewise, concentrations of butyrate ranging from 1-5 mM increased the TER in rat tissue as shown in Ussing chamber studies; however, high doses of butyrate (10 mM) decreased the TER (245). Exposure to concentrations >5 mM also decreased TER across Caco-2 monolayers, resulting in leaky barriers and apoptosis (239, 240, 246, 247).

Butyrate has several effects on the colon in addition to providing energy. It has long been known that a diet high in fiber provides protection against colon cancer which may explain why butyrate induces cell death in cancer-derived cell lines (248, 249). One proposed mechanism for preventing cancer progression is through the inhibition of histone deacetylase (249-251), which results in the hyperacetylation of histones, making the nucleosomal DNA more accessible to transcription factors (252-254). This process could activate apoptotic genes and inhibit cell proliferation (252, 255-257). It has been proposed that butyrate inhibits cell progression through G1 phase by inducing two inhibitors of the cell cycle, p21 and cyclin D3 (252, 253). Butyrate has also been shown to alter the plasminogen/plasmin system (PPS). Increased serum levels of PPS correlate with more aggressive colon cancer (258). However, butyrate *in vitro* has been found to decrease plasminogen activator activity (259, 260). Butyrate is also able to prevent cancer progression by inhibiting decay-accelerating factor expression (261) and pro-metastatic metalloproteinase activation (248, 249) resulting in an inhibition of tumor

migration. Finally, it is also able to inhibit tumor-induced angiogenesis through decreasing vascular endothelial growth factor and hypoxia-inducible factor-1α (249).

Another possible explanation for butyrate-induced apoptosis of cancer cell lines is that the high doses of butyrate may be toxic to the cell. Physiological concentrations of butyrate are in the 30 mM range, however, there is a thick mucus lining over the epithelial cells which may dilute the concentration of butyrate that the cells are directly exposed to (262).

4.4 Other SCFAs Cannot Replicate Butryate's Ability to Protect the Transcellular Pathway

As mentioned in section 1.4.1, several other SCFAs, namely acetate (c2) and proprionate (c3), are produced in addition to butyrate through the fermentation of non-starch soluble dietary fibers (178). As acetate is the most abundant SCFA in the colon, we administered 3 mM of acetate to the T84 colonic epithelium. We found that acetate alone did not improve the TER of T84 cells and co-administration of 3 mM acetate with DNP to T84 cells did not alter the *E. coli* HB101 transcytosis (Fig 11), nor did it correct the paracellular perturbation.

Our findings contrast with other studies. Rat caecal wall tissue was mounted in an Ussing chamber and both proprionate and acetate (20 mM and 40 mM for both SCFAs) increased the TER across the tissue. Moreover, TER increases were observed in both T84 and Caco-2 cells 30 minutes after the administration of either acetate (40 mM or 80 mM) or proprionate (20 mM and 40 mM) (238). Mariadason also found that the addition of 16 mM proprionate and 32 mM acetate induced a greater increase in TER

compared to butyrate administration in Caco-2 cells (239). We failed to see a change in TER when administering acetate most likely because the concentration used was not high enough. There is a reduced ability of acetate and proprionate to cross the cell membrane due to the lowered lipid solubility with decreasing chain lengths of SCFAs (263). Using 3 mM of acetate would likely not result in sufficient intracellular concentrations in the T84s to induce a paracellular or transcellular change. However, while the high doses of SCFAs used in other studies were closer to physiological concentrations, they may not be relevant as the thick layer of mucus would dilute the concentrations of SCFAs reaching the epithelium. Lastly, the investigators observed these effects within 30 minutes of adding the SCFAs onto the monolayer. That time point was not suitable for this study as changes with DNP and bacterial transcytosis are not apparent until 4 h post-treatment.

4.5 Butyrate Inhibits Inflammation Through Modifying the NF-κB Pathway

As described in Figure 8A and 8B, butyrate was able to inhibit transcytosis of the commensal bacteria across T84 cells that had been metabolically stressed. We have previously reported that pharmacological inhibition of the NF-κB pathway prevented bacterial transcytosis (210). Thus, we examined butyrate's interactions with the NF-κB pathway. The NF-κB family of transcription factors consists of 5 members: p50, p52, p65 (RelA), c-Rel and RelB. These members share an NH_2-terminal Rel homology domain that allows the dimers to bind to DNA while their C-terminal contains hydrophobic residues that provide a dimerization interface between subunits. The dimers bind to κB sites within the promoters or enhancers of target genes and recruit co-activators and co-repressors. The transcriptionally active domain (TAD) is necessary for

positive gene expression but is only present on p65, c-Rel and RelB. p50 and p52 lack TAD, and this represses transcription unless they are in the presence of a dimer containing TAD. In its inactive state, the dimers are associated with one of 3 typical IκB proteins: IκB-α, IκB–β or IκB-ε. The IκBs are responsible for maintaining NF-κB dimers in the cytoplasm. The IκB-α masks the nuclear localization sequence of p65 and, in conjunction with the nuclear export sequences on the IκB-α, maintains cytoplasmic localization. The IκBs are targeted for ubiquitination and degradation upon phosphorylation by the IKK molecules. IKK-β is both necessary and sufficient to phosphorylate either IκB-α or IκB–β. IKK-α can also mediate IκB-α phosphorylation (reviewed in (216)). Through western blot and ELISA analyses, we found that butyrate was able to prevent the phosphorylation of IκB-α, thus, butyrate prevented NF-κB activation (Fig 16A, B and C).

Butyrate's suppression of the NF-κB pathway has been reported by other investigators. For instance, Inan *et al.* found that pre-treatment of HT-29 epithelial cells with butyrate for 18 h was able to prevent constitutive p50 dimer activity as well as reduce NF-κB activation by TNF-α (264), potentially by preventing IκB-α degradation (133, 265). It may be argued that the mechanisms of action of butyrate are cell-line dependent, as Lurs *et al.* discovered that a 48 h pre-treatment with butyrate prevents TNF-α-mediated phosphorylation and subsequent ubiquitination of IκB-α in the colonic adenocarcinoma cells SW480/SW620 (266). However, Wu *et al.* showed that butyrate inhibits activation of the IL-8 gene by inducing the expression of the inhibitor molecule IκB-β in the Caco-2 cell line (267). Another study showed that co-treatment of Caco-2 cells with both Pam3CSK4 (a TLR-2 ligand) and butyrate prevented NF-κB activation

through inducing expression of the A20 protein, an endogenous inhibitor of the NF-κB pathway (268).

Phosphorylated IκB-α is ubiquitinated by the ubiquitin ligase complex E3-SCF$^{\beta\text{-TrCP}}$. The E3-SCF complexes are regulated themselves by covalent modifications. NEDD8 must be conjugated to the Cullin-1 subunit of the E3-SCF molecule to possess ubiquitin ligase activity (269, 270). Fifteen to 90 minute incubations with 5 mM butyrate were able to prevent constitutive neddylation of the Cullin-1 subunit in T84 cells. However, this was done in acidic conditions (pH 4.5-5). Given that butyrate's pKa is 4.5, acidic conditions would protonate butyrate, and, thus, increase the amount of butyrate-diffusion across the plasma membrane. When the cell medium was at a neutral pH, butyrate was unable to prevent the neddylation of Cullin-1. We also observed that butyrate did not neddylate Cullin-1 at neutral pH (Fig 16E). However, IκB-α phosphorylation was still prevented, indicating that butyrate must have exerted a different mechanism of action to prevent NF-κB activation.

Support of a theory involving the interaction of butyrate with NF-κB also comes from the ability of butyrate to reduce inflammation in the colon. NF-κB controls the expression of several genes including many inflammatory cytokines, chemokines, inducible nitric oxide synthase, growth factors, immune receptors and more (216). IL-8 is a member of the C-X-C family of chemokines that is responsible for the attraction of neutrophils to an infected area. Neutrophils will secrete cytokines and chemokines to recruit more inflammatory cells in order to amplify the immune response. Co-treatment of Caco-2 epithelial cells with either Pam3CSK4 or IL-1β induces IL-8 production (which causes neutrophil migration) that is reduced by co-treatment with butyrate (268,

271, 272). Others have found that butyrate reduced the production of inflammatory mediators (e.g. IL-6, prostaglandin E_2) by stimulated human intestinal microvascular endothelial cells (273). Butyrate decreased TNF-α production and pro-inflammatory cytokine mRNA expression in intestinal biopsies and lamina propria mononuclear cells from patients with CD (133). Butyrate abolished LPS-induced expression of cytokines by peripheral blood mononuclear cells (133). Song *et al.* reported that butyrate enemas may decrease IL-1β serum levels and tissue myeloperoxidase activity (an indication of neutrophil infiltration) in trinitrobenzene sulphonic acid (TNBS) induced colitis in rats (274). Fiber supplemented diets (i.e. prebiotics) also reduce TNF-α serum levels in TNBS treated rats (275). The severity of DSS-induced colitis was reduced in mice fed germinated barley foodstuff (GBF; rich in fiber and a precursor for butyrate production), as gauged by decreased tissue IL-6 levels and mucosal damage (206).

Apart from NF-κB, butyrate may also exert anti-inflammatory effects through histone deacetylase inhibition, (273), inhibition of IFN-γ-production and/or signaling (276, 277), and perhaps through PPAR- γ activation (278, 279).

4.6 Butyrate May Modulate the Barrier by Providing an Energy Source

Butyrate is the preferred energy source of colonocytes (215), so it is plausible that butyrate is inhibiting increases in transcellular transport by providing exogenous energy. Glucose added to the cell media as an exogenous energy source did not prevent the decrease in TER (Fig 14A), but was able to prevent the passage of bacteria into the basal chamber of the culture well (Fig 14B). This was not an osmotic effect as equi-molar mannitol did not prevent translocation. Likewise, it was not due to the glucose uptake as

a non-metabolizable form of glucose (3-O-methyl-D-glucopyranose) did not prevent the increase in bacterial internalization.

Hydrogen sulfide (H_2S) is a bacterial metabolite present in the lumen of the large intestine. Sulfur-reducing bacteria ferment sulfur-containing amino acids into H_2S (280, 281). H_2S has been implicated in the inhibition of β-oxidation of butyrate, thus, potentially reducing ATP generation (282). Patients with UC are found to have increased levels of hydrogen sulfide in their feces (281) which is possibly linked to the increased amount of sulfate-reducing bacteria in these patients (283). The use of NaHS *in vitro* impaired butyrate metabolism (284), but did not prevent the butyrate-induced increase in TER in confluent Caco-2 monolayers (239). Thus, butyrate may function to protect barrier integrity in different manners. First, butyrate may inhibit translocation via an energy-dependent process which is dependent upon the metabolism of butyrate. Second, the simple transportation of butyrate across the cell membrane, or the activation of a signaling cascade by intracellular butyrate may influence both the paracellular and transcellular pathways.

4.7 Future Experiments

The observed butyrate-induced reduction in: 1) bacterial transcytosis of both invasive and non-invasive bacteria (Fig 12A, B and C); 2) mitochondrial dysfunction as shown by both the MTT assay (Fig 5) and TEM images (Fig 4G); and 3) NF-κB activation (Fig 16A) suggest that butyrate prevents aberrant bacterial translocation and is important in maintaining barrier in times of metabolic stress. These findings, combined with research showing that some patients with IBD have reduced fecal concentrations of

butyrate (285), necessitate an investigation into the possible role of butyrate maintaining gut homeostasis. This research could shed some light onto the development of barrier disruption as a result of metabolic stress.

Examining bacterial dysbiosis could provide insight into the consequences of metabolic stress. Mice could be given amoxicillin-clavulanic acid, an antibiotic that causes the disappearance of butyrate producing *Clostridium* XIVa and IV species in patients within 4 days of the treatment (286) ± an intra-rectal administration of DNP. We have reported in the past that installation of DNP into the ileum of rats induces mitochondrial swelling and increased bacterial attachment within 6 h of treatment (122). It would be interesting to see if removing the major butyrate-producing bacteria would worsen the prognosis of metabolic stress induced by DNP treatment or if characteristics of stress and increased permeability in colonic epithelia can be induced in bacteria-depleted mice in the absence of DNP.

An in-depth inquisition into the mechanism by which the combination of DNP with commensal bacteria is causing or maintaining barrier dysfunction could provide insight into how butyrate is able to prevent bacterial translocation. It may be possible that cells treated with DNP are releasing a chemical mediator that alters the gene expression in bacteria. This could be determined by collecting the media from DNP-treated cells and control cells. The media would then be added to a reporter assay for bacterial genes to look for changes in gene expression.

Contrary to that approach, it should be investigated what DNP+*E. coli* are doing to the cells to increase the number of pseudopodia. *E. coli* HB101 alone does not significantly increase the number of pseudopodia compared to control monolayers, while

DNP alone does. Together, however, the treatments appear to synergistically increase the number and length of membrane extensions in T84 cells. The administration of LPS and TNF-α, which should initiate the NF-κB pathway, does not cause a significant increase in the number of pseudopodial extensions. Thus, a number of different signaling pathways including the PI-3K and MAPK pathways could be examined to determine if they are modified in the presence of DNP+*E. coli* HB101.

As discussed in section 1.3.4, there are a plethora of sources of metabolic stress. To ensure that butyrate protects against many different sources of mitochondrial dysfunction, other metabolic inhibitors such as hydrogen peroxide, Actinomycin A, oligomysin and NSAIDs could be used in DNP's place.

Moreover, other SCFAs have been implicated in having protective effects on the epithelium (239). Although acetate was assessed (Fig 11), the dose may have been too low to have a noticeable effect. Thus, a dose-response experiment should be done to assess the activities of acetate and proprionate on changes in paracellular permeability and translocation.

Butyrate's precise mechanisms of action have yet to be elucidated. It appears that butyrate improves barrier integrity through several means. For instance, inhibiting butyrate metabolism through the use of NaHS did not inhibit butyrate's ability to increase the TER in Caco-2 monolayers (239), potentially implicating the involvement of butyrate transporters in this phenomenon. Furthermore, butyrate prevented the neddylation of Cullin-1 when experiments were carried out in acidic media, though neutral media conditions did not produce this effect (217). Acidifying the media protonates butyrate and reduces the amount of the SCFA being transferred into the cell via the transporter but

increases simple diffusion of butyrate. Moreover, we found that IκB-α phosphorylation was still being inhibited under neutral conditions, indicating that the transport or metabolism of butyrate may be involved in signaling. Collectively, the data suggest that butyrate metabolism and its means of transport into the cell both play unique mechanistic roles. To elucidate these mechanisms, NaHS could be used to inhibit butyrate metabolism and its effects on signal transduction and translocation could be examined. Additionally, the selective inhibitor of the MCT-1 transporter, p-(chloromercuric) benzenesulfonic acid (287), could be employed for translocation studies.

The method by which butyrate inhibits IκB-α phosphorylation and/or degradation is unknown. PPARs are a set of three nuclear receptors (α, γ, σ). They inhibit NF-κB signaling through inhibiton of IκB-α degradation, reduced RelA nuclear translocation and decreased RelA-DNA binding (reviewed in (288)). Interestingly, the endogenous ligands of the intestinal PPAR-γ are fatty acids (reviewed in (289)). Thus, looking at reporter assays for PPAR- γ activation might provide insight into the mechanism of butyrate.

Although it is unknown if barrier defects are the cause or effect of IBD, it would be interesting to determine if butyrate may function as a prophylactic treatment in preventing aberrant breaches in barrier. IL-$10^{-/-}$ mice spontaneously develop colitis when moved out of a germ-free environment and their breach in permeability has been suggested to preceed overt inflammation (121). Thus, IL-$10^{-/-}$ mice would be given twice daily enemas of butyrate before and after their transfer out of an aseptic holding space into normal conditions. The mice would be examined histologically and given clinical scores. Also, their gut permeability would be measured to determine if butyrate may function to delay the onset of barrier disruption.

Patient compliance of butyrate treatment may be low as it is administered in the form of enemas and is notorious for having an unpleasant odor. Butyrate as a prophylactic could prevent or delay disease onset in subsets of patients with IBD, however, administration must become more pleasant. Prebiotics, as discussed in section 1.4.4, may be equally as effective as butyrate in protecting the barrier. To verify this hypothesis, mice would either be fed prebiotics or normal chow±butyrate enemas before administering dinitrobenzene sulphonic acid (DNBS) to induce colitis. The mice would be examined for changes in clinical scores, increases in permeability and histological damage. The colonic flora of the mice would also be examined before, during and after administration of DNBS to determine if there are any microflora changes due to the prebiotics and/or DNBS colitis.

4.8 Significance

The production of butyrate plays a role in maintaining gut homeostasis and a decrease in the production of butyrate, or improper metabolism thereof, results in impaired colonic barrier function. In this study, we tested the hypothesis that butyrate acts to prevent the increase in transcellular passage of commensal *E. coli* across metabolically stressed colonocytes. We have demonstrated that butyrate (3 mM) was unable to increase the TER in both confluent T84 monolayers and colonic epithelia exposed to DNP+*E. coli* HB101. However, co-incubation of butyrate with the DNP prevented *E. coli* (strains HB101 and F18) internalization and translocation at 4 h post-treatment across T84 cells. This phenomenon had waned by 24 h, however re-administration of butyrate every 4 h maintained the decreased level of translocation at

24 h post-treatment. These results were not found when an equi-molar concentration of the abundant SCFA acetate was used in butyrate's place. The decrease in bacterial internalization could have been due to butyrate's ability to reduce the number of pseudopodial extentions protruding from the metabolically stressed enterocytes.

Butryate may be exerting these effects in a few manners. As butyrate is an energy source, it is intuitive that it might counteract the reduced levels of ATP in the DNP-treated T84s, particularly since exogenous glucose was able to prevent the increase in bacterial translocation. Also, butyrate induced mitochondrial regenesis and prevented mitochondrial dysfunction as assessed by the MTT assay. Butyrate may also be interfering with signaling pathways. Butyrate prevented the activation of the NF-κB pathway by reducing IκB-α phosphorylation through an unknown mechanism.

In normal, homeostatic conditions, the microflora is composed of several different bacteria, some which will ferment dietary fibers to produce butyrate (Fig 18A). The epithelium may experience metabolic stressors induced bya variety of sources including medications, alcohol consumption, and infections. This may cause the TJs to loosen and bacteria may translocate across the epithelium. However, butyrate is present in these "normal" conditions to help maintain gut homeostasis by preventing NF-κB activation and will restore the energy imbalance once the metabolic stressor has been removed. Some individuals have bacterial dysbiosis and thus, will have insufficient butyrate production (Fig 18B). Should an insult resulting in metabolic stress occur in these individuals, butyrate will not be present to prevent NF- κB activation. Thus, abberant bacterial transcytosis will occur coupled with in increase in the paracellular permeability. This will ultimately result in inflammation (Fig 18C). We suggest that cohorts of

individuals who are susceptible to IBD (e.g. first degree relatives of patients with IBD) should be enrolled in a study monitoring the prophylactic ability of exogenous butyrate to prevent disease onset. Similarily, certainly, butyrate may not be able to "cure" active disease in individuals. However, butyrate (or substrates there of) should be given to IBD patients in times of remission to prevent disease relapse.

A

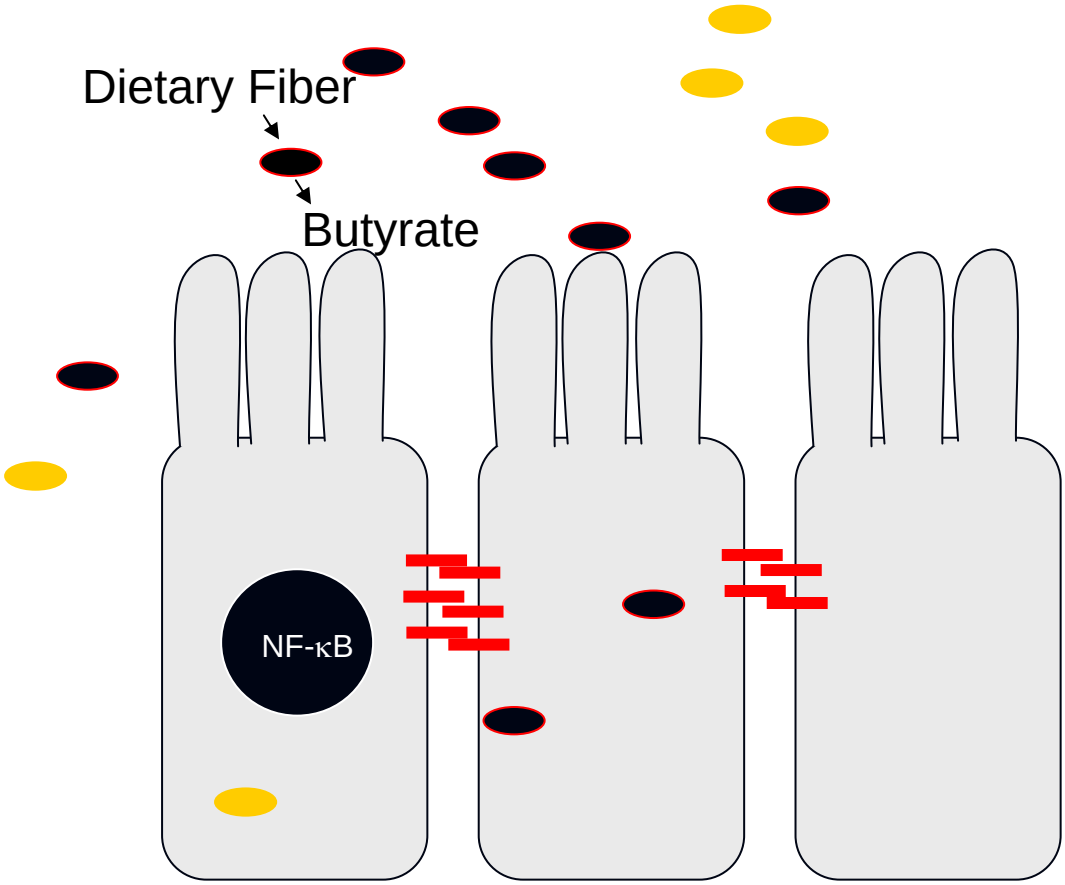

B

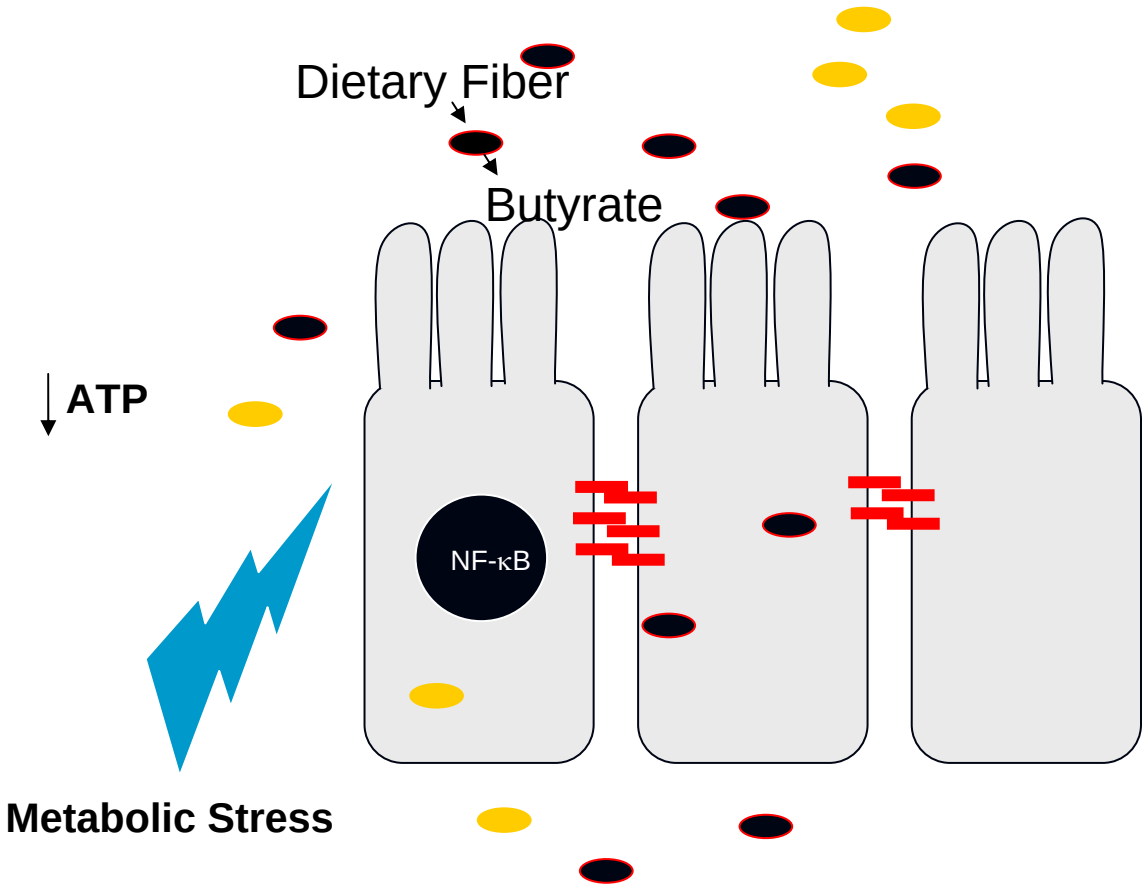

C

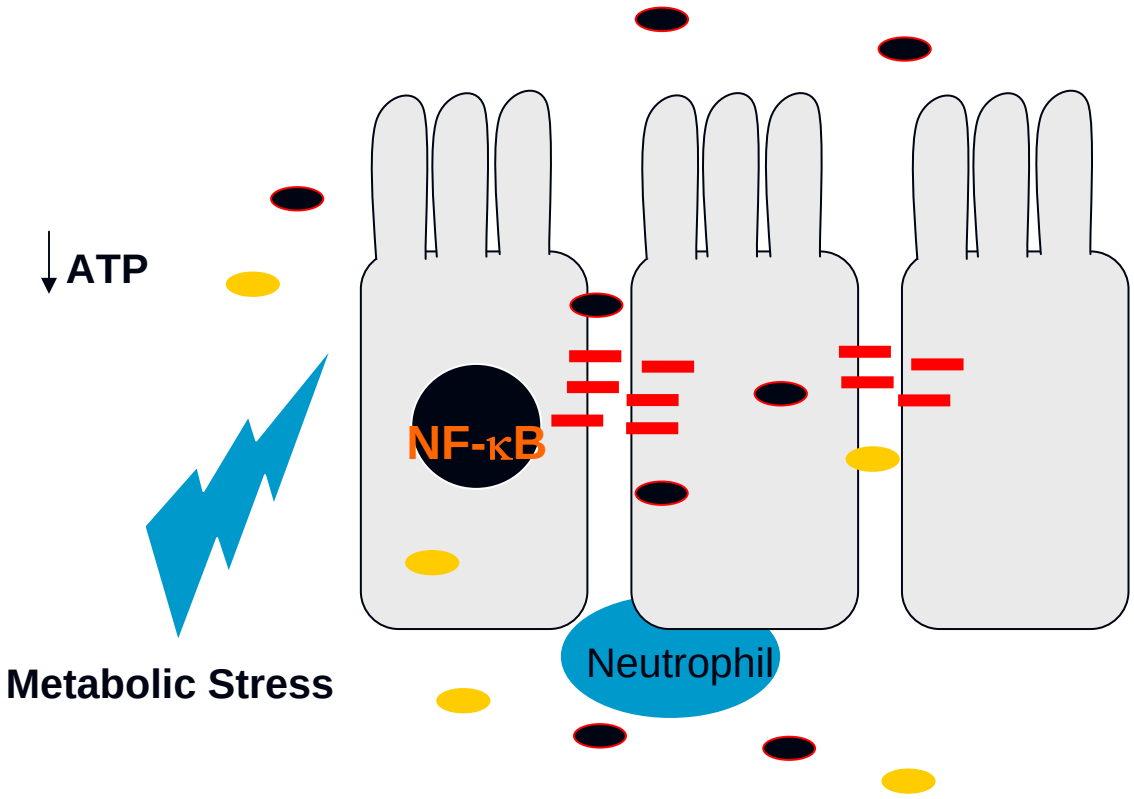

Figure 18. Butyrate prevents abberant bacterial translocation. Certain strains of bacteria in the normal microflora of the human intestine produce butyrate, a SCFA, which is the main energy source for the colonic epithelium. In this state, there is minimal bacterial translocation and the tight junction integrity is maintatined (panel A). Occasionally, sources of metabolic stress may decrease levels of colonic ATP production. This may cause a transient opening of the tight junctions and some transcellular passage of bacteria. However, once the insult is removed, butyrate will restore the cellular ATP and homeostasis will be maintained (panel B). Should the same insult occur in a patient that has bacterial dysbiosis, with a particular decrease in the butyrate-producing bacteria, butyrate will not be there to counteract the decrease in ATP production and prevent NF-κB activation, resulting in excessive amounts of bacterial translocation as well as an increase in the paracellular permeability. This will ultimately result in inflammation (panel C).

References

1. Van der Flier LG, Clevers H. Stem cells, self-renewal, and differentiation in the intestinal epithelium. *Annu Rev Physiol*. 2009;71:241-260.

2. Barrett KE. Gastrointestinal physiology. The McGraw-Hill Companies Inc., 2006:4-7.

3. Sansonetti PJ. War and peace at mucosal surfaces. *Nat Rev Immunol*. 2004;4:953-64.

4. Frank DN, St Amand AL, Feldman RA, Boedeker EC, Harpaz N, Pace NR. Molecular-phylogenetic characterization of microbial community imbalances in human inflammatory bowel diseases. *Proc Natl Acad Sci U S A*. 2007;104:13780-5.

5. Atarashi K, Nishimura J, Shima T, Umesaki Y, Yamamoto M, Onoue M, *et al*. ATP drives lamina propria T(H)17 cell differentiation. *Nature*. 2008;455:808-12.

6. Rakoff-Nahoum S, Paglino J, Eslami-Varzaneh F, Edberg S, Medzhitov R. Recognition of commensal microflora by toll-like receptors is required for intestinal homeostasis. *Cell*. 2004;118:229-41.

7. Hooper LV, Gordon JI. Commensal host-bacterial relationships in the gut. *Science*. 2001;292:1115-8.

8. Shanahan F. The host-microbe interface within the gut. *Best Pract Res Clin Gastroenterol*. 2002;16:915-31.

9. MacDonald TT, Carter PB. Requirement for a bacterial flora before mice generate cells capable of mediating the delayed hypersensitivity reaction to sheep red blood cells. *J Immunol*. 1979;122:2624-9.

10. Rook GA, Stanford JL. Give us this day our daily germs. *Immunol Today*. 1998;19:113-6.

11. Mazmanian SK, Liu CH, Tzianabos AO, Kasper DL. An immunomodulatory molecule of symbiotic bacteria directs maturation of the host immune system. *Cell*. 2005;122:107-18.

12. Madara JL, Patapoff TW, Gillece-Castro B, Colgan SP, Parkos CA, Delp C, *et al.* 5'-adenosine monophosphate is the neutrophil-derived paracrine factor that elicits chloride secretion from T84 intestinal epithelial cell monolayers. *J Clin Invest*. 1993;91:2320-5.

13. Rodal SK, Skretting G, Garred O, Vilhardt F, van Deurs B, Sandvig K. Extraction of cholesterol with methyl-beta-cyclodextrin perturbs formation of clathrin-coated endocytic vesicles. *Mol Biol Cell*. 1999;10:961-74.

14. Subtil A, Gaidarov I, Kobylarz K, Lampson MA, Keen JH, McGraw TE. Acute cholesterol depletion inhibits clathrin-coated pit budding. *Proc Natl Acad Sci U S A*. 1999;96:6775-80.

15. Nazli A, Wang A, Steen O, Prescott D, Lu J, Perdue MH, *et al*. Enterocyte cytoskeleton changes are crucial for enhanced translocation of nonpathogenic *Escherichia coli* across metabolically stressed gut epithelia. *Infect Immun*. 2006;74:192-201.

16. Alberts B, Johnson A, Lewis J, Raff M, Roberts K, Walter P. Molecular biology of the cell. 4th ed. Garland Science; 2002.

17. Gonzalez-Mariscal L, Betanzos A, Nava P, Jaramillo BE. Tight junction proteins. *Prog Biophys Mol Biol*. 2003;81:1-44.

18. Madara JL. Warner-Lambert/Parke-davis award lecture. Pathobiology of the intestinal epithelial barrier. *Am J Pathol*. 1990;137:1273-81.

19. Gewirtz AT, Liu Y, Sitaraman SV, Madara JL. Intestinal epithelial pathobiology: Past, present and future. *Best Pract Res Clin Gastroenterol*. 2002;16:851-67.

20. Perez M, Barber A, Ponz F. Effect of osmolarity on the epithelial paracellular permeability in rat jejunum. *Rev Esp Fisiol*. 1996;52:103-12.

21. Laker MF, Menzies IS. Increase in human intestinal permeability following ingestion of hypertonic solutions. *J Physiol*. 1977;265:881-94.

22. Mitic LL, Anderson JM. Molecular architecture of tight junctions. *Annu Rev Physiol*. 1998;60:121-42.

23. Niessen CM. Tight junctions/adherens junctions: Basic structure and function. *J Invest Dermatol*. 2007;127:2525-32.

24. Pappenheimer JR, Reiss KZ. Contribution of solvent drag through intercellular junctions to absorption of nutrients by the small intestine of the rat. *J Membr Biol*. 1987;100:123-36.

25. Turner JR, Cohen DE, Mrsny RJ, Madara JL. Non-invasive *in vivo* analysis of human small intestinal paracellular absorption: Regulation by Na^+-glucose cotransport. *Dig Dis Sci*. 2000;45:2122-6.

26. Turner JR, Madara JL. Physiological regulation of intestinal epithelial tight junctions as a consequence of Na^+-coupled nutrient transport. *Gastroenterology*. 1995;109:1391-6.

27. Atisook K, Madara JL. An oligopeptide permeates intestinal tight junctions at glucose-elicited dilatations: Implications for oligopeptide absorption. *Gastroenterology*. 1991;100:719-24.

28. Madara JL, Stafford J. Interferon-gamma directly affects barrier function of cultured intestinal epithelial monolayers. *J Clin Invest*. 1989;83:724-7.

29. Terpend K, Boisgerault F, Blaton MA, Desjeux JF, Heyman M. Protein transport and processing by human HT29-19A intestinal cells: Effect of interferon-gamma. *Gut*. 1998;42:538-45.

30. Mullin JM, Laughlin KV, Marano CW, Russo LM, Soler AP. Modulation of tumor necrosis factor-induced increase in renal (LLC-PK1) transepithelial permeability. *Am J Physiol*. 1992;263:915-24.

31. Schmitz H, Fromm M, Bentzel CJ, Scholz P, Detjen K, Mankertz J, *et al*. Tumor necrosis factor-alpha (TNFalpha) regulates the epithelial barrier in the human intestinal cell line HT-29/B6. *J Cell Sci*. 1999;112:137-46.

32. Bruewer M, Luegering A, Kucharzik T, Parkos CA, Madara JL, Hopkins AM, *et al*. Proinflammatory cytokines disrupt epithelial barrier function by apoptosis-independent mechanisms. *J Immunol*. 2003;171:6164-72.

33. McKay DM, Croitoru K, Perdue MH. T cell-monocyte interactions regulate epithelial physiology in a co-culture model of inflammation. *Am J Physiol*. 1996;270:C418-28.

34. Zareie M, McKay DM, Kovarik GG, Perdue MH. Monocyte/macrophages evoke epithelial dysfunction: Indirect role of tumor necrosis factor-alpha. *Am J Physiol*. 1998;275:C932-9.

35. Ozaki H, Ishii K, Horiuchi H, Arai H, Kawamoto T, Okawa K, *et al*. Cutting edge: Combined treatment of TNF-alpha and IFN-gamma causes redistribution of junctional adhesion molecule in human endothelial cells. *J Immunol*. 1999;163:553-7.

36. Di Leo V, Yang PC, Berin MC, Perdue MH. Factors regulating the effect of IL-4 on intestinal epithelial barrier function. *Int Arch Allergy Immunol*. 2002;129:219-27.

37. Berin MC, Yang PC, Ciok L, Waserman S, Perdue MH. Role for IL-4 in macromolecular transport across human intestinal epithelium. *Am J Physiol*. 1999;276:C1046-52.

38. Colgan SP, Resnick MB, Parkos CA, Delp-Archer C, McGuirk D, Bacarra AE, *et al*. IL-4 directly modulates function of a model human intestinal epithelium. *J Immunol*. 1994;153:2122-9.

39. Parkos CA. Cell adhesion and migration. Neutrophil adhesive interactions with intestinal epithelium. *Am J Physiol*. 1997;273:G763-8.

40. Zund G, Madara JL, Dzus AL, Awtrey CS, Colgan SP. Interleukin-4 and interleukin-13 differentially regulate epithelial chloride secretion. *J Biol Chem*. 1996;271:7460-4.

41. Heller F, Fromm A, Gitter AH, Mankertz J, Schulzke JD. Epithelial apoptosis is a prominent feature of the epithelial barrier disturbance in intestinal inflammation: Effect of pro-inflammatory interleukin-13 on epithelial cell function. *Mucosal Immunol*. 2008;1:S58-61.

42. Prasad S, Mingrino R, Kaukinen K, Hayes KL, Powell RM, MacDonald TT, *et al*. Inflammatory processes have differential effects on claudins 2, 3 and 4 in colonic epithelial cells. *Lab Invest*. 2005;85:1139-62.

43. Grisendi S, Arpin M, Crepaldi T. Effect of hepatocyte growth factor on assembly of zonula occludens-1 protein at the plasma membrane. *J Cell Physiol*. 1998;176:465-71.

44. Van Itallie CM, Balda MS, Anderson JM. Epidermal growth factor induces tyrosine phosphorylation and reorganization of the tight junction protein ZO-1 in A431 cells. *J Cell Sci*. 1995;108:1735-42.

45. Nusrat A, Turner JR, Madara JL. Molecular physiology and pathophysiology of tight junctions. IV. Regulation of tight junctions by extracellular stimuli: Nutrients, cytokines, and immune cells. *Am J Physiol Gastrointest Liver Physiol*. 2000;279:G851-7.

46. Sandilands A, Sutherland C, Irvine AD, McLean WH. Filaggrin in the frontline: Role in skin barrier function and disease. *J Cell Sci*. 2009;122:1285-94.

47. Cossart P, Sansonetti PJ. Bacterial invasion: The paradigms of enteroinvasive pathogens. *Science*. 2004;304:242-8.

48. Fasano A, Nataro JP. Intestinal epithelial tight junctions as targets for enteric bacteria-derived toxins. *Adv Drug Deliv Rev*. 2004;56:795-807.

49. Gruenheid S, Finlay BB. Microbial pathogenesis and cytoskeletal function. *Nature*. 2003;422:775-81.

50. Peralta-Ramirez J, Hernandez JM, Manning-Cela R, Luna-Munoz J, Garcia-Tovar C, Nougayrede JP, *et al*. EspF interacts with nucleation-promoting factors to recruit junctional proteins into pedestals for pedestal maturation and disruption of paracellular permeability. *Infect Immun*. 2008;76:3854-68.

51. Pothoulakis C. Effects of *Clostridium difficile* toxins on epithelial cell barrier. *Ann N Y Acad Sci*. 2000;915:347-56.

52. Hecht G, Koutsouris A, Pothoulakis C, LaMont JT, Madara JL. *Clostridium difficile* toxin B disrupts the barrier function of T84 monolayers. *Gastroenterology*. 1992;102:416-23.

53. Schmitz H, Barmeyer C, Fromm M, Runkel N, Foss HD, Bentzel CJ, *et al*. Altered tight junction structure contributes to the impaired epithelial barrier function in ulcerative colitis. *Gastroenterology*. 1999;116:301-9.

54. Meddings JB, Sutherland LR, May GR. Intestinal permeability in patients with Crohn's disease. *Gut*. 1994;35:1675-6.

55. Nikolaus S, Schreiber S. Diagnostics of inflammatory bowel disease. *Gastroenterology*. 2007;133:1670-89.

56. Clayburgh DR, Shen L, Turner JR. A porous defense: The leaky epithelial barrier in intestinal disease. *Lab Invest*. 2004;84:282-91.

57. Rogers BH, Clark LM, Kirsner JB. The epidemiologic and demographic characteristics of inflammatory bowel disease: An analysis of a computerized file of 1400 patients. *Journal of Chronic Diseases*. 1971;24:743-73.

58. Hendrickson BA, Gokhale R, Cho JH. Clinical aspects and pathophysiology of inflammatory bowel disease. *Clin Microbiol Rev*. 2002;15:79-94.

59. Sanchez-Munoz F, Dominguez-Lopez A, Yamamoto-Furusho JK. Role of cytokines in inflammatory bowel disease. *World J Gastroenterol*. 2008;14:4280-8.

60. Xavier RJ, Podolsky DK. Unravelling the pathogenesis of inflammatory bowel disease. *Nature*. 2007;448:427-34.

61. Podolsky DK. Inflammatory bowel disease. *N Engl J Med*. 2002;347:417-29.

62. Mathew CG. New links to the pathogenesis of Crohn disease provided by genome-wide association scans. *Nat Rev Genet*. 2008;9:9-14.

63. Hampe J, Cuthbert A, Croucher PJ, Mirza MM, Mascheretti S, Fisher S, *et al*. Association between insertion mutation in NOD2 gene and Crohn's disease in German and British populations. *Lancet*. 2001;357:1925-8.

64. Hugot JP, Chamaillard M, Zouali H, Lesage S, Cezard JP, Belaiche J, *et al*. Association of NOD2 leucine-rich repeat variants with susceptibility to Crohn's disease. *Nature*. 2001;411:599-603.

65. Barrett JC, Hansoul S, Nicolae DL, Cho JH, Duerr RH, Rioux JD, *et al*. Genome-wide association defines more than 30 distinct susceptibility loci for Crohn's disease. *Nat Genet*. 2008;40:955-62

66. Duchmann R, Kaiser I, Hermann E, Mayet W, Ewe K, Meyer zum Buschenfelde KH. Tolerance exists towards resident intestinal flora but is broken in active inflammatory bowel disease (IBD). *Clin Exp Immunol*. 1995;102:448-55.

67. Madsen KL, Malfair D, Gray D, Doyle JS, Jewell LD, Fedorak RN. Interleukin-10 gene-deficient mice develop a primary intestinal permeability defect in response to enteric microflora. *Inflamm Bowel Dis*. 1999;5:262-70.

68. Song F, Ito K, Denning TL, Kuninger D, Papaconstantinou J, Gourley W, *et al*. Expression of the neutrophil chemokine KC in the colon of mice with enterocolitis and by intestinal epithelial cell lines: Effects of flora and proinflammatory cytokines. *J Immunol*. 1999;162:2275-80.

69. Contractor NV, Bassiri H, Reya T, Park AY, Baumgart DC, Wasik MA, *et al*. Lymphoid hyperplasia, autoimmunity, and compromised intestinal intraepithelial lymphocyte development in colitis-free gnotobiotic IL-2-deficient mice. *J Immunol*. 1998;160:385-94.

70. Matsumoto S, Okabe Y, Setoyama H, Takayama K, Ohtsuka J, Funahashi H, *et al*. Inflammatory bowel disease-like enteritis and caecitis in a senescence accelerated mouse P1/Yit strain. *Gut*. 1998;43:71-8.

71. Strober W, Fuss IJ, Blumberg RS. The immunology of mucosal models of inflammation. *Annu Rev Immunol*. 2002;20:495-549.

72. Panwala CM, Jones JC, Viney JL. A novel model of inflammatory bowel disease: Mice deficient for the multiple drug resistance gene, *mdr1a*, spontaneously develop colitis. *J Immunol*. 1998;161:5733-44.

73. Blumberg RS, Saubermann LJ, Strober W. Animal models of mucosal inflammation and their relation to human inflammatory bowel disease. *Curr Opin Immunol*. 1999;11:648-56.

74. Macpherson A, Khoo UY, Forgacs I, Philpott-Howard J, Bjarnason I. Mucosal antibodies in inflammatory bowel disease are directed against intestinal bacteria. *Gut*. 1996;38:365-75.

75. D'Haens GR, Geboes K, Peeters M, Baert F, Penninckx F, Rutgeerts P. Early lesions of recurrent Crohn's disease caused by infusion of intestinal contents in excluded ileum. *Gastroenterology*. 1998;114:262-7.

76. Castiglione F, Del Vecchio Blanco G, Rispo A, Petrelli G, Amalfi G, Cozzolino A, *et al*. Orocecal transit time and bacterial overgrowth in patients with Crohn's disease. *J Clin Gastroenterol*. 2000;31:63-6.

77. Sutherland L, Singleton J, Sessions J, Hanauer S, Krawitt E, Rankin G, *et al*. Double blind, placebo controlled trial of metronidazole in Crohn's disease. *Gut*. 1991;32:1071-5.

78. Ursing B, Alm T, Barany F, Bergelin I, Ganrot-Norlin K, Hoevels J, *et al*. A comparative study of metronidazole and sulfasalazine for active Crohn's disease: The cooperative Crohn's disease study in Sweden. *Gastroenterology*. 1982;83:550-62.

79. Rutgeerts P, Hiele M, Geboes K, Peeters M, Penninckx F, Aerts R, *et al*. Controlled trial of metronidazole treatment for prevention of Crohn's recurrence after ileal resection. *Gastroenterology*. 1995;108:1617-21.

80. Burke DA, Axon AT, Clayden SA, Dixon MF, Johnston D, Lacey RW. The efficacy of tobramycin in the treatment of ulcerative colitis. *Aliment Pharmacol Ther*. 1990;4:123-9.

81. Turunen U, Farkkila, Valtonen V. Long-term treatment of ulcerative colitis with ciprofloxacin. *Gastroenterology*. 1999;117:282-3.

82. Leiper K, Morris AI, Rhodes JM. Open label trial of oral clarithromycin in active Crohn's disease. *Aliment Pharmacol Ther*. 2000;14:801-6.

83. Aberra FN, Brensinger CM, Bilker WB, Lichtenstein GR, Lewis JD. Antibiotic use and the risk of flare of inflammatory bowel disease. *Clin Gastroenterol Hepatol*. 2005;3:459-65.

84. Singh S, Graff LA, Bernstein CN. Do NSAIDs, antibiotics, infections, or stress trigger flares in IBD? *Am J Gastroenterol.* 2009;104:1298-1314.

85. Perencevich M, Burakoff R. Use of antibiotics in the treatment of inflammatory bowel disease. *Inflamm Bowel Dis*. 2006;12:651-64.

86. Greenfield C, Aguilar Ramirez JR, Pounder RE, Williams T, Danvers M, Marper SR, *et al*. *Clostridium difficile* and inflammatory bowel disease. *Gut*. 1983;24:713-7.

87. Swidsinski A, Ladhoff A, Pernthaler A, Swidsinski S, Loening-Baucke V, Ortner M, *et al*. Mucosal flora in inflammatory bowel disease. *Gastroenterology*. 2002;122:44-54.

88. Cartun RW, Van Kruiningen HJ, Pedersen CA, Berman MM. An immunocytochemical search for infectious agents in Crohn's disease. *Mod Pathol*. 1993;6:212-9.

89. Martinez-Medina M, Aldeguer X, Lopez-Siles M, Gonzalez-Huix F, Lopez-Oliu C, Dahbi G, *et al*. Molecular diversity of *Escherichia coli* in the human gut: New ecological evidence supporting the role of adherent-invasive *E. coli* (AIEC) in Crohn's disease. *Inflamm Bowel Dis*. 2009;15:872-82.

90. Darfeuille-Michaud A, Boudeau J, Bulois P, Neut C, Glasser AL, Barnich N, *et al*. High prevalence of adherent-invasive *Escherichia coli* associated with ileal mucosa in Crohn's disease. *Gastroenterology*. 2004;127:412-21.

91. Kotlowski R, Bernstein CN, Sepehri S, Krause DO. High prevalence of *Escherichia coli* belonging to the B2+D phylogenetic group in inflammatory bowel disease. *Gut*. 2007;56:669-75.

92. Sepehri S, Kotlowski R, Bernstein CN, Krause DO. Microbial diversity of inflamed and noninflamed gut biopsy tissues in inflammatory bowel disease. *Inflamm Bowel Dis*. 2007;13:675-83.

93. Sasaki M, Sitaraman SV, Babbin BA, Gerner-Smidt P, Ribot EM, Garrett N, *et al*. Invasive *Escherichia coli* are a feature of Crohn's disease. *Lab Invest*. 2007;87:1042-54.

94. Boudeau J, Glasser AL, Masseret E, Joly B, Darfeuille-Michaud A. Invasive ability of an *Escherichia coli* strain isolated from the ileal mucosa of a patient with Crohn's disease. *Infect Immun*. 1999;67:4499-509.

95. Peeters M, Geypens B, Claus D, Nevens H, Ghoos Y, Verbeke G, *et al*. Clustering of increased small intestinal permeability in families with Crohn's disease. *Gastroenterology*. 1997;113:802-7.

96. Soderholm JD, Olaison G, Lindberg E, Hannestad U, Vindels A, Tysk C, *et al*. Different intestinal permeability patterns in relatives and spouses of patients with Crohn's disease: An inherited defect in mucosal defence? *Gut*. 1999;44:96-100.

97. Breslin NP, Nash C, Hilsden RJ, Hershfield NB, Price LM, Meddings JB, *et al*. Intestinal permeability is increased in a proportion of spouses of patients with Crohn's disease. *Am J Gastroenterol*. 2001;96:2934-8.

98. Persson PG, Ahlbom A, Hellers G. Diet and inflammatory bowel disease: A case-control study. *Epidemiology*. 1992;3:47-52.

99. Farrokhyar F, Swarbrick ET, Irvine EJ. A critical review of epidemiological studies in inflammatory bowel disease. *Scand J Gastroenterol*. 2001;36:2-15.

100. Jayanthi V, Probert CS, Pinder D, Wicks AC, Mayberry JF. Epidemiology of Crohn's disease in Indian migrants and the indigenous population in Leicestershire. *Q J Med*. 1992;82:125-38.

101. Lakatos L, Mester G, Erdelyi Z, Balogh M, Szipocs I, Kamaras G, *et al*. Striking elevation in incidence and prevalence of inflammatory bowel disease in a province of western Hungary between 1977-2001. *World J Gastroenterol*. 2004;10:404-9.

102. Sonnenberg A. Geographic and temporal variations of sugar and margarine consumption in relation to Crohn's disease. *Digestion*. 1988;41:161-71.

103. Reif S, Klein I, Lubin F, Farbstein M, Hallak A, Gilat T. Pre-illness dietary factors in inflammatory bowel disease. *Gut*. 1997;40:754-60.

104. Kugathasan S, Amre D. Inflammatory bowel disease-environmental modification and genetic determinants. *Pediatr Clin North Am*. 2006;53:727-49.

105. Gilat T, Hacohen D, Lilos P, Langman MJ. Childhood factors in ulcerative colitis and Crohn's disease. An international co-operative study. *Scand J Gastroenterol*. 1987;22:1009-24.

106. Baron S, Turck D, Leplat C, Merle V, Gower-Rousseau C, Marti R, *et al*. Environmental risk factors in paediatric inflammatory bowel diseases: A population based case control study. *Gut*. 2005;54:357-63.

107. Amre DK, Lambrette P, Law L, Krupoves A, Chotard V, Costea F, *et al*. Investigating the hygiene hypothesis as a risk factor in pediatric onset Crohn's disease: A case-control study. *Am J Gastroenterol*. 2006;101:1005-11.

108. Buhner S, Buning C, Genschel J, Kling K, Herrmann D, Dignass A, *et al*. Genetic basis for increased intestinal permeability in families with Crohn's disease: Role of CARD15 mutation? *Gut*. 2006;55:342-7.

109. Irvine EJ, Marshall JK. Increased intestinal permeability precedes the onset of Crohn's disease in a subject with familial risk. *Gastroenterology*. 2000;119:1740-4.

110. Soderholm JD, Olaison G, Peterson KH, Franzen LE, Lindmark T, Wiren M, *et al*. Augmented increase in tight junction permeability by luminal stimuli in the non-inflamed ileum of Crohn's disease. *Gut*. 2002;50:307-13.

111. Wyatt J, Vogelsang H, Hubl W, Waldhoer T, Lochs H. Intestinal permeability and the prediction of relapse in Crohn's disease. *Lancet*. 1993;341:1437-9.

112. Arnott ID, Kingstone K, Ghosh S. Abnormal intestinal permeability predicts relapse in inactive Crohn's disease. *Scand J Gastroenterol*. 2000;35:1163-9.

113. D'Inca R, Di Leo V, Corrao G, Martines D, D'Odorico A, Mestriner C, *et al*. Intestinal permeability test as a predictor of clinical course in Crohn's disease. *Am J Gastroenterol*. 1999;94:2956-60.

114. Strober W, Fuss I, Mannon P. The fundamental basis of inflammatory bowel disease. *J Clin Invest*. 2007;117:514-21.

115. Wallace JL. Nonsteroidal anti-inflammatory drugs and gastroenteropathy: The second hundred years. *Gastroenterology*. 1997;112:1000-16.

116. Olson TS, Reuter BK, Scott KG, Morris MA, Wang XM, Hancock LN, *et al*. The primary defect in experimental ileitis originates from a nonhematopoietic source. *J Exp Med*. 2006;203:541-52.

117. Schwab M, Schaeffeler E, Marx C, Fromm MF, Kaskas B, Metzler J, *et al*. Association between the C3435T MDR1 gene polymorphism and susceptibility for ulcerative colitis. *Gastroenterology*. 2003;124:26-33.

118. Yacyshyn B, Maksymowych W, Bowen-Yacyshyn MB. Differences in P-glycoprotein-170 expression and activity between Crohn's disease and ulcerative colitis. *Hum Immunol*. 1999;60:677-87.

119. Resta-Lenert S, Smitham J, Barrett KE. Epithelial dysfunction associated with the development of colitis in conventionally housed *mdr1a*$^{-/-}$ mice. *Am J Physiol Gastrointest Liver Physiol*. 2005;289:G153-62.

120. Saclarides TJ, Jakate SM, Coon JS, Bhattacharyya AK, Dominguez JM, Szeluga DJ, *et al*. Variable expression of P-glycoprotein in normal, inflamed, and dysplastic areas in ulcerative colitis. *Dis Colon Rectum.* 1992;35:747-52.

121. Sydora BC, Macfarlane SM, Walker JW, Dmytrash AL, Churchill TA, Doyle J, *et al*. Epithelial barrier disruption allows nondisease-causing bacteria to initiate and sustain IBD in the IL-10 gene-deficient mouse. *Inflamm Bowel Dis*. 2007;13:947-54.

122. Nazli A, Yang PC, Jury J, Howe K, Watson JL, Soderholm JD, *et al*. Epithelia under metabolic stress perceive commensal bacteria as a threat. *Am J Pathol*. 2004;164:947-57.

123. Schurmann G, Bruwer M, Klotz A, Schmid KW, Senninger N, Zimmer KP. Transepithelial transport processes at the intestinal mucosa in inflammatory bowel disease. *Int J Colorectal Dis*. 1999;14:41-6.

124. Roediger WE. The colonic epithelium in ulcerative colitis: An energy-deficiency disease? *Lancet.* 1980;2:712-5.

125. Hadjiagapiou C, Schmidt L, Dudeja PK, Layden TJ, Ramaswamy K. Mechanism(s) of butyrate transport in Caco-2 cells: Role of monocarboxylate transporter 1. *Am J Physiol Gastrointest Liver Physiol*. 2000;279:G775-80.

126. Ganapathy V, Thangaraju M, Gopal E, Martin PM, Itagaki S, Miyauchi S, *et al*. Sodium-coupled monocarboxylate transporters in normal tissues and in cancer. *AAPS J*. 2008;10:193-9.

127. Voet D, Voet JG, Pratt CW. Fundamentals of biochemistry. Wiley & Sons Inc.; 2005.

128. Allan ES, Winter S, Light AM, Allan A. Mucosal enzyme activity for butyrate oxidation; no defect in patients with ulcerative colitis. *Gut*. 1996;38:886-93.

129. Bernardi P, Broekemeier KM, Pfeiffer DR. Recent progress on regulation of the mitochondrial permeability transition pore; a cyclosporin-sensitive pore in the inner mitochondrial membrane. *J Bioenerg Biomembr*. 1994;26:509-17.

130. Bernardi P, Colonna R, Costantini P, Eriksson O, Fontaine E, Ichas F, *et al*. The mitochondrial permeability transition. *Biofactors*. 1998;8:273-81.

131. Weiss JN, Korge P, Honda HM, Ping P. Role of the mitochondrial permeability transition in myocardial disease. *Circ Res*. 2003;93:292-301.

132. Manichanh C, Rigottier-Gois L, Bonnaud E, Gloux K, Pelletier E, Frangeul L, *et al*. Reduced diversity of faecal microbiota in Crohn's disease revealed by a metagenomic approach. *Gut*. 2006;55:205-11.

133. Segain JP, Raingeard de la Bletiere D, Bourreille A, Leray V, Gervois N, Rosales C, *et al*. Butyrate inhibits inflammatory responses through NF-kappaB inhibition: Implications for Crohn's disease. *Gut*. 2000;47:397-403.

134. Barcenilla A, Pryde SE, Martin JC, Duncan SH, Stewart CS, Henderson C, *et al*. Phylogenetic relationships of butyrate-producing bacteria from the human gut. *Appl Environ Microbiol*. 2000;66:1654-61.

135. Humphrey CD, Montag DM, Pittman FE. Morphologic observations of experimental *Campylobacter jejuni* infection in the hamster intestinal tract. *Am J Pathol*. 1986;122:152-9.

136. Zareie M, Riff J, Donato K, McKay DM, Perdue MH, Soderholm JD, *et al*. Novel effects of the prototype translocating *Escherichia coli*, strain C25 on intestinal epithelial structure and barrier function. *Cell Microbiol*. 2005;7:1782-97.

137. Ma C, Wickham ME, Guttman JA, Deng W, Walker J, Madsen KL, *et al*. *Citrobacter rodentium* infection causes both mitochondrial dysfunction and intestinal epithelial barrier disruption *in vivo*: Role of mitochondrial associated protein (map). *Cell Microbiol*. 2006;8:1669-86.

138. He D, Hagen SJ, Pothoulakis C, Chen M, Medina ND, Warny M, *et al*. *Clostridium difficile* toxin A causes early damage to mitochondria in cultured cells. *Gastroenterology*. 2000;119:139-50.

139. Dickman KG, Hempson SJ, Anderson J, Lippe S, Zhao L, Burakoff R, *et al*. Rotavirus alters paracellular permeability and energy metabolism in Caco-2 cells. *Am J Physiol Gastrointest Liver Physiol*. 2000;279:G757-66.

140. Helzer JE, Stillings WA, Chammas S, Norland CC, Alpers DH. A controlled study of the association between ulcerative colitis and psychiatric diagnoses. *Dig Dis Sci*. 1982;27:513-8.

141. Bernstein CN, Walker JR, Graff LA. On studying the connection between stress and IBD. *Am J Gastroenterol*. 2006;101:782-5.

142. Grace WJ. Life stress and gastro-intestinal diseases. *Am Pract Dig Treat*. 1953;4:848-52.

143. Mawdsley JE, Rampton DS. Psychological stress in IBD: New insights into pathogenic and therapeutic implications. *Gut*. 2005;54:1481-91.

144. Mittermaier C, Dejaco C, Waldhoer T, Oefferlbauer-Ernst A, Miehsler W, Beier M, *et al*. Impact of depressive mood on relapse in patients with inflammatory bowel disease: A prospective 18-month follow-up study. *Psychosom Med*. 2004;66:79-84.

145. Barclay GR, Turnberg LA. Effect of psychological stress on salt and water transport in the human jejunum. *Gastroenterology*. 1987;93:91-7.

146. Santos J, Saperas E, Nogueiras C, Mourelle M, Antolin M, Cadahia A, *et al*. Release of mast cell mediators into the jejunum by cold pain stress in humans. *Gastroenterology*. 1998;114:640-8.

147. Saunders PR, Kosecka U, McKay DM, Perdue MH. Acute stressors stimulate ion secretion and increase epithelial permeability in rat intestine. *Am J Physiol*. 1994;267:G794-9.

148. Meddings JB, Swain MG. Environmental stress-induced gastrointestinal permeability is mediated by endogenous glucocorticoids in the rat. *Gastroenterology*. 2000;119:1019-28.

149. Soderholm JD, Perdue MH. Stress and gastrointestinal tract. II. Stress and intestinal barrier function. *Am J Physiol Gastrointest Liver Physiol*. 2001;280:G7-G13.

150. Soderholm JD, Yang PC, Ceponis P, Vohra A, Riddell R, Sherman PM, *et al*. Chronic stress induces mast cell-dependent bacterial adherence and initiates mucosal inflammation in rat intestine. *Gastroenterology*. 2002;123:1099-108.

151. Somasundaram S, Sigthorsson G, Simpson RJ, Watts J, Jacob M, Tavares IA, *et al*. Uncoupling of intestinal mitochondrial oxidative phosphorylation and inhibition of cyclooxygenase are required for the development of NSAID-enteropathy in the rat. *Aliment Pharmacol Ther*. 2000;14:639-50.

152. Atherton C, Jones J, McKaig B, Bebb J, Cunliffe R, Burdsall J, *et al*. Pharmacology and gastrointestinal safety of lumiracoxib, a novel cyclooxygenase-2 selective inhibitor: An integrated study. *Clin Gastroenterol Hepatol*. 2004;2:113-20.

153. Somasundaram S, Rafi S, Hayllar J, Sigthorsson G, Jacob M, Price AB, *et al*. Mitochondrial damage: A possible mechanism of the "topical" phase of NSAID induced injury to the rat intestine. *Gut*. 1997;41:344-53.

154. Basivireddy J, Vasudevan A, Jacob M, Balasubramanian KA. Indomethacin-induced mitochondrial dysfunction and oxidative stress in villus enterocytes. *Biochem Pharmacol*. 2002;64:339-49.

155. Gabe SM, Bjarnason I, Tolou-Ghamari Z, Tredger JM, Johnson PG, Barclay GR, *et al*. The effect of tacrolimus (FK506) on intestinal barrier function and cellular energy production in humans. *Gastroenterology*. 1998;115:67-74.

156. Madsen KL, Yanchar NL, Sigalet DL, Reigel T, Fedorak RN. FK506 increases permeability in rat intestine by inhibiting mitochondrial function. *Gastroenterology*. 1995;109:107-14.

157. Taylor CT, Dzus AL, Colgan SP. Autocrine regulation of epithelial permeability by hypoxia: Role for polarized release of tumor necrosis factor alpha. *Gastroenterology*. 1998;114:657-68.

158. Gellerich FN, Trumbeckaite S, Opalka JR, Gellerich JF, Chen Y, Neuhof C, *et al*. Mitochondrial dysfunction in sepsis: Evidence from bacteraemic baboons and endotoxaemic rabbits. *Biosci Rep*. 2002;22:99-113.

159. Willoughby RP, Harris KA, Carson MW, Martin CM, Troster M, DeRose G, *et al*. Intestinal mucosal permeability to ^{51}Cr-ethylenediaminetetraacetic acid is increased after bilateral lower extremity ischemia-reperfusion in the rat. *Surgery*. 1996;120:547-53.

160. Ramachandran A, Patra S, Balasubramanian KA. Intestinal mitochondrial dysfunction in surgical stress. *J Surg Res*. 2001;99:120-8.

161. Kim NH, Kang JH. Oxidative damage of DNA induced by the cytochrome *c* and hydrogen peroxide system. *J Biochem Mol Biol*. 2006;39:452-6.

162. Ma YS, Wu SB, Lee WY, Cheng JS, Wei YH. Response to the increase of oxidative stress and mutation of mitochondrial DNA in aging. *Biochim Biophys Acta*. 2009 [Epub ahead of print].

163. Dean RT, Fu S, Stocker R, Davies MJ. Biochemistry and pathology of radical-mediated protein oxidation. *Biochem J*. 1997;324:1-18.

164. Breen AP, Murphy JA. Reactions of oxyl radicals with DNA. *Free Radic Biol Med.* 1995;18:1033-77.

165. Frank H, Thiel D, MacLeod J. Mass spectrometric detection of cross-linked fatty acids formed during radical-induced lesion of lipid membranes. *Biochem J*. 1989;260:873-8.

166. Bowie A, O'Neill LA. Oxidative stress and nuclear factor-kappaB activation: A reassessment of the evidence in the light of recent discoveries. *Biochem Pharmacol*. 2000;59:13-23.

167. Hadjigogos K. The role of free radicals in the pathogenesis of rheumatoid arthritis. *Panminerva Med.* 2003;45:7-13.

168. Warner TD, Giuliano F, Vojnovic I, Bukasa A, Mitchell JA, Vane JR. Nonsteroid drug selectivities for cyclo-oxygenase-1 rather than cyclo-oxygenase-2 are associated with human gastrointestinal toxicity: A full *in vitro* analysis. *Proc Natl Acad Sci U S A.* 1999;96:7563-8.

169. Yamazaki R, Kusunoki N, Matsuzaki T, Hashimoto S, Kawai S. Nonsteroidal anti-inflammatory drugs induce apoptosis in association with activation of peroxisome proliferator-activated receptor gamma in rheumatoid synovial cells. *J Pharmacol Exp Ther*. 2002;302:18-25.

170. Tegeder I, Pfeilschifter J, Geisslinger G. Cyclooxygenase-independent actions of cyclooxygenase inhibitors. *FASEB J.* 2001;15:2057-72.

171. Harper JA, Dickinson K, Brand MD. Mitochondrial uncoupling as a target for drug development for the treatment of obesity. *Obes Rev*. 2001;2:255-65.

172. Jenkins DJ, Kendall CW. Plant sterols, health claims and strategies to reduce cardiovascular disease risk. *J Am Coll Nutr*. 1999;18:559-62.

173. Jenkins DJ, Kendall CW, Vuksan V. Inulin, oligofructose and intestinal function. *J Nutr*. 1999;129:1431S-3S.

174. Louis P, Scott KP, Duncan SH, Flint HJ. Understanding the effects of diet on bacterial metabolism in the large intestine. *J Appl Microbiol*. 2007;102:1197-208.

175. Cummings JH. Fermentation in the human large intestine: Evidence and implications for health. *Lancet.* 1983;1:1206-9.

176. Miller TL, Wolin MJ. Fermentations by saccharolytic intestinal bacteria. *Am J Clin Nutr*. 1979;32:164-72.

177. Silk DB. Fibre and enteral nutrition. *Gut*. 1989;30:246-64.

178. Topping DL, Clifton PM. Short-chain fatty acids and human colonic function: Roles of resistant starch and nonstarch polysaccharides. *Physiol Rev*. 2001;81:1031-64.

179. Cummings JH, Hill MJ, Bone ES, Branch WJ, Jenkins DJ. The effect of meat protein and dietary fiber on colonic function and metabolism. II. Bacterial metabolites in feces and urine. *Am J Clin Nutr*. 1979;32:2094-101.

180. Andoh A, Tsujikawa T, Fujiyama Y. Role of dietary fiber and short-chain fatty acids in the colon. *Curr Pharm Des*. 2003;9:347-58.

181. Roberfroid MB. Introducing inulin-type fructans. *Br J Nutr*. 2005;93:S13-25.

182. Roediger WE. Utilization of nutrients by isolated epithelial cells of the rat colon. *Gastroenterology*. 1982;83:424-9.

183. Chapman MA, Grahn MF, Hutton M, Williams NS. Butyrate metabolism in the terminal ileal mucosa of patients with ulcerative colitis. *Br J Surg*. 1995;82:36-8.

184. Roediger WE, Nance S. Selective reduction of fatty acid oxidation in colonocytes: Correlation with ulcerative colitis. *Lipids*. 1990;25:646-52.

185. Roediger WE, Nance S. Metabolic induction of experimental ulcerative colitis by inhibition of fatty acid oxidation. *Br J Exp Pathol*. 1986;67:773-82.

186. Roediger WE, Heyworth M, Willoughby P, Piris J, Moore A, Truelove SC. Luminal ions and short chain fatty acids as markers of functional activity of the mucosa in ulcerative colitis. *J Clin Pathol*. 1982;35:323-6.

187. Thibault R, De Coppet P, Daly K, Bourreille A, Cuff M, Bonnet C, *et al*. Down-regulation of the monocarboxylate transporter 1 is involved in butyrate deficiency during intestinal inflammation. *Gastroenterology*. 2007;133:1916-27.

188. Daly K, Cuff MA, Fung F, Shirazi-Beechey SP. The importance of colonic butyrate transport to the regulation of genes associated with colonic tissue homoeostasis. *Biochem Soc Trans*. 2005;33:733-5.

189. Vernia P, Monteleone G, Grandinetti G, Villotti G, Di Giulio E, Frieri G, *et al*. Combined oral sodium butyrate and mesalazine treatment compared to oral mesalazine alone in ulcerative colitis: Randomized, double-blind, placebo-controlled pilot study. *Dig Dis Sci*. 2000;45:976-81.

190. Talley NA, Chen F, King D, Jones M, Talley NJ. Short-chain fatty acids in the treatment of radiation proctitis: A randomized, double-blind, placebo-controlled, cross-over pilot trial. *Dis Colon Rectum*. 1997;40:1046-50.

191. Scheppach W, Christl SU, Bartram HP, Richter F, Kasper H. Effects of short-chain fatty acids on the inflamed colonic mucosa. *Scand J Gastroenterol Suppl*. 1997;222:53-7.

192. Scheppach W, Muller JG, Boxberger F, Dusel G, Richter F, Bartram HP, *et al*. Histological changes in the colonic mucosa following irrigation with short-chain fatty acids. *Eur J Gastroenterol Hepatol*. 1997;9:163-8.

193. Di Sabatino A, Morera R, Ciccocioppo R, Cazzola P, Gotti S, Tinozzi FP, *et al*. Oral butyrate for mildly to moderately active Crohn's disease. *Aliment Pharmacol Ther*. 2005;22:789-94.

194. Scheppach W, Sommer H, Kirchner T, Paganelli GM, Bartram P, Christl S, *et al*. Effect of butyrate enemas on the colonic mucosa in distal ulcerative colitis. *Gastroenterology*. 1992;103:51-6.

195. Vernia P, Annese V, Bresci G, d'Albasio G, D'Inca R, Giaccari S, *et al*. Topical butyrate improves efficacy of 5-ASA in refractory distal ulcerative colitis: Results of a multicentre trial. *Eur J Clin Invest*. 2003;33:244-8.

196. Vernia P, Marcheggiano A, Caprilli R, Frieri G, Corrao G, Valpiani D, *et al*. Short-chain fatty acid topical treatment in distal ulcerative colitis. *Aliment Pharmacol Ther*. 1995;9:309-13.

197. Venkatraman A, Ramakrishna BS, Shaji RV, Kumar NS, Pulimood A, Patra S. Amelioration of dextran sulfate colitis by butyrate: Role of heat shock protein 70 and NF-kappaB. *Am J Physiol Gastrointest Liver Physiol*. 2003;285:G177-84.

198. Patz J, Jacobsohn WZ, Gottschalk-Sabag S, Zeides S, Braverman DZ. Treatment of refractory distal ulcerative colitis with short chain fatty acid enemas. *Am J Gastroenterol*. 1996;91:731-4.

199. Pinto A, Fidalgo P, Cravo M, Midoes J, Chaves P, Rosa J, *et al*. Short chain fatty acids are effective in short-term treatment of chronic radiation proctitis: Randomized, double-blind, controlled trial. *Dis Colon Rectum*. 1999;42:795-6.

200. Steinhart AH, Hiruki T, Brzezinski A, Baker JP. Treatment of left-sided ulcerative colitis with butyrate enemas: A controlled trial. *Aliment Pharmacol Ther*. 1996;10:729-36.

201. Breuer RI, Soergel KH, Lashner BA, Christ ML, Hanauer SB, Vanagunas A, *et al*. Short chain fatty acid rectal irrigation for left-sided ulcerative colitis: A randomised, placebo controlled trial. *Gut*. 1997;40:485-91.

202. Guillemot F, Colombel JF, Neut C, Verplanck N, Lecomte M, Romond C, *et al*. Treatment of diversion colitis by short-chain fatty acids. prospective and double-blind study. *Dis Colon Rectum*. 1991;34:861-4.

203. Hallert C, Kaldma M, Petersson BG. Ispaghula husk may relieve gastrointestinal symptoms in ulcerative colitis in remission. *Scand J Gastroenterol*. 1991;26:747-50.

204. Fernandez-Banares F, Hinojosa J, Sanchez-Lombrana JL, Navarro E, Martinez-Salmeron JF, Garcia-Puges A, *et al*. Randomized clinical trial of *Plantago ovata* seeds (dietary fiber) as compared with mesalamine in maintaining remission in ulcerative colitis. *Am J Gastroenterol*. 1999;94:427-33.

205. Kanauchi O, Suga T, Tochihara M, Hibi T, Naganuma M, Homma T, *et al*. Treatment of ulcerative colitis by feeding with germinated barley foodstuff: First report of a multicenter open control trial. *J Gastroenterol*. 2002;37:67-72.

206. Kanauchi O, Serizawa I, Araki Y, Suzuki A, Andoh A, Fujiyama Y, *et al*. Germinated barley foodstuff, a prebiotic product, ameliorates inflammation of colitis through modulation of the enteric environment. *J Gastroenterol*. 2003;38:134-41.

207. Kanauchi O, Mitsuyama K, Homma T, Takahama K, Fujiyama Y, Andoh A, *et al*. Treatment of ulcerative colitis patients by long-term administration of germinated barley foodstuff: Multi-center open trial. *Int J Mol Med*. 2003;12:701-4.

208. Hanai H, Kanauchi O, Mitsuyama K, Andoh A, Takeuchi K, Takayuki I, *et al*. Germinated barley foodstuff prolongs remission in patients with ulcerative colitis. *Int J Mol Med*. 2004;13:643-7.

209. Anderson AD, McNaught CE, Jain PK, MacFie J. Randomised clinical trial of synbiotic therapy in elective surgical patients. *Gut*. 2004;53:241-5.

210. Lewis K, Caldwell J, Phan V, Prescott D, Nazli A, Wang A, *et al*. Decreased epithelial barrier function evoked by exposure to metabolic stress and nonpathogenic *E. coli* is enhanced by TNF-alpha. *Am J Physiol Gastrointest Liver Physiol*. 2008;294:G669-78.

211. Compton SJ, Jones CG. Mechanism of dye response and interference in the Bradford protein assay. *Anal Biochem*. 1985;151:369-74.

212. Bradford MM. A rapid and sensitive method for the quantitation of microgram quantities of protein utilizing the principle of protein-dye binding. *Anal Biochem.* 1976;72:248-54.

213. Reisner AH, Nemes P, Bucholtz C. The use of Coomassie brilliant blue G250 perchloric acid solution for staining in electrophoresis and isoelectric focusing on polyacrylamide gels. *Anal Biochem*. 1975;64:509-16.

214. Slater TF, Sawyer B, Straeuli U. Studies on succinate-tetrazolium reductase systems. iii. Points of coupling of four different tetrazolium salts. *Biochim Biophys Acta*. 1963;77:383-93.

215. Roediger WE. Role of anaerobic bacteria in the metabolic welfare of the colonic mucosa in man. *Gut*. 1980;21:793-8.

216. Hayden MS, Ghosh S. Shared principles in NF-kappaB signaling. *Cell*. 2008;132:344-62.

217. Kumar A, Wu H, Collier-Hyams LS, Kwon YM, Hanson JM, Neish AS. The bacterial fermentation product butyrate influences epithelial signaling via reactive oxygen species-mediated changes in cullin-1 neddylation. *J Immunol*. 2009;182:538-46.

218. Sartor RB. Microbial influences in inflammatory bowel diseases. *Gastroenterology*. 2008;134:577-94.

219. Linskens RK, Huijsdens XW, Savelkoul PH, Vandenbroucke-Grauls CM, Meuwissen SG. The bacterial flora in inflammatory bowel disease: Current insights in pathogenesis and the influence of antibiotics and probiotics. *Scand J Gastroenterol*. 2001;234:29-40.

220. Ma C, Wickham ME, Guttman JA, Deng W, Walker J, Madsen KL, *et al*. *Citrobacter rodentium* infection causes both mitochondrial dysfunction and intestinal epithelial barrier disruption *in vivo*: Role of mitochondrial associated protein (map). *Cell Microbiol*. 2006;8:1669-86.

221. Soderholm JD, Peterson KH, Olaison G, Franzen LE, Westrom B, Magnusson KE, *et al*. Epithelial permeability to proteins in the noninflamed ileum of Crohn's disease? *Gastroenterology*. 1999;117:65-72.

222. Kameyama J, Narui H, Inui M, Sato T. Energy level in large intestinal mucosa in patients with ulcerative colitis. *J Exp Med*. 1984;143:253-4.

223. Dharmsathaphorn K, McRoberts JA, Mandel KG, Tisdale LD, Masui H. A human colonic tumor cell line that maintains vectorial electrolyte transport. *Am J Physiol*. 1984;246:G204-8.

224. Murakami H, Masui H. Hormonal control of human colon carcinoma cell growth in serum-free medium. *Proc Natl Acad Sci U S A*. 1980;77:3464-8.

225. Linsinger G, Wilhelm S, Wagner H, Hacker G. Uncouplers of oxidative phosphorylation can enhance a fas death signal. *Mol Cell Biol*. 1999;19:3299-311.

226. Eguchi Y, Shimizu S, Tsujimoto Y. Intracellular ATP levels determine cell death fate by apoptosis or necrosis. *Cancer Res*. 1997;57:1835-40.

227. Shimizu S, Eguchi Y, Kamiike W, Waguri S, Uchiyama Y, Matsuda H, *et al*. Retardation of chemical hypoxia-induced necrotic cell death by bcl-2 and ICE inhibitors: Possible involvement of common mediators in apoptotic and necrotic signal transductions. *Oncogene*. 1996;12:2045-50.

228. Sanchez-Duffhues G, Calzado MA, de Vinuesa AG, Appendino G, Fiebich BL, Loock U, *et al*. Denbinobin inhibits nuclear factor-kappaB and induces apoptosis via reactive oxygen species generation in human leukemic cells. *Biochem Pharmacol*. 2009;77:1401-9.

229. Zhang M, Liu B, Zhang Y, Wei H, Lei Y, Zhao L. Structural shifts of mucosa-associated *Lactobacilli* and *Clostridium leptum* subgroup in patients with ulcerative colitis. *J Clin Microbiol*. 2007;45:496-500.

230. Sokol H, Pigneur B, Watterlot L, Lakhdari O, Bermudez-Humaran LG, Gratadoux JJ, *et al*. *Faecalibacterium prausnitzii* is an anti-inflammatory commensal bacterium identified by gut microbiota analysis of Crohn's disease patients. *Proc Natl Acad Sci U S A*. 2008;105:16731-6.

231. Barnich N, Darfeuille-Michaud A. Role of bacteria in the etiopathogenesis of inflammatory bowel disease. *World J Gastroenterol*. 2007;13:5571-6.

232. Baumgart M, Dogan B, Rishniw M, Weitzman G, Bosworth B, Yantiss R, *et al*. Culture independent analysis of ileal mucosa reveals a selective increase in invasive *Escherichia coli* of novel phylogeny relative to depletion of clostridiales in Crohn's disease involving the ileum. *ISME J*. 2007;1:403-18.

233. Ambrose NS, Johnson M, Burdon DW, Keighley MR. Incidence of pathogenic bacteria from mesenteric lymph nodes and ileal serosa during Crohn's disease surgery. *Br J Surg*. 1984;71:623-5.

234. Tabaqchali S, O'Donoghue DP, Bettelheim KA. *Escherichia coli* antibodies in patients with inflammatory bowel disease. *Gut*. 1978;19:108-13.

235. Arnott ID, Landers CJ, Nimmo EJ, Drummond HE, Smith BK, Targan SR, *et al*. Sero-reactivity to microbial components in Crohn's disease is associated with disease severity and progression, but not NOD2/CARD15 genotype. *Am J Gastroenterol*. 2004;99:2376-84.

236. Burke DA, Axon AT. Adhesive *Escherichia coli* in inflammatory bowel disease and infective diarrhoea. *BMJ*. 1988;297:102-4.

237. Meconi S, Vercellone A, Levillain F, Payre B, Al Saati T, Capilla F, *et al*. Adherent-invasive *Escherichia coli* isolated from Crohn's disease patients induce granulomas *in vitro*. *Cell Microbiol*. 2007;9:1252-61.

238. Suzuki T, Yoshida S, Hara H. Physiological concentrations of short-chain fatty acids immediately suppress colonic epithelial permeability. *Br J Nutr*. 2008;100:297-305.

239. Mariadason JM, Barkla DH, Gibson PR. Effect of short-chain fatty acids on paracellular permeability in Caco-2 intestinal epithelium model. *Am J Physiol*. 1997;272:G705-12.

240. Peng L, He Z, Chen W, Holzman IR, Lin J. Effects of butyrate on intestinal barrier function in a Caco-2 cell monolayer model of intestinal barrier. *Pediatr Res*. 2007;61:37-41.

241. Yamane M, Yamane S. The induction of colonocyte differentiation in Caco-2 cells by sodium butyrate causes an increase in glucosylceramide synthesis in order to avoid apoptosis based on ceramide. *Arch Biochem Biophys*. 2007;459:159-68.

242. Hara A, Hibi T, Yoshioka M, Toda K, Watanabe N, Hayashi A, *et al*. Changes of proliferative activity and phenotypes in spontaneous differentiation of a colon cancer cell line. *Jpn J Cancer Res*. 1993;84:625-32.

243. Madara JL, Trier JS, Neutra MR. Structural changes in the plasma membrane accompanying differentiation of epithelial cells in human and monkey small intestine. *Gastroenterology*. 1980;78:963-75.

244. Musch MW, Bookstein C, Xie Y, Sellin JH, Chang EB. SCFA increase intestinal Na absorption by induction of NHE3 in rat colon and human intestinal C2/bbe cells. *Am J Physiol Gastrointest Liver Physiol.* 2001;280:G687-93.

245. Mariadason JM, Kilias D, Catto-Smith A, Gibson PR. Effect of butyrate on paracellular permeability in rat distal colonic mucosa *ex vivo*. *J Gastroenterol Hepatol*. 1999;14:873-9.

246. Ruemmele FM, Dionne S, Qureshi I, Sarma DS, Levy E, Seidman EG. Butyrate mediates Caco-2 cell apoptosis via up-regulation of pro-apoptotic BAK and inducing caspase-3 mediated cleavage of poly-(ADP-ribose) polymerase (PARP). *Cell Death Differ*. 1999;6:729-35.

247. Ruemmele FM, Schwartz S, Seidman EG, Dionne S, Levy E, Lentze MJ. Butyrate induced Caco-2 cell apoptosis is mediated via the mitochondrial pathway. *Gut*. 2003;52:94-100.

248. Zeng H, Briske-Anderson M. Prolonged butyrate treatment inhibits the migration and invasion potential of HT1080 tumor cells. *J Nutr*. 2005;135:291-5.

249. Zgouras D, Wachtershauser A, Frings D, Stein J. Butyrate impairs intestinal tumor cell-induced angiogenesis by inhibiting HIF-1alpha nuclear translocation. Biochem *Biophys Res Commun*. 2003;300:832-8.

250. Gibson PR, Rosella O, Wilson AJ, Mariadason JM, Rickard K, Byron K, *et al*. Colonic epithelial cell activation and the paradoxical effects of butyrate. *Carcinogenesis*. 1999;20:539-44.

251. Daly K, Shirazi-Beechey SP. Microarray analysis of butyrate regulated genes in colonic epithelial cells. *DNA Cell Biol*. 2006;25:49-62.

252. Hinnebusch BF, Meng S, Wu JT, Archer SY, Hodin RA. The effects of short-chain fatty acids on human colon cancer cell phenotype are associated with histone hyperacetylation. *J Nutr*. 2002;132:1012-7.

253. Davie JR. Inhibition of histone deacetylase activity by butyrate. *J Nutr*. 2003;133:2485S-93S.

254. Gibson PR. The intracellular target of butyrate's actions: HDAC or HDON'T? *Gut*. 2000;46:447-8.

255. Chirakkal H, Leech SH, Brookes KE, Prais AL, Waby JS, Corfe BM. Upregulation of BAK by butyrate in the colon is associated with increased Sp3 binding. *Oncogene*. 2006;25:7192-200.

256. Comalada M, Bailon E, de Haro O, Lara-Villoslada F, Xaus J, Zarzuelo A, *et al*. The effects of short-chain fatty acids on colon epithelial proliferation and survival depend on the cellular phenotype. *J Cancer Res Clin Oncol*. 2006;132:487-97.

257. Hodin RA, Meng S, Archer S, Tang R. Cellular growth state differentially regulates enterocyte gene expression in butyrate-treated HT-29 cells. *Cell Growth Differ*. 1996;7:647-53.

258. Berger DH. Plasmin/plasminogen system in colorectal cancer. *World J Surg*. 2002;26:767-71.

259. Mortensen FV, Jorgensen B, Christiansen HM, Sloth-Nielsen J, Wolff B, Hessov I. Short-chain fatty acid enemas stimulate plasminogen activator inhibitor-1 after abdominal aortic graft surgery: A double-blinded, placebo-controlled study. *Thromb Res*. 2000;98:361-6.

260. Gibson PR, Kilias D, Rosella O, Day JM, Abbott M, Finch CF, *et al*. Effect of topical butyrate on rectal epithelial kinetics and mucosal enzyme activities. *Clin Sci (Lond)*. 1998;94:671-6.

261. Andoh A, Shimada M, Araki Y, Fujiyama Y, Bamba T. Sodium butyrate enhances complement-mediated cell injury via down-regulation of decay-accelerating factor expression in colonic cancer cells. *Cancer Immunol Immunother*. 2002;50:663-72.

262. McIntyre A, Young GP, Taranto T, Gibson PR, Ward PB. Different fibers have different regional effects on luminal contents of rat colon. *Gastroenterology*. 1991;101:1274-81.

263. DeSoignie R, Sellin JH. Propionate-initiated changes in intracellular pH in rabbit colonocytes. Gastroenterology. 1994;107:347-56.

264. Inan MS, Rasoulpour RJ, Yin L, Hubbard AK, Rosenberg DW, Giardina C. The luminal short-chain fatty acid butyrate modulates NF-kappaB activity in a human colonic epithelial cell line. *Gastroenterology*. 2000;118:724-34.

265. Yin L, Laevsky G, Giardina C. Butyrate suppression of colonocyte NF-kappa B activation and cellular proteasome activity. *J Biol Chem*. 2001;276:44641-6.

266. Luhrs H, Gerke T, Schauber J, Dusel G, Melcher R, Scheppach W, *et al*. Cytokine-activated degradation of inhibitory kappaB protein alpha is inhibited by the short-chain fatty acid butyrate. *Int J Colorectal Dis*. 2001;16:195-201.

267. Wu GD, Huang N, Wen X, Keilbaugh SA, Yang H. High-level expression of I kappa B-beta in the surface epithelium of the colon: *In vitro* evidence for an immunomodulatory role. *J Leukoc Biol*. 1999;66:1049-56.

268. Weng M, Walker WA, Sanderson IR. Butyrate regulates the expression of pathogen-triggered IL-8 in intestinal epithelia. *Pediatr Res*. 2007;62:542-6.

269. Kamitani T, Kito K, Nguyen HP, Yeh ET. Characterization of NEDD8, a developmentally down-regulated ubiquitin-like protein. *J Biol Chem*. 1997 7;272:28557-62.

270. Parry G, Estelle M. Regulation of cullin-based ubiquitin ligases by the NEDD8/RUB ubiquitin-like proteins. *Semin Cell Dev Biol*. 2004;15:221-9.

271. Bocker U, Nebe T, Herweck F, Holt L, Panja A, Jobin C, *et al*. Butyrate modulates intestinal epithelial cell-mediated neutrophil migration. *Clin Exp Immunol*. 2003;131:53-60.

272. Huang N, Katz JP, Martin DR, Wu GD. Inhibition of IL-8 gene expression in Caco-2 cells by compounds which induce histone hyperacetylation. *Cytokine*. 1997;9:27-36.

273. Ogawa H, Rafiee P, Fisher PJ, Johnson NA, Otterson MF, Binion DG. Butyrate modulates gene and protein expression in human intestinal endothelial cells. *Biochem Biophys Res Commun*. 2003;309:512-9.

274. Song M, Xia B, Li J. Effects of topical treatment of sodium butyrate and 5-aminosalicylic acid on expression of trefoil factor 3, interleukin 1beta, and nuclear factor kappaB in trinitrobenzene sulphonic acid induced colitis in rats. *Postgrad Med J*. 2006;82:130-5.

275. Rodriguez-Cabezas ME, Galvez J, Lorente MD, Concha A, Camuesco D, Azzouz S, *et al*. Dietary fiber down-regulates colonic tumor necrosis factor alpha and nitric oxide production in trinitrobenzenesulfonic acid-induced colitic rats. *J Nutr*. 2002;132:3263-71.

276. Klampfer L, Huang J, Sasazuki T, Shirasawa S, Augenlicht L. Inhibition of interferon gamma signaling by the short chain fatty acid butyrate. *Mol Cancer Res*. 2003;1:855-62.

277. Stempelj M, Kedinger M, Augenlicht L, Klampfer L. Essential role of the JAK/STAT1 signaling pathway in the expression of inducible nitric-oxide synthase in intestinal epithelial cells and its regulation by butyrate. *J Biol Chem*. 2007;282:9797-804.

278. Schwab M, Reynders V, Loitsch S, Steinhilber D, Stein J, Schroder O. Involvement of different nuclear hormone receptors in butyrate-mediated inhibition of inducible NF kappa B signalling. *Mol Immunol*. 2007;44:3625-32.

279. Wachtershauser A, Loitsch SM, Stein J. PPAR-gamma is selectively upregulated in Caco-2 cells by butyrate. *Biochem Biophys Res Commun*. 2000;272:380-5.

280. Roediger WE, Duncan A, Kapaniris O, Millard S. Sulphide impairment of substrate oxidation in rat colonocytes: A biochemical basis for ulcerative colitis? *Clin Sci (Lond)*. 1993;85:623-7.

281. Roediger WE, Duncan A, Kapaniris O, Millard S. Reducing sulfur compounds of the colon impair colonocyte nutrition: Implications for ulcerative colitis. *Gastroenterology*. 1993;104:802-9.

282. Moore JW, Babidge W, Millard S, Roediger WE. Effect of sulphide on short chain acyl-CoA metabolism in rat colonocytes. *Gut*. 1997;41:77-81.

283. Pitcher MC, Beatty ER, Cummings JH. The contribution of sulphate reducing bacteria and 5-aminosalicylic acid to faecal sulphide in patients with ulcerative colitis. *Gut*. 2000;46:64-72.

284. Leschelle X, Goubern M, Andriamihaja M, Blottiere HM, Couplan E, Gonzalez-Barroso MD, *et al*. Adaptative metabolic response of human colonic epithelial cells to the adverse effects of the luminal compound sulfide. *Biochim Biophys Acta*. 2005;1725:201-12.

285. Marchesi JR, Holmes E, Khan F, Kochhar S, Scanlan P, Shanahan F, *et al*. Rapid and noninvasive metabonomic characterization of inflammatory bowel disease. *J Proteome Res*. 2007;6:546-51.

286. Young VB, Schmidt TM. Antibiotic-associated diarrhea accompanied by large-scale alterations in the composition of the fecal microbiota. *J Clin Microbiol*. 2004;42:1203-6.

287. Hosoi R, Matsuyama Y, Hirose S, Koyama Y, Matsuda T, Gee A, *et al*. Characterization of (14)C-acetate uptake in cultured rat astrocytes. *Brain Res*. 2009;1253:69-73.

288. Remels AH, Langen R, Gosker HR, Russell A, Spaapen F, Voncken W, *et al*. PPAR-gamma inhibits NF-kappaB-dependent transcriptional activation in skeletal muscle. *Am J Physiol Endocrinol Metab*. 2009;297:E174-183.

289. Francis GA, Fayard E, Picard F, Auwerx J. Nuclear receptors and the control of metabolism. *Annu Rev Physiol*. 2003;65:261-311.